UNIVERSITY OF MINNESOTA

This is to certify that I have examined this copy of a master's thesis by

Laurence H. Lin

and have found that it is complete and satisfactory in all respects,
and that any and all revisions requireed by the final
examining commitee have been made.

Name of Faculty Adviser

Signature of Faculty Adviser

Date

GRADUATE SCHOOL

A STOICHIOMETRIC MODEL OF TWO PRODUCERS AND ONE CONSUMER

SUBMITTED TO THE FACULTY OF THE GRADUATE SCHOOL
OF THE UNIVERSITY OF MINNESOTA
BY

LAURENCE HAO-RAN LIN

IN PARTIAL FULFILLMENT OF THE REQUIREMENTS
FOR THE DEGREE OF
MASTER OF SCIENCE

Bruce Peckham

June 2008

Abstract

A stoichiometric population model of two producers and one consumer is a generalization of the Rosenzweig and MacArthur population growth model, which is a single-producer-single-consumer population model without stoichiometry. The generalization involves two steps: 1) add a second producer which competes with the first, and 2) introduce stoichiometry into the system. Both generalizations introduce additional equilibria and bifurcations to the single-producer-single-consumer model without stoichiometry.

The primary focus of this paper is to study the equilibria and bifurcations of the two-producer-one-consumer model with stoichiometry. The nutrient cycle in this model is closed. The primary parameters are the growth rates of both producers, and the secondary parameter is the total nutrient in the system. Depending on the parameters, the possible equilibria are: no-life, one-producer, coexistence with both producers, the consumer coexisting with either producer, and the consumer coexisting with both producers. Limit cycles exist in the latter three coexistence combinations. Additionally, variations on producer and competitions between the two producers are considered in this model. Bifurcation diagrams along with corresponding phase portraits summarize the results presented in this paper.

Acknowledgments

I would like to express my deep-felt gratitude to my adviser, Dr. Bruce Peckham, Undergraduate Director of Mathematics and Statistics Department at University of Minnesota Duluth, for his advice, encouragement, enduring patience and constant support. He was never lost his belief in me (though I often felt uncertain about my abilities); always providing clear explanations when I got lost; constantly driving me when I was tired, and always, *always* giving me his time, in spite of anything else that was going on. I wish all students would have the honor and opportunity to experience his ability to perform at that job.

I also thank other committee members, Dr. Harlan Stech of Mathematics and Statistics Department and Dr. John Pastor of the Biology Department, both at University of Minnesota. Their suggestions, comments and additional guidance were invaluable to the completion of this work.

Additionally, I want to thank the professors and staff of University of Minnesota Mathematics and Statistics Department for all their hard work and dedication, providing me the means to complete my degree and prepare for a career as a mathematician.

Contents

1 Introduction

A stoichiometric population model of two producers and one consumer is developed and studied by equilibrium and bifurcation analysis in this paper. Consumers and producers are often referred as predators and prey. This model is a generalization of the Rosenzweig and MacArthur population growth model, which is a single-producer-single-consumer population model. The generalization involves two steps: 1) add a second producer which competes with the first, and 2) introduce stoichiometry into the system. The orders of generalization should not change the final result.

We first introduce a stoichiometric mechanism into the Rosenzweig and MacArthur model; thus, leading to the study of a one-producer-one-consumer model with stoichiometry. The stoichiometry in the one-producer model provides additional bifurcations (including a saddle node, which destroys a limit cycle) and "low nutrient" equilibrium solutions.

Starting from Rosenzweig and MacArthur model again without stoichiometry, we add the second producer, which competes with each the first. The producers are distinguished by their growth rates. Adding a second producer also leads to additional bifurcations (including a transcritical bifurcation of periodic orbits). Due to the additional bifurcation of the periodic orbits, the geometry of the limit cycles becomes an interesting feature.

Finally, we apply both generalizations together. The two-producer-single-consumer model with stoichiometry has all the features above. Additionally, the transitions from one producer to two producers, and the bifurcations occurring between different "side planes" and the interior of the positive quadrant are studied. Bifurcation diagrams along with the corresponding phase portraits summarize the results.

To simplify the system for equilibrium analysis, we divide the models into two cases. If the food source has a high nutrient value to the consumer, we call that to be case H. Otherwise, we have case L if the food source has a low nutrient value to the consumer. We found all equilibrium solutions in both cases and numerically generated curves in the primary parameter plane corresponding to changes in eigenvalues of the equilibria. By running simulations, we obtain phase portraits corresponding to different regions of the parameter plane and identify bifurcations induced as we change the producer growth rates.

A brief review of relevant population models is in the background review section. The relevant population models are Lotka-Voltera model, Rosenzweig and MacArthur model, and the LKE model (Loladze, Kuang, and Elser). The term "stoichiometry" means the ratio of two or more nutrients in an organism. We restrict our attention to carbon and one other nutrient. To construct our model, both carbon flows and nutrient cycles are considered. There are five differential equations and two primary parameters investigated

in the bifurcations. The two primary parameters are the growth rates of the producers. A secondary parameter investigated in the bifurcations is the total nutrient in the system, N_T. All other parameters remain fixed in this study.

The organization of this paper is the following: Section 1 is the introduction; Section 2 is the background review to the Lotka-Voltera model, the Rosenzweig MacArthur model, and the LKE (Loladze, Kuang, Esler) model; Section 3 contains the model construction. The assumptions and compartment diagrams are stated and shown in this section. Section 4 describes the one-producer-one-consumer model. A stoichiometric mechanism is introduced into Rosenzweig and MacArthur model. The equilibrium solutions and bifurcation diagrams of this one-producer model are presented in this section. Section 5 describes the two-producer-one-consumer model. A second producer is first added to the Rosenzweig and MacArthur model without stoichiometry. Then a stoichiometric mechanism is introduced into this two-producer model. The corresponding equilibrium solutions and bifurcation diagrams are presented in this section. Section 6 describes the conclusions of this study. Section 7 is an appendix.

2 Background Review

Many Producer-Consumer models have been developed and studied, usually with a single population of producers assumed in the models. The Lotka-Voltera model was proposed independently in 1925 by the American biophysicist Alfred Lotka and the Italian mathematician Vito Volterra [1]. It was one of the first models to incorporate interactions between producers (prey) and consumers (predators). In the Lotka-Voltera model, the population densities of producers and consumers are thought as the functions against time, with population growth, mortality, and predation including fluxes (interactions) between producers and consumers. To describe the changes of the two population densities, two ordinary differential equations are used, one for producers and another for consumers. Formulas (2.0.1) are differential equations for the Lotka-Voltera model, where P and C represent the population densities of producers and consumers, respectively.

$$\begin{cases} \frac{dP}{dt} &= \alpha P - \beta PC \\ \frac{dC}{dt} &= e\beta PC - dC \end{cases} \tag{2.0.1}$$

α is the natural growth rate of producers in the absence of predation.
β is the death rate per encounter of producer due to predation.
d is the natural death rate of consumers.
e is the efficiency of turning predated food into consumer biomass.

This model describes the interactions between producers and consumers in a simple fashion, in which (i) the population growth of the consumers depends on the population of the producers. If there is a large population of producers available for consumers as food, the population of consumers will increase in size. (ii) The population of producers gets low when the population of consumers is too high. As a result, the number of consumers drops and the producer population increases again.

However, there are two significant problems with the model. (i) If the population of consumers is removed from the system ($C = 0$), the population of producers will grow infinitely without any upper bounds over time according to the formula (1). Obviously, this is not correct because of the limited living resources in the environment. (ii) If the number of producers is doubled, then the growth of consumer will be twice as fast according to the formula (2.0.1). This is the result of ignoring the fact that consumers have saturation on food. Consumers cannot eat twice as much food even if the amount of food is doubled. In other words, the amount of food available and the amount of food consumed are not linearly related.

To improve the Lotka-Voltera model, Rosenzweig and MacArthur [2] suggested introducing the logistic growth function and the food saturation into the model in 1963. Formulas (2) are the equations for a version of the Rosenzweig-MacArthur model.

$$\begin{cases} \frac{dP}{dt} &= \alpha P(1-\frac{P}{K}) - f(P)C \\ \frac{dC}{dt} &= ef(P)C - dC \\ f(P) &= \frac{\beta P}{\chi + P} \end{cases} \tag{2.0.2}$$

α is the natural growth rate of producers in the absence of predation.
d is the natural death rate of consumers.
e is the efficiency of turning predated food into consumers' own biomass.
K is the carrying capacity of producers.
$f(P)$ is a Holling Type II or Michaelis-Menten function that describes consumers saturation on food.
β is the maximal death rate per encounter of producer due to predation.
χ is the half-saturation of predation.

Solutions to system (2.0.2) are more realistic than the solutions to (2.0.1). If the growth rate α of producers is too low, the ecosystem becomes a monoculture system. This is because there is not enough food to maintain the consumers. When the growth rate α is high enough passing a transcritical value, both producers and consumers will be able to coexist together and approach some constant values. As the producer's growth rate α increases further, population solutions approach a limit cycle, and the amptitude of the cycle grows with increasing growth rate α.

Around 2000, a new model was constructed based on the Rosenzweig-MacArthur model to explain the "paradox of enrichment" [3]. Loladze, Kuang and Elser (LKE) [4] introduced the idea of nutrient cycling into the ecology models. Every organism has its own ratio of nutrient to carbon in its body, and that ratio is called the "stoichiometric ratio". The stoichiometric ratio is very specific for most animals, but plants can have a wide range of values over time. Food that has a very low stoichiometric ratio to the consumer's ratio is not as much benefit to the consumer. The result model is described in equations (2.0.3).

The paradox of enrichment is a phenomenon in which the population of consumer declines when the population of producers increases. This observed result is in contrast to the prediction from the Rosenzweig-MacArthur model. Although the number of producers in-

creases, the stoichiometric ratio of producers drops below what the consumer needs. As a result, the consumer can not get enough nutrients from the food (producers), causing the consumer's population to decline.

$$\begin{cases} \frac{dP}{dt} &= \alpha P(1 - \frac{P}{\min(K, (N_T - \theta C)/q)}) - f(P)C \\ \frac{dC}{dt} &= \widehat{e}\ \min(1, \frac{(N_T - \theta C)/P}{\theta}) f(P)C - dC \end{cases} \tag{2.0.3}$$

α is the natural growth rate of producers in the absence of predation.
K is the carrying capacity of producers.
$f(P)$ is a Holling Type II function to describe consumers' saturation on food.
d is the natural death rate of consumers.
$\widehat{e}$ is the maximal production efficiency.
θ is a fixed stoichiometric ratio of consumers.
q is the minimum stoichiometric ratio of producers.
N_T is total amount of nutrient in the model.

From the Lotka-Voltera model to the LKE stoichiometric model, the parameters of the population carrying capacity, the saturation on food, and the nutrient cycling are introduced into the models. Naturally, another concern may be the number of different types of producers and consumers. For example, a variety of grazing species in a corn field would require a model of one producer and multiple consumers. Yet an ecosystem of a garden of various flowers might be a model of multiple producers (flowers and green plants) and one consumer (a certain type of insect). In the paper "Herbivores, the Functional Diversity of Plants, and Cycling of Nutrients in Ecosystems" by Pastor and Cohen [5], a model of one consumer, two producers, and a single nutrient was addressed. The focus of the model was to determine the criteria of coexistence in terms of plants' growth rates in open and closed environments. An open environment means there are nutrient inputs from and exports to the surrounding environments for some components, and a closed environment corresponds to those being a fixed total amount of nutrient cycling through the components in the model. There are still many interesting questions associated with a model of two producers. (i) Are there any coexistence limit cycles? (ii) How does the consumer's food preference affect the populations of both producers? (ii) Are the resource competitions and the variations among the producers related to criteria of coexistence? (iv) What are the transitions when a system moves from one producer to two producers? This paper includes a further study of the model of two producers, focusing on the questions above.

3 Model Construction

This model contains two populations of producers and a single population of consumers. We assume that the consumers will feed on both producers and convert them into its biomass. Since this is a stoichiometric model, both quality and quantity of producers and consumers are measured. A common way to monitor a population density is to measure the total biomass of that population. Approximately 50% of the dry mass is carbon. Therefore, we can measure the flows of carbon to determine the biomass transfers among the populations. The word "flow" is used because carbon does not stay in the system forever. In fact, carbon comes into the model through photosynthesis and leaves when living beings die and decompose.

The quality of a food to the consumer is a relative term. We think of it as the ratio of the amount of nutrient to the amount of carbon. Modelers have traditionally used carbon in the system as a measurement of population densities. So now we need to keep track of the amount of nutrient, such as nitrogen, in each population in the model. Unlike carbon which flows through the model, nutrients cycle within the model. Initially, there is a certain amount of nutrient in the soil. Plants take up the nutrient from soil and grow. Consumers gain nutrients by feeding on plants. When plants and consumers die, their bodies will be decomposed and the nutrient contained in the bodies will return to the soil. Therefore, there is a component of mineralized nutrients in the nutrient cycle to represent the amount of nutrient in the soil. The graph (3.0.1) shows the flows of two elements in the model.

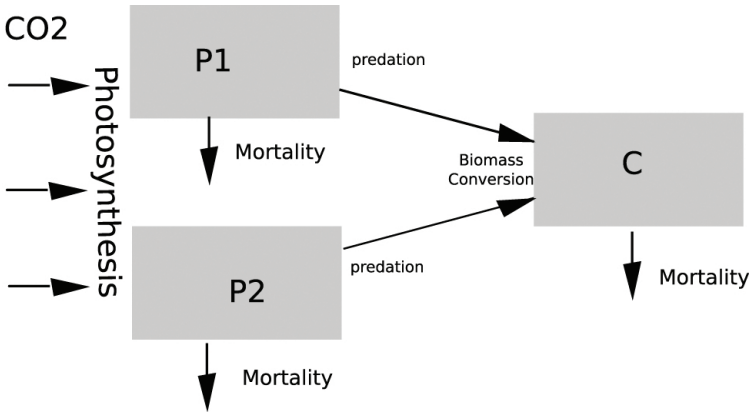

(a) Flow of Carbon

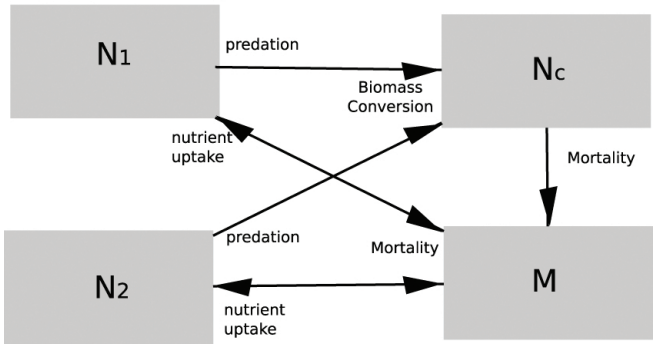

(b) Cycle of Nutrient

Figure 3.0.1: Graphs of Carbon and Nutrient

Regarding the flow of carbon, P_1, P_2 and C are the amounts of carbon in the populations of producer one, producer two, and consumer. For the cycle of nutrient, N_1, N_2 and N_c are the amounts of nutrient in the populations of producer one, producer two, and consumer. M is the amount of mineralized nutrient.

3.1 General assumptions

There is no carbon sediment class in the model. We assume that the rates of litter decomposition and nutrient mineralization are independent of sediment nutrient concentration. Thus, mortality is considered as an exit of carbon flow in the system. (See 3.0.1(a))

This is a closed nutrient model. The amount of nutrient in the system is fixed. There are no external nutrient input and output in any components. In other words, all nutrients are cycling within the model. Let N_T be the total sum of all nutrient in system. Then, by this assumption, the amount of mineralized nutrient, $M = N_T - N_c - N_1 - N_2$.

3.2 Assumptions on Producers

The two producers are assumed to be competing with each other. Like the other models, the parameter that we are going to change for the producers is the growth rate. We assume that two producers are very similar, but differ by their growth rates, respectively b_1 and b_2. By making this assumption, we can see how sensitive the system and the long-term solutions are to small variations in growth rates of the two producers. Note that the two producers are not identical even if their growth rates are the same ($b_1 = b_2$). This is because the interference coefficients λ_{12} and λ_{21} differ from the self-limitation coefficients λ_{11} and λ_{22}.

The equations and the equilibrium solutions in this paper are for the general parameter settings. In the future, one could study the bifurcations of the same system by varying some sets of parameters other than the growth rates, such as transpiration rates and interference coefficients.

Regarding the flow of carbon, both producers absorb carbon dioxide from the air and generate carbohydrates through photosynthesis. We assume that the biomass (carbon) growth for each producer alone is logistic in form: b_1/λ_{11} and b_2/λ_{22} are the carrying capacities for producer P_1 and P_2 without the competitions. The interference terms $\lambda_{12}P_2$ and $\lambda_{21}P_1$ represent the competitions between the two producers in P_1 growth rate and P_2 growth rate, respectively. The growth terms in $\frac{dP_1}{dt}$ and $\frac{dP_2}{dt}$ are $P_1 g_1(P_1, P_2)$ and $P_2 g_2(P_1, P_2)$, where $g_1(P_1, P_2) = (b_1 - \lambda_{11}P_1 - \lambda_{12}P_2)^+$ and $g_2(P_1, P_2) = (b_2 - \lambda_{21}P_1 - \lambda_{22}P_2)^+$. The

$(x)^+$ function is defined as $\max(0, x)$ to prevent the growth terms from being negative. Carbon leaves the system when producers die. Let d_{P_1} and d_{P_2} be the death rates of producer one and producer two. The amounts of carbon loss are $P_i d_{P_i}, i = 1, 2$. When producers are consumed by consumers, the producer biomasses decrease. Since the consumption rate by consumers depends on the total amount of food available, we calculate the total amount of food, which is the total sum of producers, $P_1 + P_2$ as the consuming function input P. Let $f(P) = \frac{\alpha P}{h+P}$ be the Rosenzweig - MacArthur's rate of producers being consumed by consumers (Holling Type II). The total amount of consumed biomass is $f(P_1 + P_2)C = \frac{\alpha(P_1+P_2)C}{h+P_1+P_2}$.

Regarding the nutrient cycle, we assume that the producer absorbs the mineralized nutrients from the soil via transpiration. The nutrient uptake of producers is assumed to be proportional to the mineralized nutrient M and the growth $P_i g_i(P_1, P_2)$ of the producer. Denoting the transpiration efficiency by $T(P_i)$. we model the amount of nutrient absorbed by one producer as $MT(P_i)$. The total amount of nutrient absorbed by a population of producers is $MT(P_i)P_i g_i(P_1, P_2)$. To simplify the calculation, we let $T(P_i)$ be some constant β_i. Once a producer dies, its body will decompose and its nutrients will return to the nutrient pool underground. Thus, the amounts of producer-held nutrient loss due to mortality are $d_{P_i} N_i, i = 1, 2$. A major assumption we will make is that the first two phases of decomposition, leaching and immobilization, take no time. In reality, immobilization is not a simple process that can be done in a short period of time. However, to keep this model simple enough to analyze, we make this assumption. When producers are consumed, a certain amount of nutrient is transferred from producers to consumers. The amounts of producer-bound nutrient loss due to the predation are $f(P_1 + P_2)C\frac{N_i}{P_i}, i = 1, 2$.

3.3 Assumptions on Consumer

Animals typical have a small deviation of their stoichiometric ratio, while plants can tolerate a very large range of stoichiometric ratios. Therefore, the stoichiometric ratio of consumers is assumed to be a constant. Let q be the consumer stoichiometric ratio. Then the amount of nutrient in consumers N_c can be rewritten as Cq, where C is the amount of carbon in consumers. Furthermore, the change of consumer nutrient over time is the change of consumer carbon times the stoichiometric ratio. That is, $\frac{dN_c}{dt} = \frac{dC}{dt}q$. With this relationship, we can solve for C from the system of equations first and then calculate $N_c = Cq$.

A consumer can convert only a portion of carbon from the food they eat. Assume that the portion of converted carbon is proportional to the total amount of carbon contained in food. Let γ be the optimal biomass conversion efficiency. Then the maximum amount of carbon consumers gain from food is $\gamma f(P_1 + P_2)C$. The actual amount of absorbed carbon

is based on the quality of food. A high quality food means the stoichiometric ratio of the food is "close" to the stoichiometric ratio of the consumer's body. With high quality food, consumers can convert food into carbon at the most efficient rate. Therefore, the amount of gained carbon is $\gamma f(P_1 + P_2)C$. However, a consumer cannot maintain the carbon conversion process at the most efficient rate when the food quality is poor. Consequently, the consumer will convert less carbon from the low nutrient food. We approximate that lower rate by Q/q, where Q is the stoichiometric ratio of the food source. Since we have two food sources, Q is $\frac{P_1Q_1+P_2Q_2}{P_1+P_2}$ and the biomass conversion rate is $\min(\gamma, \frac{1}{q}\frac{Q_1P_1+Q_2P_2}{P_1+P_2})f(P_1+P_2)C$, where Q_1 and Q_2 are the stoichiometric ratios of producer P_1 and P_2. (See Appendix I)

In the nutrient cycle, a consumer can absorb nutrients only from the producers. Once the consumer dies, its nutrient content will be returned to the nutrient pool M.

We assume that the food preference of consumers is based the amount that is available. In other words, a consumer will prefer the producer that can be found easily, meaning the producer that has higher population density. Let $a = \frac{P_1}{P_1+P_2}$ be the probability of consumers feeding on producer P_1. Then the probability of consumers feeding on producer P_2 is $(1 - a)$ since there are only two producers in the model.

3.4 The mathematical equations for this model

$$\begin{cases} \frac{dP_1}{dt} &= g_1(P_1, P_2)P_1 - d_{p_1}P_1 - af(P_1 + P_2)C \\ \frac{dP_2}{dt} &= g_2(P_1, P_2)P_2 - d_{p_2}P_2 - (1-a)f(P_1 + P_2)C \\ \frac{dC}{dt} &= \min(\gamma, \frac{1}{q}\frac{Q_1P_1+Q_2P_2}{P_1+P_2})f(P_1 + P_2)C - d_cC \\ \frac{dN_1}{dt} &= MT(P_1)g_1(P_1, P_2)P_1 - af(P_1 + P_2)C\frac{N_1}{P_1} - d_{p_1}N_1 \\ \frac{dN_2}{dt} &= MT(P_2)g_2(P_1, P_2)P_2 - (1-a)f(P_1 + P_2)C\frac{N_2}{P_2} - d_{p_2}N_2 \end{cases} \tag{3.4.1}$$

$$\text{where} \begin{cases} a = \frac{P_1}{P_1+P_2} \\ g_1(P_1,P_2) = (b_1 - \lambda_{11}P_1 - \lambda_{12}P_2)^+ \\ g_2(P_1,P_2) = (b_2 - \lambda_{21}P_1 - \lambda_{22}P_2)^+ \\ f(P_1+P_2) = \frac{\alpha(P_1+P_2)}{h+(P_1+P_2)} \\ T(P_i) = \beta_i, i = 1,2 \\ M = N_T - N_c - N_1 - N_2 \end{cases}$$

$g_1(P_1, P_2)$ and $g_2(P_1, P_2)$ are the logistic growth functions with interference terms.
$T(P_i)$ are the transpiration coefficients.
Function f is the amount of consumed producer by a single consumer.
a is the probability that producer P_1 is consumed.

To reduce the complexity of formulas (3.4.1), we use $Q_i = \frac{N_i}{P_i}, i = 1, 2$ to replace N_1 and N_2. Q_i is the stoichiometric ratio for producer P_i, where $P_i > 0$.

$$\frac{dQ_i}{dt} = \frac{dN_i}{dt}\frac{1}{P_i} - \frac{N_i}{P_i^2}\frac{dP_i}{dt} \tag{3.4.2}$$

Substituting $\frac{dN_i}{dt}$ and $\frac{dP_i}{dt}$ into (3.4.2), we get the differential equations for $\frac{dQ_1}{dt}$ and $\frac{dQ_2}{dt}$. Now the system equations are shown in (3.4.3).

$$\begin{cases} \frac{dP_1}{dt} = ((b_1 - \lambda_{11}P_1 - \lambda_{22}P_2)^+ - d_{p_1} - \frac{\alpha C}{h+(P_1+P_2)})P_1 \\ \frac{dP_2}{dt} = ((b_2 - \lambda_{21}P_1 - \lambda_{22}P_2)^+ - d_{p_2} - \frac{\alpha C}{h+(P_1+P_2)})P_2 \\ \frac{dC}{dt} = (\min(\gamma, \frac{1}{q}\frac{P_1Q_1+P_2Q_2}{P_1+P_2})\frac{\alpha(P_1+P_2)}{h+(P_1+P_2)} - d_c)C \\ \frac{dQ_1}{dt} = ((N_T - qC - Q_1P_1 - Q_2P_2)\beta_1 - Q_1)(b_1 - \lambda_{11}P_1 - \lambda_{22}P_2)^+ \\ \frac{dQ_2}{dt} = ((N_T - qC - Q_1P_1 - Q_2P_2)\beta_2 - Q_2)(b_2 - \lambda_{21}P_1 - \lambda_{22}P_2)^+ \end{cases} \tag{3.4.3}$$

4 One-Producer-One-Consumer Model

In order to understand the model (3.4.3), we first consider the special case where there is a single producer in the system. We set $P_2 = 0$ and reduce the model into a one-producer-one-consumer model (see equations 4.0.1). As we shall see, it is sufficient to drop the reference to the positive part function. The single-producer-single-consumer system now leads equations (4.0.1).

$$\begin{cases} \frac{dP_1}{dt} &= (b_1 - \lambda_{11}P_1 - d_{P_1} - \frac{\alpha C}{h+P_1})P_1 \\ \frac{dC}{dt} &= (\min(\gamma, \frac{Q_1}{q})\frac{\alpha P_1}{h+P_1} - d_c)C \\ \frac{dQ_1}{dt} &= ((N_T - qC - Q_1P_1)\beta_1 - Q_1)(b_1 - \lambda_{11}P_1) \end{cases} \tag{4.0.1}$$

For the purpose of numerical simulation and stability analysis, the parameter values for the model are listed below.
Logistic equation constant $\lambda_{11} = 0.5$,
Producer death rates $d_{P_1} = d_{P_2} = 0.05$,
Consumer death rate $d_c = 0.17$,
Consumer Stoichiometric ratio $q = 0.05$,
The efficient conversation rate $\gamma = 0.1$,
The maximal and half-saturation efficients in the predation function are $\alpha = 2.75$ and $h = 0.75$,
Transpiration constant $\beta_1 = 0.3$ (even if $P_1 = 0$).

4.1 Invariant Regions

Based on the model's biological origins, we hold some basic expectations about the variables and equations.

1) P_1, C, and Q_1 should be non-negative at any time t.

2) The growth function $(b_1 - \lambda_{11}P_1)$ and the amount of mineralized nutrient $(N_T - qC - Q_1P_1)$ cannot be negative.

Proposition 4.1.1. *Assume λ_{11} , d_{P_1}, d_c, q, γ, α, h, and β_1 are > 0. If $(b_1 - \lambda_{11}P_1)$ and $(N - qC - Q_1P_1)$ are initially non-negative, then $(b_1 - \lambda_{11}P_1)$ and $(N_T - qC - Q_1P_1)$*

should be always non-negative at any time t along the solution, assuming P_1, C, and Q_1 are positive.

Proof. Assume that the growth function is equal to zero at some time t'. ${P_1}' = P_1(t')$, $C' = C(t')$, and ${Q_1}' = Q_1(t')$.

Consider the derivative of the growth function $(b_1 - \lambda_{11}P_1) = 0$ at $t = t'$

$$\begin{aligned}
\tfrac{d}{dt}(b_1 - \lambda_{11}P_1)|_{t=t'} = -\lambda_{11}\tfrac{dP_1}{dt}|_{t=t'} &= -\lambda_{11}(b_1 - \lambda_{11}{P_1}' - d_{P_1} - \tfrac{\alpha C'}{h+{P_1}'}){P_1}' \\
&= -\lambda_{11}(-d_{P_1} - \tfrac{\alpha C'}{h+{P_1}'}){P_1}' \\
&= \lambda_{11}{P_1}'(d_{P_1} + \tfrac{\alpha C'}{h+{P_1}'}) \geq 0
\end{aligned}$$

This means the growth function cannot become negative if a solution starts with a non-negative growth rate.

Assume that $(N_T - qC - Q_1P_1)$ is equal to zero at some time t'.

Consider the derivative of $(N_T - qC - Q_1P_1)$ at $t = t'$

$$\begin{aligned}
\tfrac{d}{dt}(N_T - qC - Q_1P_1)|_{t=t'} &= -q\tfrac{dC}{dt}|_{t=t'} - Q_1\tfrac{dP_1}{dt}|_{t=t'} - P_1\tfrac{dQ_1}{dt}|_{t=t'} \\
&= -q(\min(\gamma, \tfrac{{Q_1}'}{q})\tfrac{\alpha {P_1}'}{h+({P_1}')} - d_c)C' \\
&\quad -{Q_1}'(b_1 - \lambda_{11}{P_1}' - d_{P_1} - \tfrac{\alpha C'}{h+{P_1}'}){P_1}' \\
&\quad -{P_1}'((N_T - qC' - {Q_1}'{P_1}')\beta_1 - {Q_1}')(b_1 - \lambda_{11}{P_1}') \\
&= -q\min(\gamma, \tfrac{{Q_1}'}{q})\tfrac{\alpha {P_1}'C'}{h+{P_1}'} + qC'd_c \\
&\quad -{Q_1}'{P_1}'(b_1 - \lambda_{11}{P_1}' - d_{P_1} - \tfrac{\alpha C'}{h+{P_1}'}) \\
&\quad +{Q_1}'{P_1}'(b_1 - \lambda_{11}{P_1}') \\
&= qC'd_c + {Q_1}'{P_1}'d_{P_1} + q\tfrac{\alpha {P_1}'C'}{h+{P_1}'}(\tfrac{{Q_1}'}{q} - \min(\gamma, \tfrac{{Q_1}'}{q}))
\end{aligned}$$

If $\gamma \leq \frac{{Q_1}'}{q}$, then $qC'd_c + {Q_1}'{P_1}'d_{P_1} + q\frac{\alpha {P_1}'C'}{h+{P_1}'}(\frac{{Q_1}'}{q} - \gamma) \geq 0$.

If $\gamma > \frac{Q_1{}'}{q}$, then $qC'd_c + Q_1{}'P_1{}'d_{P_1} + q\frac{\alpha P_1{}'C'}{h+P_1{}'}(\frac{Q_1{}'}{q} - \frac{Q_1{}'}{q}) \geq 0$.

This implies that that $(N_T - qC - Q_1P_1)$ cannot become negative if a solution starts with a non-negative value of $(N_T - qC - Q_1P_1)$.

□

Proposition 4.1.2. *An invariant region of model (4.0.1) is* $0 \leq P_1 \leq \frac{b_1}{\lambda_{11}}$, $0 \leq C \leq \frac{N}{q}$, $0 \leq Q_1 \leq N_T\beta$, *and* $(N_T - qC - Q_1P_1) \geq 0$. *If a solution initially starts in the interior of the invariant region or on the boundary of the invariant region, the solution will stay in this region.*

Proof. If the solution initially starts on the boundary but does not cross the boundary, then all solutions start initially in this invariant region should stay in this region at any future time t. There are seven "sides" to the region boundary.

a) and b) For solutions on the side planes $P_1 = 0$ or $C = 0$, the solutions cannot cross the side planes since $\frac{dP_1}{dt} = 0$ and $\frac{dC}{dt} = 0$, respectively.

c) For solutions on the side plane $Q_1 = 0$,

$$\frac{dQ_1}{dt} = (N_T - qC)\beta_1(b_1 - \lambda_{11}P_1) \geq 0$$

Let $\frac{dQ_1}{dt} \geq 0$ since $C \leq \frac{N_T}{q}$ and $P_1 \leq \frac{b_1 - d_{P_1}}{\lambda_{11}}$. This implies that solutions cannot exit the invariant region through $Q_1 = 0$.

d) For solutions on the side plane $P_1 = \frac{b_1}{\lambda_{11}}$,

$$\frac{dP_1}{dt} = (0 - d_{P_1} - \frac{\alpha C}{h + \frac{b_1}{\lambda_{11}}})\frac{b_1}{\lambda_{11}} < 0$$

That implies solutions cannot exit the invariant region through $P_1 = \frac{b_1}{\lambda_{11}}$.

e) For solutions on the surface of $(N_T - qC - Q_1P_1) = 0$, by Proposition (4.0.1), it has been shown that $(N_T - qC - Q_1P_1)$ increases. Thus, the solution cannot exit the invariant region through the surface.

f) For solutions on the boundary $C = \frac{N_T}{q}$, either $Q_1 = 0$ or $P_1 = 0$ (since $(N_T - qC - Q_1P_1)$ is equal to zero).

If $P_1 = 0$, $\frac{dC}{dt} = (0 - d_c)\frac{N_T}{q}$. C is decreasing since $\frac{dC}{dt} < 0$.

If $Q_1 = 0$, $\frac{dC}{dt} = (-d_c)\frac{N_T}{q}$. C is decreasing since $\frac{dC}{dt} < 0$.

g) For solutions on the boundary $Q_1 = N_T\beta$ and $P_1 \leq \frac{b_1}{\lambda_{11}}$,

$$\frac{dQ_1}{dt} = ((N_T - qC - Q_1P_1)\beta_1 - N_T\beta)(b_1 - \lambda_{11}P_1) \leq 0$$

Solutions cannot exit the invariant region through the plane $Q_1 = N_T\beta$.

The highlighted region in the graph (4.1.1) illustrates the invariant region in space P_1CQ_1. □

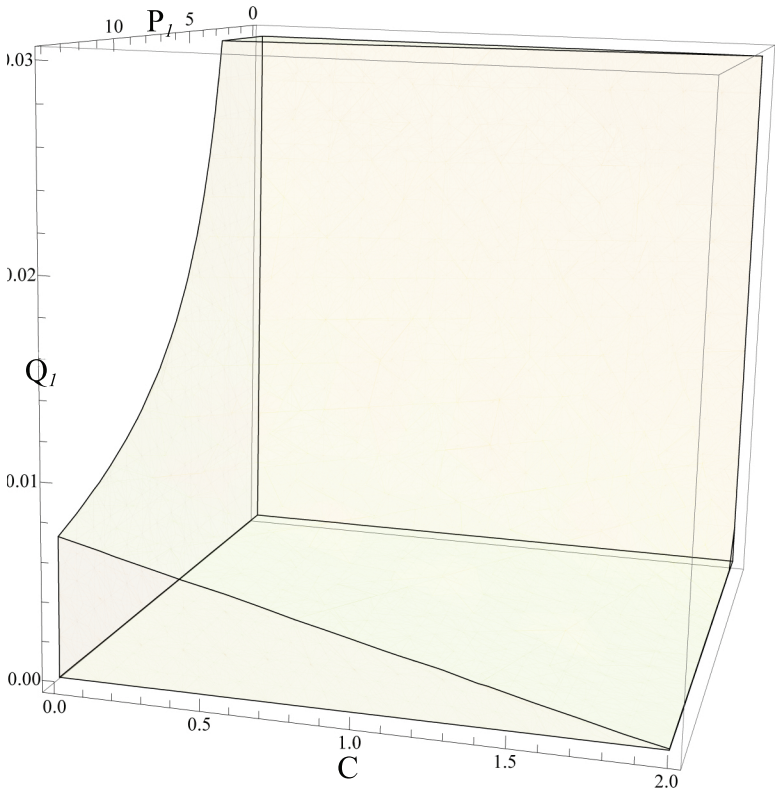

Figure 4.1.1: **An Invariant Region for Model (4.0.1)**

4.2 Equilibria In One-Producer-One-Consumer Model

Assume that the amount of nutrient is abundant in the system. Consumer then converts food into biomass at the optimal rate γ. Under this assumption, γ will always satisfy the biomass converison efficiency min function on the right hand side of $\frac{dC}{dt}$. We call this case H. On the other hand, consumer converts food into biomass at the lower rate $\frac{Q_1}{q} < \gamma$ depending on the stoichiometric ratio of producers. We call this system case L.

Equilibria In Case H

The producer's stoichiometric ratio does not affect the growth of consumer or producer. This is similar to the Rosenzweig - MacArthur model, in which stoichiometry is not present. The primary parameter is the growth rate of producer b_1. As the growth rate b_1 increases, the solution of (P_1, C) changes from approaching an equilibrium point to approaching a limit cycle. The equations for case H are the following.

$$\begin{cases} \frac{dP_1}{dt} &= (b_1 - \lambda_{11}P_1 - d_{p_1} - \frac{\alpha C}{h+(P_1)})P_1 \\ \frac{dC}{dt} &= (\gamma\frac{\alpha P_1}{h+P_1} - d_c)C \\ \frac{dQ_1}{dt} &= ((N_T - qC - Q_1P_1)\beta_1 - Q_1)(b_1 - \lambda_{11}P_1) \end{cases} \tag{4.2.2}$$

The equilibrium solutions are the following (in terms of (P_1, C, Q_1)):
The origin $(\mathrm{O})_H$: $(0, 0, N_T\beta_1)$, where producer and consumer do not exist, but the producer stoichiometric ratio is not necessary to be zero.

The monoculture equilibrium $(\mathrm{P1})_H$: $(\frac{b_1-d_{p1}}{\lambda_{11}}, 0, \frac{N_T\lambda_{11}\beta_1}{\lambda_{11}+(b_1-d_{p_1})\beta_1})$. In the absence of consumers, the population of producers follows the logistic growth and reaches its carrying capacity $\frac{b_1-d_{p1}}{\lambda_{11}}$ over time.

The coexistence equilibrium $(\mathrm{P1C})_H$: $(\frac{d_ch}{\alpha\gamma-d_c}, \frac{h\gamma(b_1-d_{p_1})}{\alpha\gamma-d_c} - \frac{\gamma d_c\lambda_{11}h^2}{(\alpha\gamma-d_c)^2}, \frac{\beta(N_T(\alpha\gamma-d_c)-hq\gamma(b_1-d_{p_1})+\frac{k\gamma q d_c h^2}{\alpha\gamma-d_c})}{\alpha\gamma-d_c(h\beta_1-1)})$.
Note that, due to the consumption by consumers, the population of producers remains constant over time, regardless to the growth rate b_1.

The eigenvalue diagrams for the equilibria in case H and associated phase portraits are given in Appendix II. A bifurcation diagram for case H is shown in figure (4.2.2).

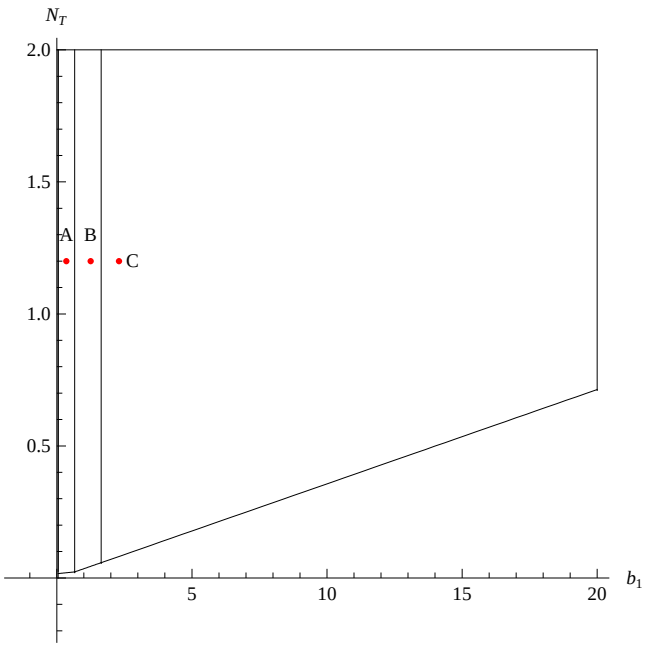

Figure 4.2.2: **A Bifurcation Diagram for Model (4.2.2) In Case H**
On the left boundary of region A, there is a transcritical bifurcation separating the region of "no life" (not labelled) from the region of producer monoculture (A). From region A to B, there is a second transcritical bifurcation. Region B, the consumer enters the system. From region B to C, there is Hopf bifurcation and populations of producer and consumer begin to have regular oscillations. On the lower right corner of the graph, $(\text{P1C})_H$ does not satisfy the biomass conversion efficiency condition. Thus, it is not relevant to the bifurcation diagram in case H.

Equilibria In Case L

Here we assume that the system is nutrient poor, so $\frac{Q_1}{q}$ satisfies the biomass conversion efficiency min function in $\frac{dC}{dt}$. The equilibrium solutions $(\mathrm{O})_L$ and $(\mathrm{P1})_L$ are the same as the ones in case H. The solution $(\mathrm{P1C})_L$, however, is different. Since the stoichiometry of producers is no longer independent of the populations of consumers and producers, both b_1 and N_T are taken as the primary parameters for this model.

$$\begin{cases} \frac{dP_1}{dt} &= (b_1 - \lambda_{11}P_1 - d_{p_1} - \frac{\alpha C}{h+(P_1)})P_1 \\ \frac{dC}{dt} &= (\frac{Q_1}{q}\frac{\alpha P_1}{h+P_1} - d_c)C \\ \frac{dQ_1}{dt} &= ((N_T - qC - Q_1P_1)\beta_1 - Q_1)(b_1 - \lambda_{11}P_1) \end{cases} \tag{4.2.3}$$

The origin $(\mathrm{O})_L$ is at $(0, 0, N_T\beta_1)$ and the monoculture equilibrium $(\mathrm{P1})_L$ is at

$(\frac{b_1-d_{p_1}}{\lambda_{11}}, 0, \frac{N_T\lambda_{11}\beta_1}{\lambda_{11}+(b_1-d_{p_1})\beta_1})$. The coexistence equilibrium (P1C) are the roots of a cubic equation (4.2.4). (See Appendix III)

$$F(P_1) = (P_1)^3c3 + (P_1)^2c2 + (P_1)c1 + c0 = 0, \tag{4.2.4}$$

where

$c3 = -\lambda_{11}$
$c2 = b_1 - d_{p_1} + d_c - h\lambda_{11}$
$c1 = (b_1 - d_{p_1} + d_c)h - \frac{N_T\alpha}{q} + \frac{d_c}{\beta_1}$
$c0 = \frac{hd_c}{\beta_1}$

The y-intercept of F is $\frac{hd_c}{\beta} > 0$ and the slope at that intercept is $c1$. The two local extremes P_+ and P_- are at $P_1 = \frac{c2}{3\lambda_{11}} + \sqrt{(\frac{c2}{3\lambda_{11}})^2 + \frac{c1}{3\lambda_{11}}}$ and $P_1 = \frac{c2}{3\lambda_{11}} - \sqrt{(\frac{c2}{3\lambda_{11}})^2 + \frac{c1}{3\lambda_{11}}}$. Generally speaking, as b_1 increases, the solution values of P_1 also increases. When $F(P_+) = 0$, F begins to have three real solutions. However, two of the real root solutions collapse and vanish when $F(P_-) = 0$. The number of solutions indicates that the coexistence equilibrium (P1C) has saddle node bifurcations at $F(P_+) = 0$ and $F(P_-) = 0$. One creates two additional $(\mathrm{P1C})_L$s, born at $F(P_+) = 0$, and the other one causes two to disappear at $F(P_-) = 0$. This can be illustrated by the graph (4.2.3).

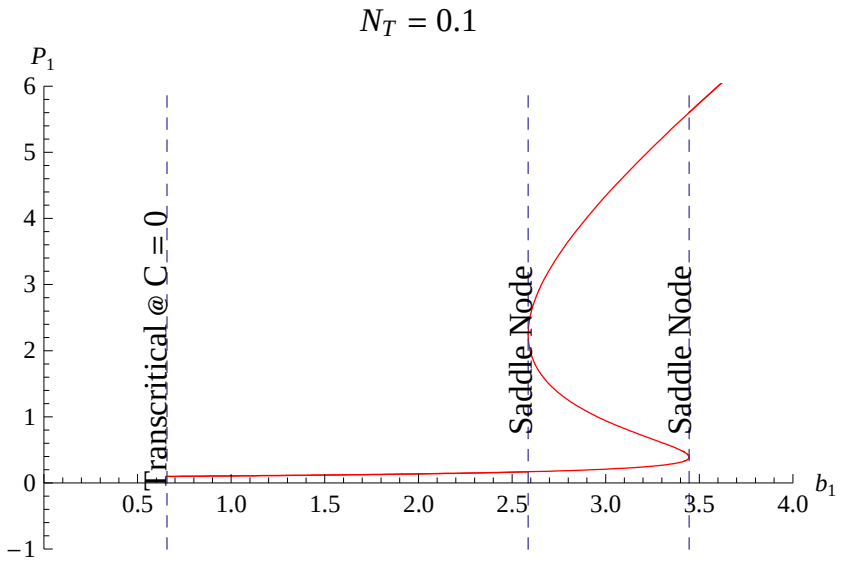

Figure 4.2.3: **Solutions of P_1 For The Coexistence Equilibrium In Case L**
Fixing $N_T = 0.1$, the red curve represents the solutions of P_1 from the cubic equation (4.2.4) as b_1 increase from 0 to 4.

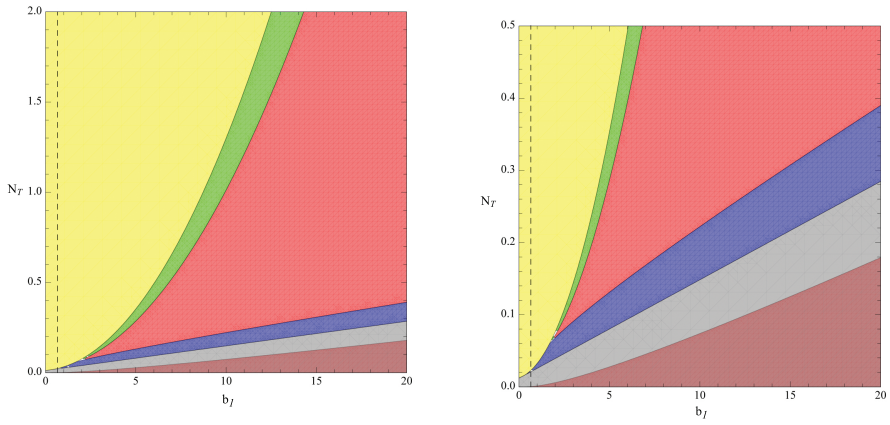

(a) Zoom Out

(b) Zoom In

Figure 4.2.4: **Number of Real Roots of Equation (4.2.4) in the parameter space** $b_1 : [0, 20] \times N_T : [0, 2]$ (The color scheme is described in table (4.2.1).)

When the slope of the graph of F at the y-intercept is negative, and $F(P_+) < 0$ and $F(P_-) < 0$, there is only one root. When $F(P_+) > 0$ and $F(P_-) < 0$, there are three roots. As b_1 increases, $F(P_-)$ passes zero and cubic equation starts to have one root again. When b_1 is large enough ($b_1 > \frac{N_T\alpha}{qh} - \frac{d_c}{\beta_1 h} + d_{P_1} - d_c$), the slope becomes positive but P_- becomes less than zero. Thus, there is only one positive root for equation (4.2.4). Note that the real roots of the cubic equation F are the solution of P_1 at the coexistence equilibrium. When root solution P_1 is positive, the corresponding C solution is not necessary to be positive. With the parameter settings in equations (4.0.1), the positive coexistence equilibrium does not exist in the brown region in figure (4.2.4).

The graph (4.2.4) shows the number of real roots in the parameter space $b_1 : [0, 20] \times N_T : [0, 2]$.

Color	Slope at the y-intersection	Number of real roots	Note
Yellow	(-)	1	P_+ and P_- are complex
Green	(-)	1	$f(P_+) < 0$ and $f(P_-) < 0$
Red	(-)	3	$f(P_+) > 0$ and $f(P_-) < 0$
Blue	(-)	1	$f(P_+) > 0$ and $f(P_-) > 0$
Gray	(+)	1	$f(P_+) > 0$ and $P_- < 0$
Brown	(+)	3	one positive root and 2 negative roots

Table 4.2.1: A Table Of Color Scheme For Figure (4.2.4)

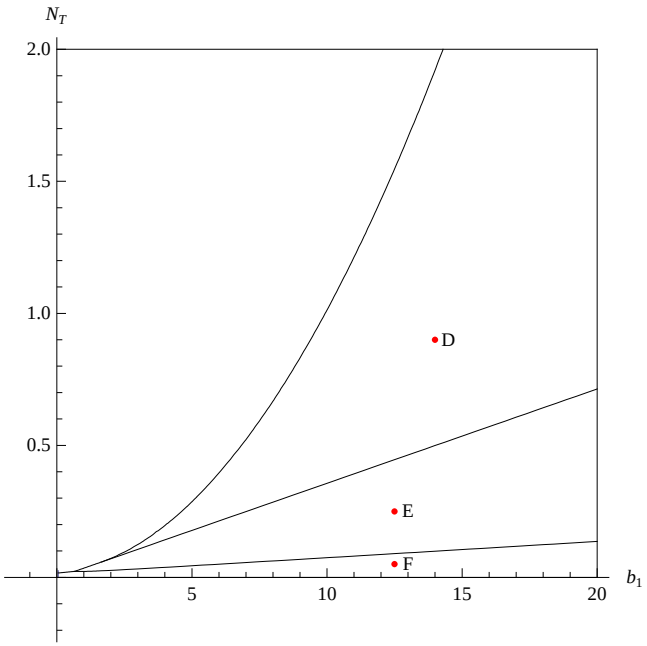

Figure 4.2.5: **A Bifurcation Diagram of Model (4.2.3)**
In case L region D is a saddle and a node region. There are two $(\text{P1C})_L$ solutions. One is a node and other one is a saddle. In region E, the saddle branch of $(\text{P1C})_L$ does not satisfy the condition $\frac{Q_1}{q}$. Thus, there is only one $(\text{P1C})_L$ (a node) left. In region F, the consumer dies out due to the low food quality. Comparing to the bifurcation diagram in case H, the transcritical bifurcation of $(\text{P1})_L$ and $(\text{P1C})_L$ now depends on both b_1 and N_T.

The border line between the green and the red is the location where a saddle node bifurcation occurs. It creates two $(\text{P1C})_L$ equilibria. On the border line between the red and the blue, however, another saddle node bifurcation occurs and changes the system to have one $(\text{P1C})_L$ solution again. Although there are possibly three equilibrium solution $(\text{P1C})_L$ in case L, not all of them satisfy the requirement $\frac{Q_1}{q} < \gamma$. The details of selecting valid coexistence equilibria is shown in the next section figure (4.3.6)).

The eigenvalue plot of each equilibrium solution is showed in Appendix IV. A bifurcation diagram for case L is shown in figure (4.2.5).

4.3 The Full Model of One Producer And One Consumer

The full model of one producer and one consumer (4.0.1) contains the equilibrium solutions in case H and case L. At a fixed $N_T > 0.06$, as the producer's growth rate b_1 increases, the min function of biomass conversion efficiency serves as a switch, changing the equilibrium (P1C) from case H to case L. (P1C) in the full model is the same as $(\text{P1C})_H$ in case H when b_1 satisfies $F(P_+) < 0$ or P_+ is complex. At $F(P_+) = 0$, a saddle node bifurcation occurs and creates two additional equilibrium $(\text{P1C})_L$ solutions. Since the stoichiometric ratios are low at those equilibrium points (satisfy $\frac{Q_1}{q} < \gamma$), the biomass conversation rate can switch to $\frac{Q_1}{q}$ from γ. At the same time, $(\text{P1C})_H$ still satisfies $\frac{Q_1}{q} \geq \gamma$. So there are three (P1C) equilibria. As b_1 increases further, $(\text{P1C})_H$ reaches its limit $\frac{Q_1}{q} = \gamma$ and intersects with one of the $(\text{P1C})_L$ solutions. After that $(\text{P1C})_H$ and one of the $(\text{P1C})_L$ solutions are no longer an equilibrium solution in the system. This is a (non-smooth) saddle node bifurcation caused by the min function. It can be illustrated by the figure (4.3.6). In graph (4.2.4), there is no red region when $N_T < 0.06$. In other words, a saddle node bifurcation does not occur at such a low nutrient level. However, there is still a switch of equilibrium (P1C) from case H to case L on the border line between the yellow and the other colors. For example, set $N_T = 0.05$ and calculate the biomass conversion efficiency at the equilibrium. (Shown in figure (4.3.7))

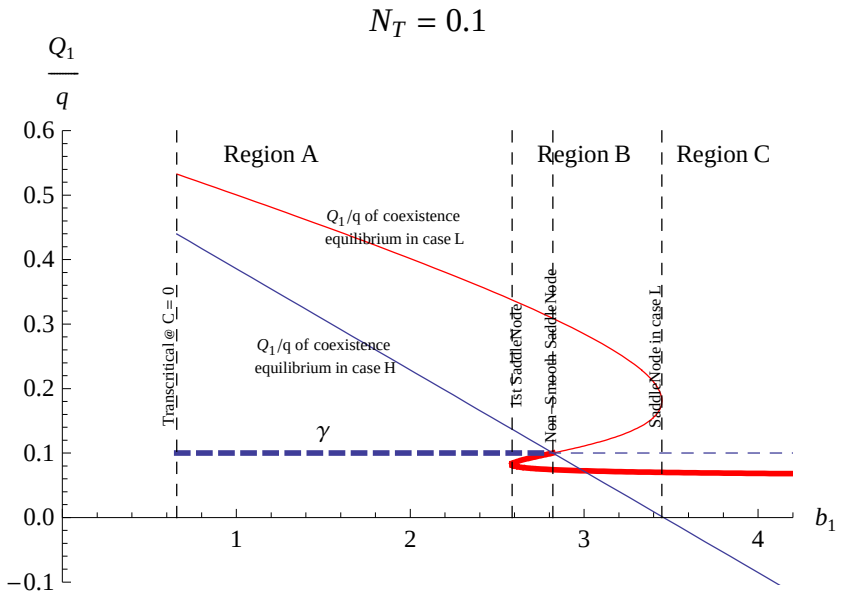

Figure 4.3.6: **A Plot of $\frac{Q_1}{q}$ At Coexistence Equilibrium Against b_1 for moderate N_T**

In region A, there is a single $(\text{P1C})_L$ solution in case L but its efficiency is above γ. Thus, there is no $(\text{P1C})_L$ equilibrium in region A. In region B, there are three $(\text{P1C})_L$ solutions. However, only two of them satisfy the condition $\frac{Q_1}{q} < \gamma$. In region C, case L has one $(\text{P1C})_L$ solution, and it satisfies the condition. It seems that the $(\text{P1C})_L$ equilibrium in case L are born by the saddle node bifurcation at $f(P_+) = 0$. In the full system of equations, the min function plays a role in choosing the biomass conversion efficiency. In region A, there is only one equilibrium (P1C) and it behaves as in case H. In region B, however, two additional equilibrium (P1C)s are born by the the saddle node bifurcation in case L. In the first half of the region B, the solution of $(\text{P1C})_H$ in case H is still able to provide enough nutrient to consumer until the solution $(\text{P1C})_H$ satisfies $\frac{Q_1}{q} = \gamma$. Thus, the full system has three (P1C) equilibria in the first half of region B. At $\frac{Q_1}{q} = \gamma$, a non-smooth saddle node bifurcation occurs and both $(\text{P1C})_H$ and one of the $(\text{P1C})_L$ disappears along the bifurcation.

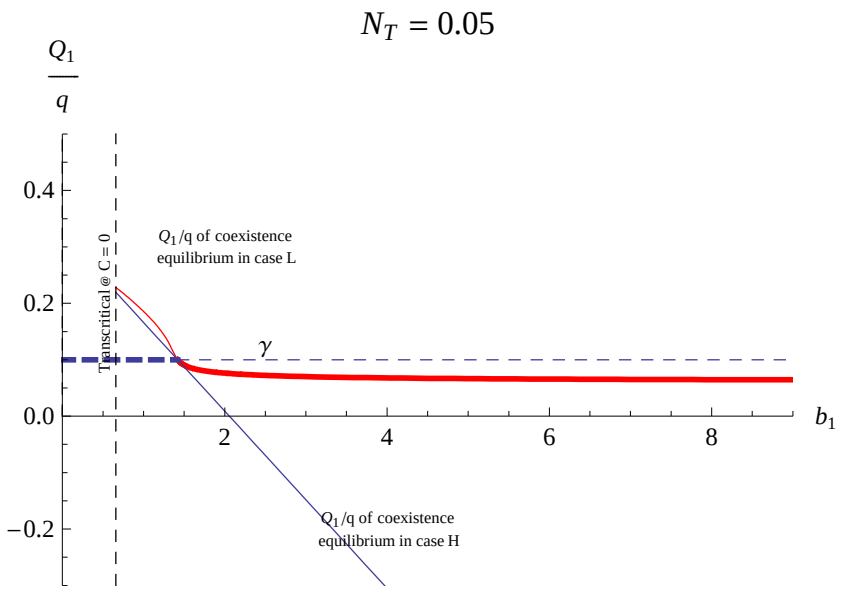

Figure 4.3.7: **A Plot of $\frac{Q_1}{q}$ At Coexistence Equilibrium Against b_1 for low N_T**

The bifurcation diagram of the full system is shown in figure (4.3.8), and the corresponding phase portraits are shown in figure (4.3.10), (4.3.11),(4.3.12),(4.3.13),(4.3.14), and (4.3.15). In each phase portrait, solutions of P_1, C, and Q_1 with initial values are plotted against the time. Solution orbits are also projected onto the P_1C plane, and the center of the equilibria labels are the locations of the equilibria. As a comparison, figure (4.3.9) shows a bifurcation diagram of a model without stoichiometry.

For any $N_T > 0$, there is a transcritical bifurcation at $b_1 = d_{P_1}$, left to region A. For $0 < b_1 < d_{P_1}$, both producers and consumers die out as described in appendix II. On the boundary of regions A and B, there is a second transcritical bifurcation allowing the consumer to enter and survive in the system. A Hopf bifurcation occurs on the boundary of regions B and C. Solutions now approach a limit cycle in region C. On the boundary of regions C and D, a saddle-node bifurcation occurs and a pair of equilibria are born. There are three coexistence equilibria in region D, one attracting and two saddles. Almost all solutions now approach the attracting equilibrium. On the boundary of regions D and E, a non-smooth saddle-node bifurcation occurs and the two saddle equilibria meet and vanish. There is a third transcritical bifurcation on the boundary of regions E and F. The consumer is unable to survive in region F.

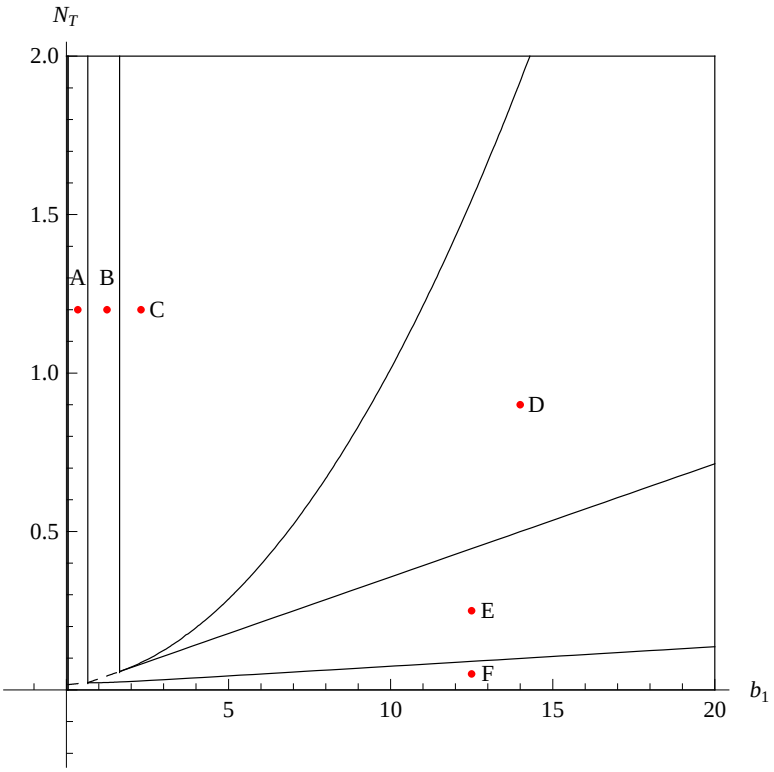

Figure 4.3.8: **A Bifurcation diagram of Model (4.0.1)**
The parameter space $b_1 \times N_T$ is divided into six regions. Regions A and F, and regions B and E are connected. The differences between A and F, and B and E are the biomass conversion rates. In regions A and B, the biomass conversion rate is γ, but it is $\frac{Q_1}{q}$ in regions E and F. The red dot in each region is chosen to show the standard phase portrait in the region.

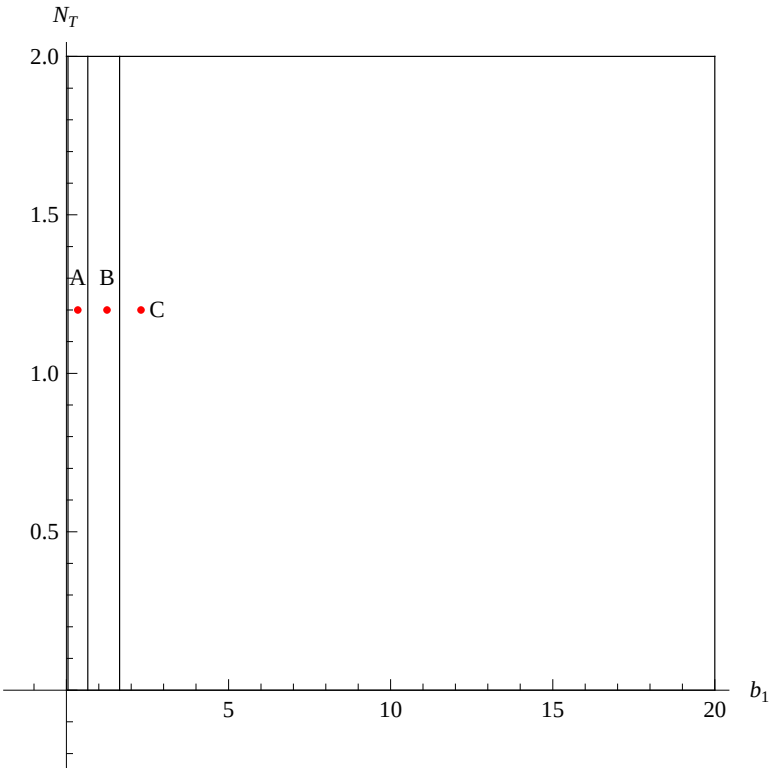

Figure 4.3.9: **A Bifurcation Diagram of One-Producer-And-One-Consumer Model Without Stoichiometry**

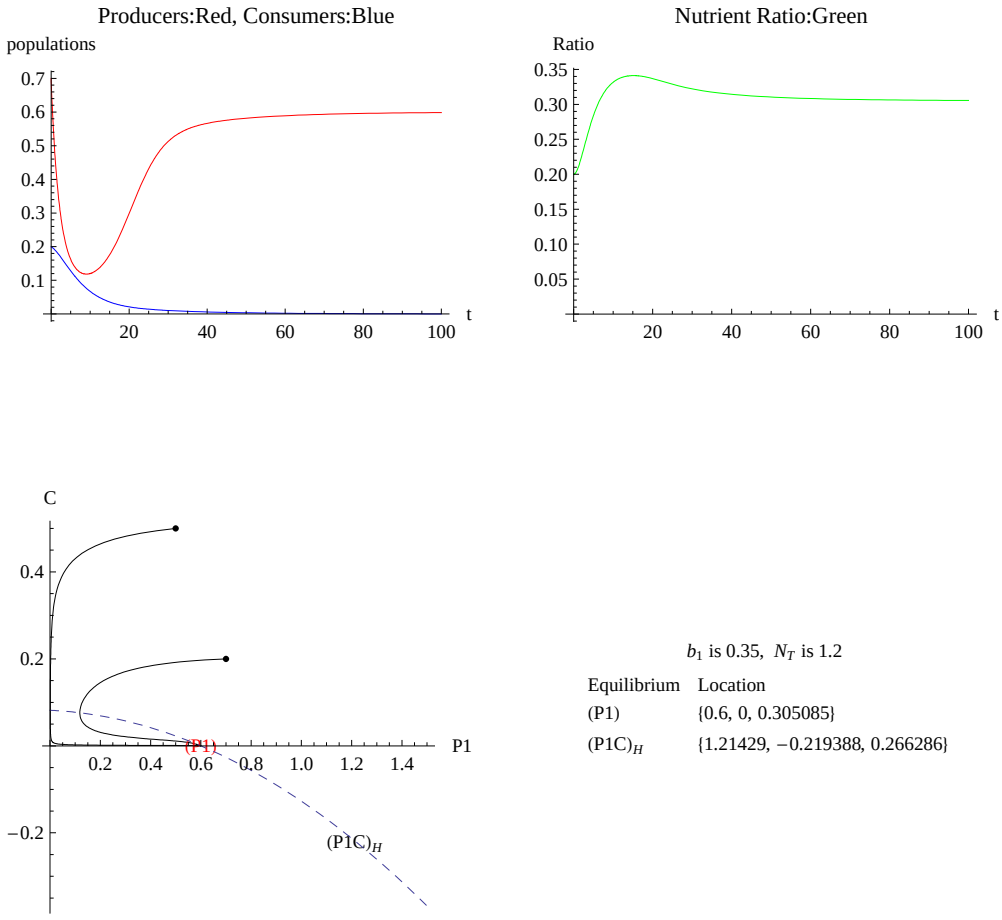

Figure 4.3.10: **Phase Portrait in region A**
The equilibrium (P1) is attracting, but (P1C) is still a saddle and not yet in the first quadrant. Illustrated by the simulation, the population of consumers goes extinct and producers remain. The producer-consumer system turns into a monoculture system.

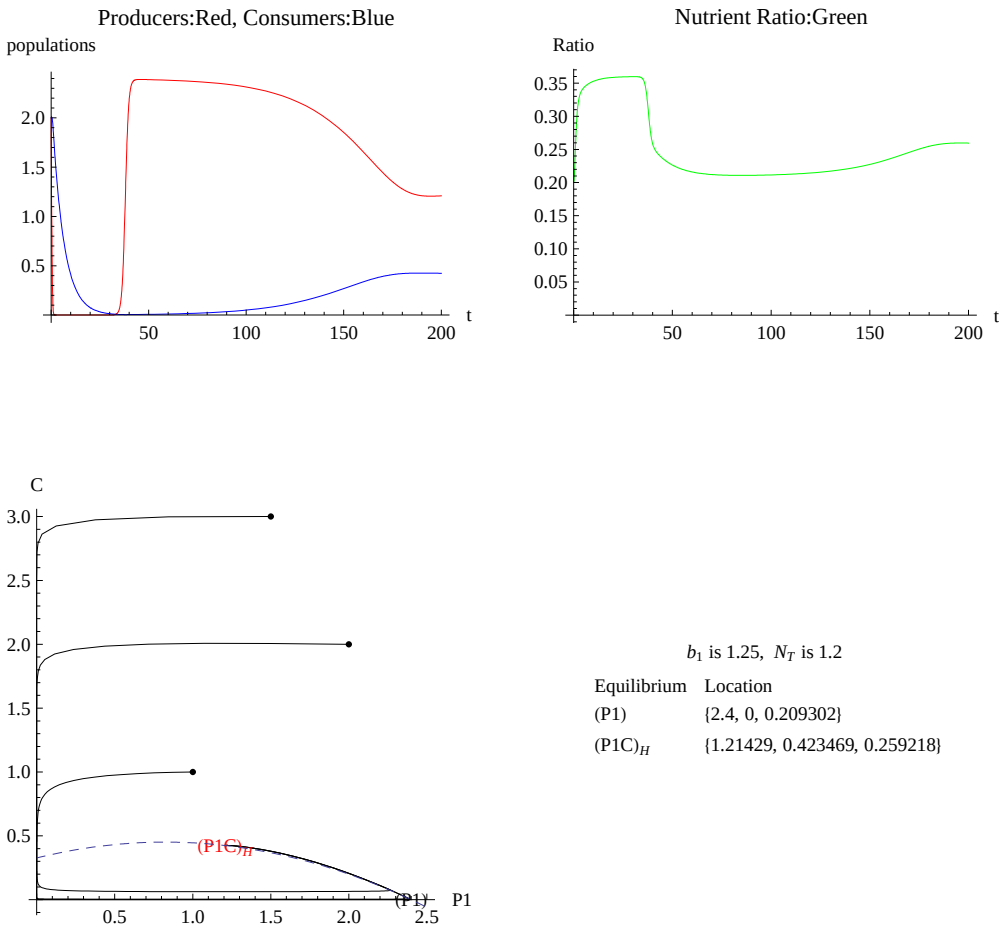

Figure 4.3.11: **Phase Portrait in region B**
The coexistence equilibrium $(\text{P1C})_H$ is attracting. Populations of producers and consumers both coexist and tend to certain constant population sizes.

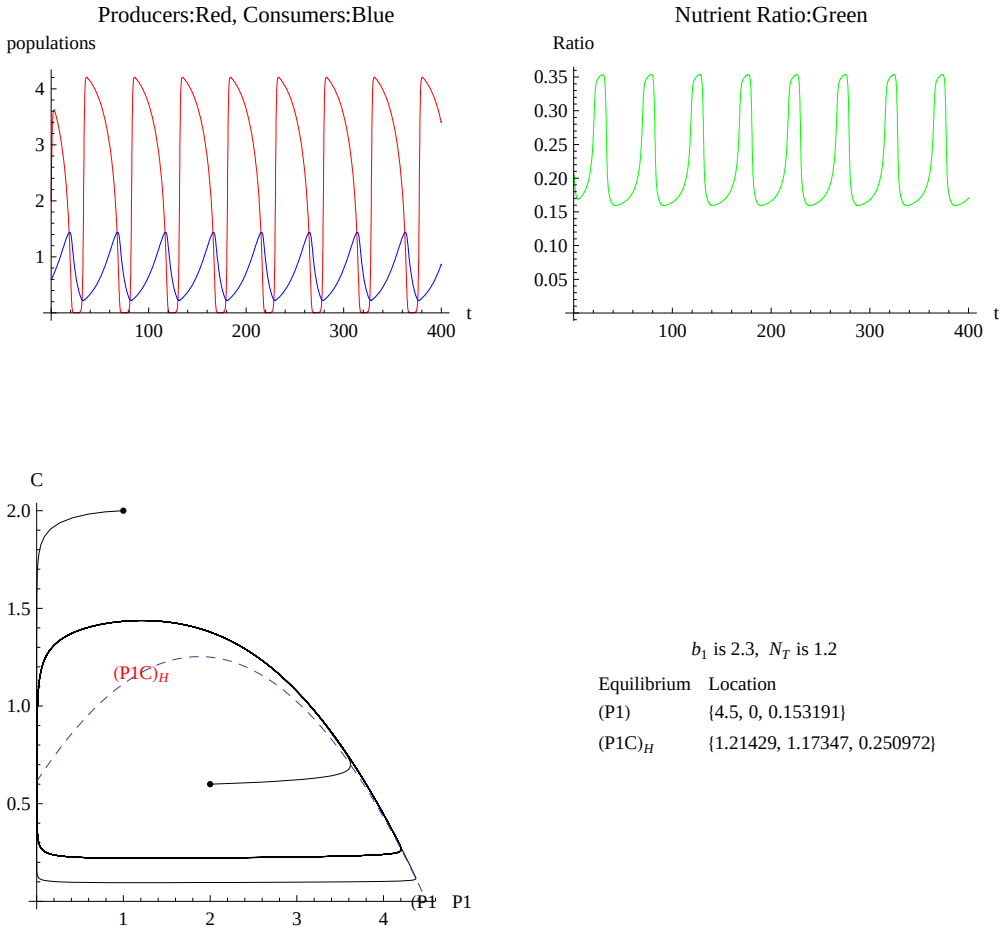

Figure 4.3.12: **Phase Portrait in region C**
Solutions in region C approach a limit cycle. The geometry of the cycle is influenced by parameters in the system. For example, the growth rate b_1 can influence the amplitude of the cycle. When solutions approach a limit cycle, the populations of producers and consumers oscillate periodically in the long run.

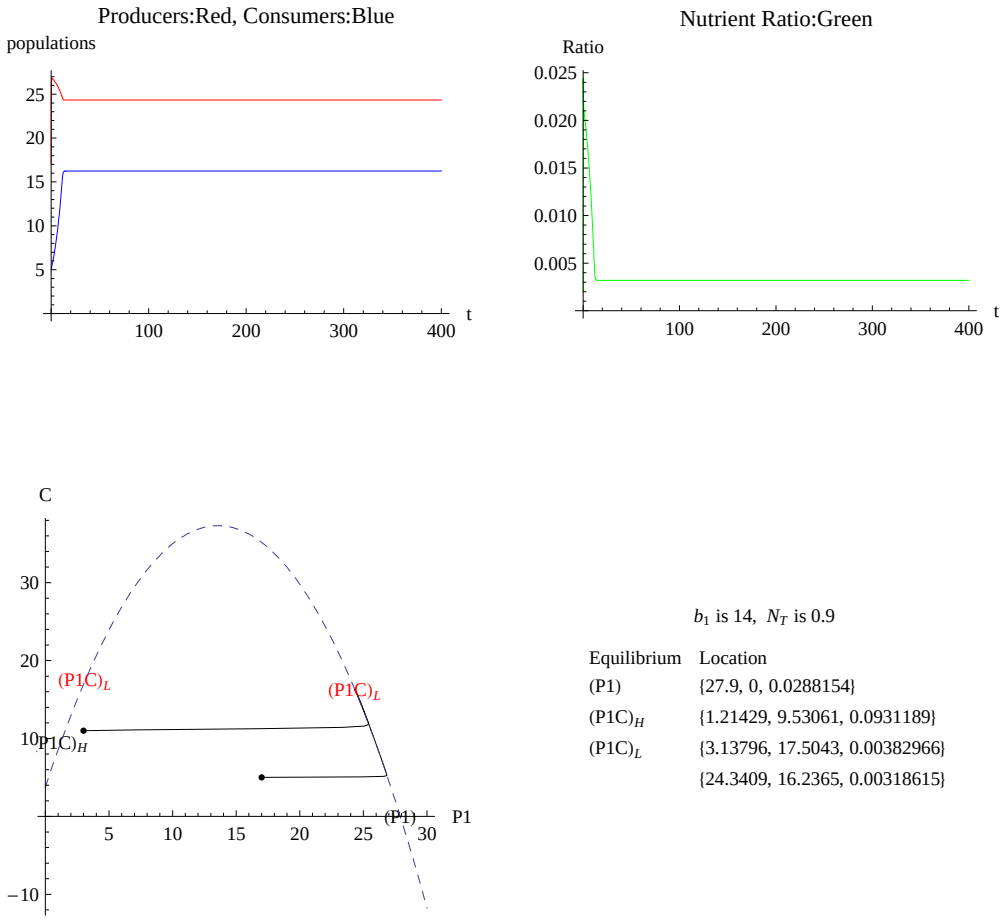

Figure 4.3.13: **Phase Portrait in region D**

However, only one (P1C) which is born from the saddle-node bifurcation is stable. The (P1C) from case H is saddle in region D. The other (P1C) from the saddle-node bifurcation is also saddle. The large oscillated cycles of producers and consumers stop, and the populations approach to certain stable size. The nutrient carbon ratio in producers, however, becomes very low, $\frac{Q_1}{q} < \gamma$.

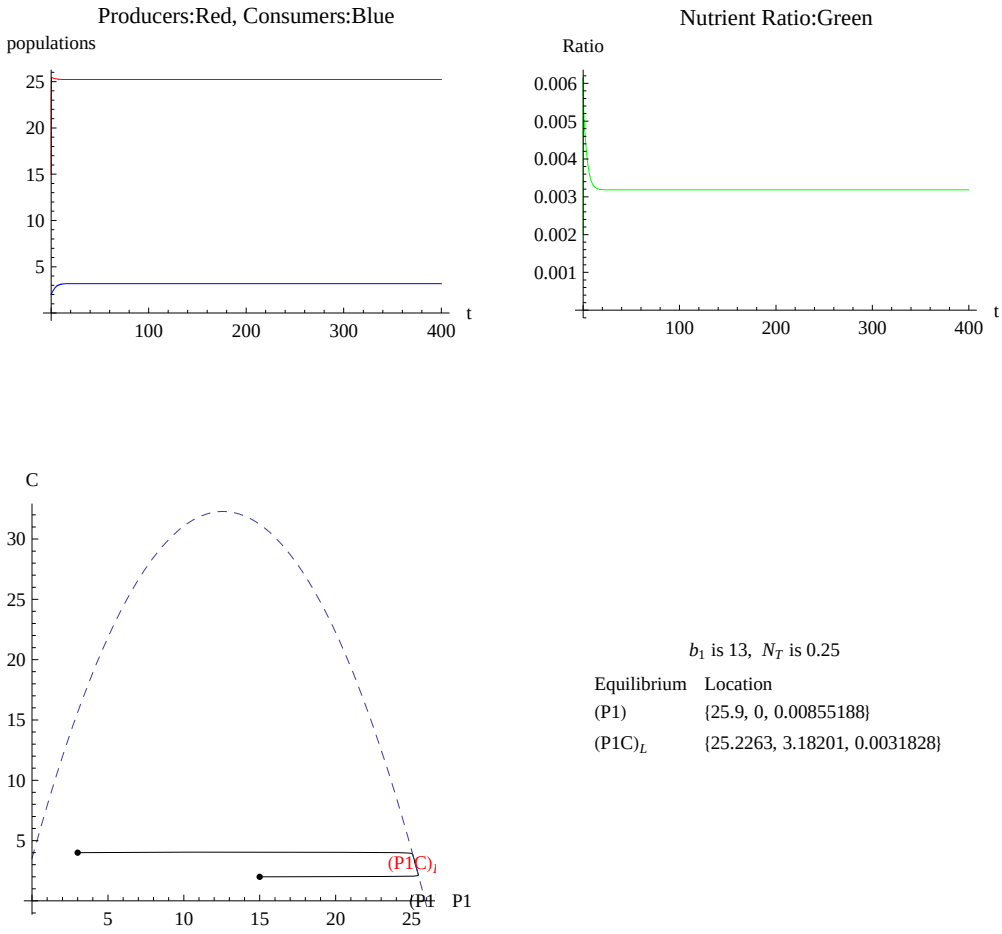

Figure 4.3.14: **Phase Portrait in region E**
The solutions are similar to the solutions in region D. However, there is only one coexistence equilibrium in region D.

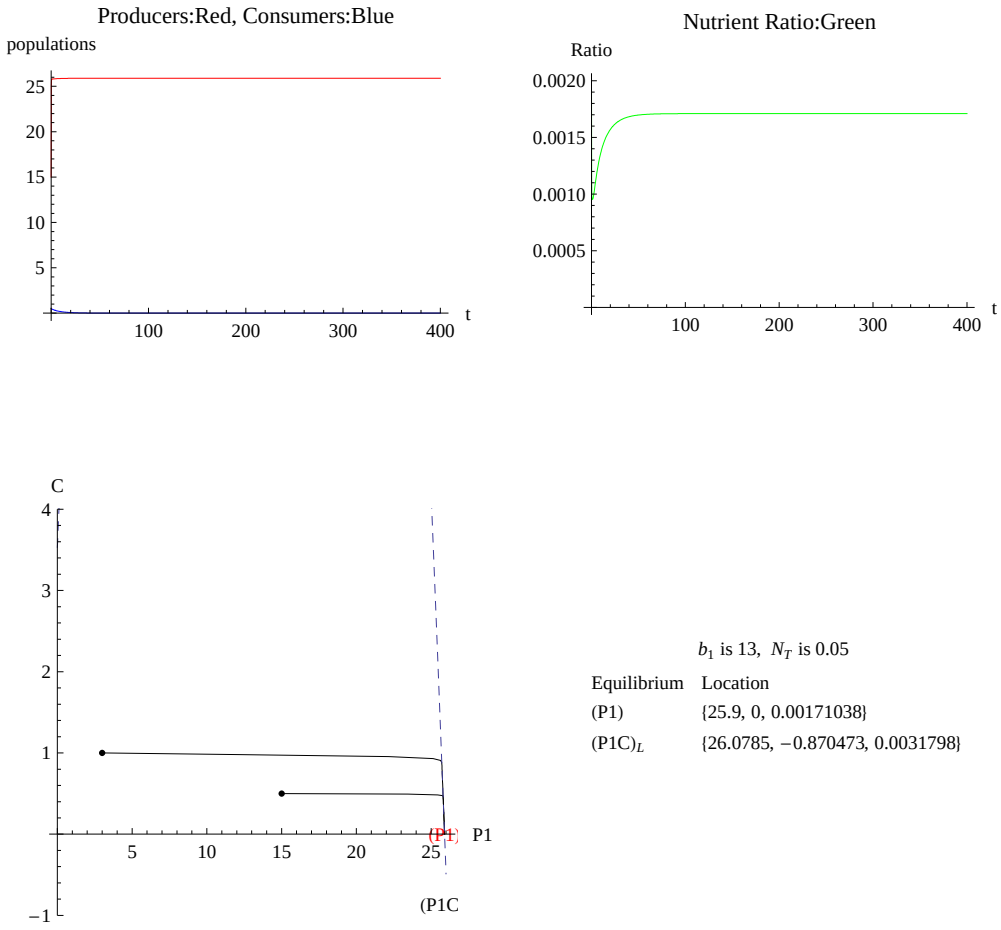

Figure 4.3.15: **Phase Portrait in region F**
Equilibrium (P1C) is now a saddle in the fourth quadrant while (P1) is the stable attractor. This system is similar to the system in region A except the nutrient carbon ratio in producers is very low.

5 Two-Producers-One-Consumer Model

Let P_2 be the population density of the second producer. λ_{11} and λ_{22} are the self-limiting population growth coefficients. λ_{12} and λ_{21} are the interference coefficients from producer P_2 to producer P_1 and from producer P_1 to producer P_2.

$$\begin{cases} \frac{dP_1}{dt} &= ((b_1 - \lambda_{12}P_2 - \lambda_{11}P_1)^+ - d_{P_1} - \frac{\alpha C}{h+P_1+P_2})P_1 \\ \frac{dP_2}{dt} &= ((b_2 - \lambda_{21}P_1 - \lambda_{22}P_2)^+ - d_{p_2} - \frac{\alpha C}{h+P_1+P_2})P_2 \\ \frac{dC}{dt} &= (\min(\gamma, \frac{1}{q}\frac{Q_1P_1+Q_2P_2}{P_1+P_2})\frac{\alpha(P_1+P_2)}{h+P_1+P_2} - d_c)C \\ \frac{dQ_1}{dt} &= ((N_T - qC - Q_1P_1 - Q_2P_2)\beta_1 - Q_1)(b_1 - \lambda_{12}P_2 - \lambda_{11}P_1)^+ \\ \frac{dQ_2}{dt} &= ((N_T - qC - Q_1P_1 - Q_2P_2)\beta_2 - Q_2)(b_2 - \lambda_{21}P_1 - \lambda_{22}P_2)^+ \end{cases} \tag{5.0.1}$$

Note that $\frac{dC}{dt}$ is not defined for $P_1 = P_2 = 0$, but it can be continuously extended to $\frac{dC}{dt} = -d_C$.
For our numerical investigrations, the parameter values for the model are listed below.
Self-limiting coefficients $\lambda_{11} = \lambda_{22} = 0.5$,
Interference coefficients $\lambda_{12} = \lambda_{21} = 0.2$,
Producer death rates $d_{P_1} = d_{P_2} = 0.05$,
Consumer death rate $d_c = 0.17$,
Consumer stoichiometric ratio $q = 0.05$,
The efficient conversation rate $\gamma = 0.1$,
The maximal and half-saturation coefficients in the predation function $\alpha = 2.75$ and $h = 0.75$,
Transpiration constants $\beta_1 = \beta_2 = 0.3$ (even if $P_1 = 0$).

5.1 Invariant Regions

Based on the biological Interpretation of the model, we expect that

1) P_1, C, and Q_1 should be non-negative at any time t.

2) The amount of mineralized nutrient $(N_T - qC - Q_1P_1 - Q_2P_2)$ cannot be negative.

3) The growth functions $(b_1 - \lambda_{12}P_2 - \lambda_{11}P_1)^+ = \max(0, b_1 - \lambda_{12}P_2 - \lambda_{11}P_1)$ and $(b_2 - \lambda_{21}P_1 - \lambda_{22}P_2)^+ = \max(0, b_2 - \lambda_{21}P_1 - \lambda_{22}P_2)$ should be greater than or equal to zero.

The Q_i is defined as $\frac{N_i}{P_i}$. When $P_i = 0$, Q_i is not defined.

Proposition 5.1.1. *Assume λ_{11}, λ_{12}, λ_{21}, λ_{22}, d_{P_1}, d_{P_2}, d_c, q, γ, α, h, β_1, and β_2 are > 0. If $(N_T - qC - Q_1P_1 - Q_2P_2)$ is non-negative at the initial value of a solution, then $(N_T - qC - Q_1P_1 - Q_2P_2)$ should always remain non-negative at any time t along the solution, assuming P_1, P_2, C, Q_1, and Q_2 are positive.*

Proof. Assume $(N_T - qC - Q_1P_1 - Q_2P_2)$ is equal to zero at some time t'. Let ${P_1}'$, ${P_2}'$, C', ${Q_1}'$, and ${Q_2}'$ be the values of P_1, P_2, C, Q_1, and Q_2 at time t'.

Consider the derivative of $(N_T - qC - Q_1P_1 - Q_2P_2)$ at $t = t'$.

$$
\begin{aligned}
& \tfrac{d}{dt}(N_T - qC - Q_1P_1 - Q_2P_2)|_{t=t'} \\
= \; & -q\tfrac{dC}{dt}|_{t=t'} - {Q_1}'\tfrac{dP_1}{dt}|_{t=t'} - {P_1}'\tfrac{dQ_1}{dt}|_{t=t'} - {Q_2}'\tfrac{dP_2}{dt}|_{t=t'} - {P_2}'\tfrac{dQ_2}{dt}|_{t=t'} \\
= \; & -qC'(\min(\gamma, \tfrac{1}{q}\tfrac{{Q_1}'{P_1}' + {Q_2}'{P_2}'}{{P_1}' + {P_2}'})\tfrac{\alpha({P_1}' + {P_2}')}{h + {P_1}' + {P_2}'} - d_c) \\
& -{Q_1}'((b_1 - \lambda_{12}{P_2}' - \lambda_{11}{P_1}')^+ - d_{P_1} - \tfrac{\alpha C'}{h + {P_1}' + {P_2}'}){P_1}' \\
& -{P_1}'((N_T - qC' - {Q_1}'{P_1}' - {Q_2}'{P_2}')\beta_1 - {Q_1}')(b_1 - \lambda_{12}{P_2}' - \lambda_{11}{P_1}')^+ \\
& -{Q_2}'((b_2 - \lambda_{21}{P_1}' - \lambda_{22}{P_2}')^+ - d_{P_2} - \tfrac{\alpha C'}{h + {P_1}' + {P_2}'}){P_2}' \\
& -{P_2}'((N_T - qC' - {Q_1}'{P_1}' - {Q_2}'{P_2}')\beta_2 - {Q_2}')(b_2 - \lambda_{21}{P_1}' - \lambda_{22}{P_2}')^+
\end{aligned}
$$

$$
\begin{aligned}
= \quad & -qC'(\min(\gamma, \tfrac{1}{q}\tfrac{Q_1{}'P_1{}'+Q_2{}'P_2{}'}{P_1{}'+P_2{}'})\tfrac{\alpha(P_1{}'+P_2{}')}{h+P_1{}'+P_2{}'} - d_c) \\
& -Q_1{}'((b_1 - \lambda_{12}P_2{}' - \lambda_{11}P_1{}')^+ - d_{P_1} - \tfrac{\alpha C'}{h+P_1{}'+P_2{}'})P_1{}' \\
& -P_1{}'(0 - Q_1{}')(b_1 - \lambda_{12}P_2{}' - \lambda_{11}P_1{}')^+ \\
& -Q_2{}'((b_2 - \lambda_{21}P_1{}' - \lambda_{22}P_2{}')^+ - d_{P_2} - \tfrac{\alpha C'}{h+P_1{}'+P_2{}'})P_2{}' \\
& -P_2{}'(0 - Q_2{}')(b_2 - \lambda_{21}P_1{}' - \lambda_{22}P_2{}')^+ \\
= \quad & -qC'(\min(\gamma, \tfrac{1}{q}\tfrac{Q_1{}'P_1{}'+Q_2{}'P_2{}'}{P_1{}'+P_2{}'})\tfrac{\alpha(P_1{}'+P_2{}')}{h+P_1{}'+P_2{}'} - d_c) \\
& -Q_1{}'(-d_{P_1} - \tfrac{\alpha C'}{h+P_1{}'+P_2{}'})P_1{}' \\
& -Q_2{}'(-d_{P_2} - \tfrac{\alpha C'}{h+P_1{}'+P_2{}'})P_2{}' \\
= \quad & -qC'(\min(\gamma, \tfrac{1}{q}\tfrac{Q_1{}'P_1{}'+Q_2{}'P_2{}'}{P_1{}'+P_2{}'})\tfrac{\alpha(P_1{}'+P_2{}')}{h+P_1{}'+P_2{}'} - d_c) + Q_1{}'P_1{}'(d_{P_1} + \tfrac{\alpha C'}{h+P_1{}'+P_2{}'}) \\
& +Q_2{}'P_2{}'(d_{P_2} + \tfrac{\alpha C'}{h+P_1{}'+P_2{}'}) \\
= \quad & qC'd_c + Q_1{}'P_1{}'d_{P_1} + Q_2{}'P_2{}'d_{P_2} - \tfrac{q\alpha C'(P_1{}'+P_2{}')}{h+P_1{}'+P_2{}'}(\tfrac{Q_1{}'P_1{}'+Q_2{}'P_2{}'}{q(P_1{}'+P_2{}')} - Min(\gamma, \tfrac{1}{q}\tfrac{Q_1{}'P_1{}'+Q_2{}'P_2{}'}{P_1{}'+P_2{}'}))
\end{aligned}
$$

If $\gamma \leq \frac{Q_1{}'P_1{}'+Q_2{}'P_2{}'}{q(P_1{}'+P_2{}')}$, then $qC'd_c+Q_1{}'P_1{}'d_{P_1}+Q_2{}'P_2{}'d_{P_2}-\frac{q\alpha C'(P_1{}'+P_2{}')}{h+P_1{}'+P_2{}'}(\frac{Q_1{}'P_1{}'+Q_2{}'P_2{}'}{q(P_1{}'+P_2{}')}-\gamma) \geq 0$

If $\gamma > \frac{Q_1{}'P_1{}'+Q_2{}'P_2{}'}{q(P_1{}'+P_2{}')}$, then $qC'd_c + Q_1{}'P_1{}'d_{P_1} + Q_2{}'P_2{}'d_{P_2} - \frac{q\alpha C'(P_1{}'+P_2{}')}{h+P_1{}'+P_2{}'}(\frac{Q_1{}'P_1{}'+Q_2{}'P_2{}'}{q(P_1{}'+P_2{}')} - \frac{Q_1{}'P_1{}'+Q_2{}'P_2{}'}{q(P_1{}'+P_2{}')}) \geq 0$

This means $(N_T - qC - Q_1P_1 - Q_2P_2)$ cannot be negative if a solution starts with a positive $(N_T - qC - Q_1P_1 - Q_2P_2)$. □

Proposition 5.1.2. *An invariant region of model (5.0.1) is* $0 \leq P_1 \leq \frac{b_1}{\lambda_{11}}$, $0 \leq P_2 \leq \frac{b_2}{\lambda_{22}}$, $0 \leq C \leq \frac{N_T}{q}$, $0 \leq Q_1 \leq N_T\beta_1$, $0 \leq Q_2 \leq N_T\beta_2$, *and* $(N_T - qC - Q_1P_1 - Q_2P_2) \geq 0$. *If a solution initially starts in the interior of the invariant region or on the boundary of the invariant region, the solution will stay in region.*

Proof. If the solution initially starts on the boundary but does not go through the boundary, then all solutions start initially in this invariant region should stay in this region at

any future time t.

Solutions on the side planes $P_1 = 0$, $P_2 = 0$, and $C = 0$, the solutions cannot go over the side planes since $\frac{dP_1}{dt} = 0$, $\frac{dP_2}{dt} = 0$, and $\frac{dC}{dt} = 0$.

Solutions on $Q_1 = 0$ or $Q_2 = 0$ and keep other variable inside the region, the solutions would not exit the invariant region through $Q_1 = 0$ and $Q_2 = 0$ since $\frac{dQ_1}{dt} = (N_T - qC - Q_2P_2)\beta_1(b_1 - \lambda_{12}P_2 - \lambda_{11}P_1)^+ \geq 0$ and $\frac{dQ_2}{dt} = (N_T - qC - Q_1P_1)\beta_2(b_2 - \lambda_{21}P_1 - \lambda_{22}P_2)^+ \geq 0$

Solutions on the surface $(N_T - qC - Q_1P_1 - Q_2P_2) = 0$, then the solutions move to the interior of the region since the derivative of $(N_T - qC - Q_1P_1 - Q_2P_2)$ is positive by Proposition (5.1.1).

Solutions on the plane $P_1 = \frac{b_1}{\lambda_{11}}$, then P_1 decreases since $\frac{dP_1}{dt}$ is negative (see below). Similarly, the derivative of P_2 is also negative on the plane $P_2 = \frac{b_2}{\lambda_{22}}$.

$$\frac{dP_1}{dt} = ((-\lambda_{12}P_2)^+ - d_{P_1} - \frac{\alpha C}{h + b_1/\lambda_{11} + P_2})P_1 \leq 0$$

Solutions on the plane $Q_1 = N_T\beta_1$

$$\frac{dQ_1}{dt} = ((-qC - Q_1P_1 - Q_2P_2)\beta_1)(b_1 - \lambda_{12}P_2 - \lambda_{11}P_1)^+ \leq 0$$

Q_1 decreases since $\frac{dQ_1}{dt}$ is negative. If solutions are on the plane $Q_2 = N_T\beta_2$, Q_2 also decreases by the similar reason.

Solutions on the plane $C = \frac{N_T}{q}$, then $N_T - qC - Q_1P_1 - Q_2P_2 = -Q_1P_1 - Q_2P_2$. That implies $Q_1P_1 + Q_2P_2$ is zero. Assuming both P_1 and P_2 are not zero at the same time, the derivative of C is negative and C decreases (see below).

$$\frac{dC}{dt} = (\min(\gamma, 0)\frac{\alpha(P_1 + P_2)}{h + P_1 + P_2} - d_c)C = -d_cC < 0$$

The value of $\frac{1}{q}\frac{Q_1P_1+Q_2P_2}{P_1+P_2}$ is always less than $\max(Q_1, Q_2)$. If both P_1 and P_2 are both zero, by the continuous extension of (5.0.1) gives

$$\frac{dC}{dt} = -d_c C \leq 0$$

.

□

In the system of equations (5.0.1), $(b_1 - \lambda_{12}P_2 - \lambda_{11}P_1)$ and $(b_2 - \lambda_{21}P_1 - \lambda_{22}P_2)$ are set to be positive and zero only with a function $()^+$ to prevent these growth terms from becoming negative. In graph (5.1.1), both P_1 and P_2 in the red intersection of the area under the lines satisfy $b_1 - \lambda_{12}P_2 - \lambda_{11}P_1 \geq 0$ and $b_2 - \lambda_{21}P_1 - \lambda_{22}P_2 \geq 0$. The dashed line box in the graph is the projected invariant region onto P_1P_2 plane. Without the function $()^+$, the growth terms may become negative and cause mis-calculations.

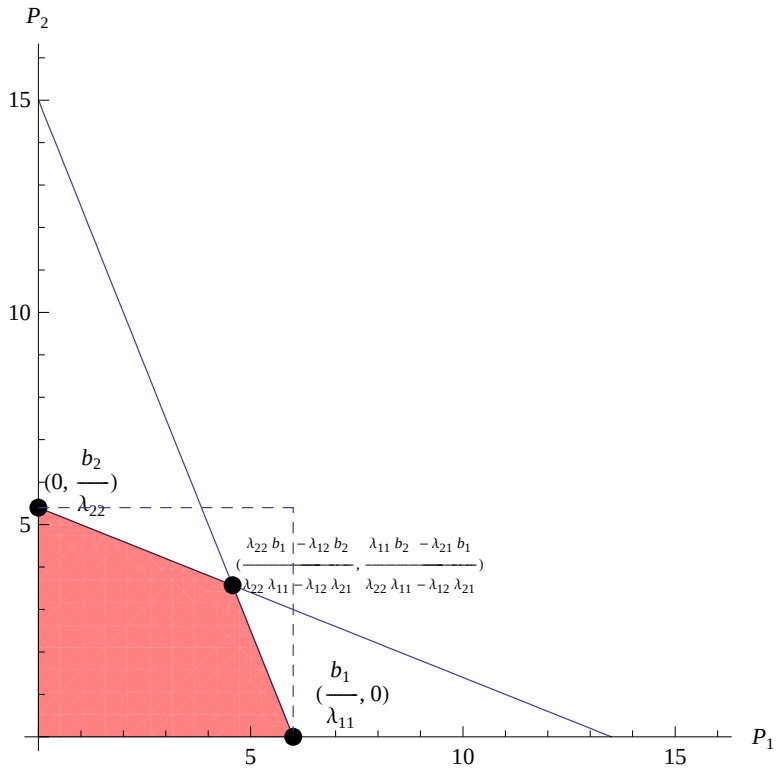

Figure 5.1.1: **The Conditions on P_1 and P_2**
The lines are the producers' growth terms $(b_1 - \lambda_{12}P_2 - \lambda_{11}P_1)$ and $(b_2 - \lambda_{21}P_1 - \lambda_{22}P_2)$. Both growth terms are positive in the red intersection.

5.2 Equilibria In Two-Producer-One-Consumer Model

Similar to the one producer model, there are case H (the biomass conversion efficiency is γ) and case L (the biomass conversion efficiency is $\frac{1}{q}\frac{Q_1P_1+Q_2P_2}{P_1+P_2}$, depending on nutrient ratio in the combined food source).

Equilibria In Case H

Let γ be the biomass conversion efficiency.

$$\begin{cases} \frac{dP_1}{dt} &= ((b_1-\lambda_{12}P_2-\lambda_{11}P_1)^+ - d_{P_1} - \frac{\alpha C}{h+P_1+P_2})P_1 \\ \frac{dP_2}{dt} &= ((b_2-\lambda_{21}P_1-\lambda_{22}P_2)^+ - d_{P_2} - \frac{\alpha C}{h+P_1+P_2})P_2 \\ \frac{dC}{dt} &= (\gamma\frac{\alpha(P_1+P_2)}{h+P_1+P_2} - d_c)C \\ \frac{dQ_1}{dt} &= ((N_T-qC-Q_1P_1-Q_2P_2)\beta_1 - Q_1)(b_1-\lambda_{12}P_2-\lambda_{11}P_1)^+ \\ \frac{dQ_2}{dt} &= ((N_T-qC-Q_1P_1-Q_2P_2)\beta_2 - Q_2)(b_2-\lambda_{21}P_1-\lambda_{22}P_2)^+ \end{cases} \tag{5.2.2}$$

Equilibrium solutions are the following (in (P_1, P_2, C, Q_1, Q_2) format):

Equilibria that are in the $P_2 = 0$ plane or $P_1 = 0$ plane are same as the equilibria in the single-producer-single-consumer model in the last chapter. They are listed below.

The origin $(\mathrm{O})_H$: $(0, 0, 0, {Q_1}^*, {Q_2}^*)$

The monoculture equilibrium $(\mathrm{P1})_H$: $(\frac{b_1-d_{P_1}}{\lambda_{11}}, 0, 0, \frac{N_T\beta_1\lambda_{11}}{\lambda_{11}+(b_1-d_{P_1})\beta_1}, {Q_2}^*)$

The monoculture equilibrium $(\mathrm{P2})_H$: $(0, \frac{b_2-d_{P_2}}{\lambda_{22}}, 0, {Q_1}^*, \frac{N_T\beta_2\lambda_2 2}{\lambda_2 2+(b_2-d_{P_2})\beta_2})$

The one-producer coexistence equilibrium $(\mathrm{P1C})_H$:

$$(\frac{d_ch}{\gamma\alpha-d_c}, 0, \frac{\gamma h(b_1-d_{P_1})}{\alpha\gamma-d_c} - \frac{\gamma d_ch^2\lambda_{11}}{(\alpha\gamma-d_c)^2}, \frac{\beta_1(N_T(\alpha\gamma-d_c)-hq\gamma(b_1-d_{P_1})-\frac{d_cq\gamma h^2\lambda_{11}}{\alpha\gamma-d_c})}{\alpha\gamma-d_c(h\beta_1-1)}, {Q_2}^*).$$

The one-producer coexistence equilibrium $(\mathrm{P2C})_H$:

$$(0, \frac{d_c h}{\gamma\alpha - d_c}, \frac{\gamma h(b_2 - d_{P_2})}{\alpha\gamma - d_c} - \frac{\gamma d_c h^2 \lambda_{22}}{(\alpha\gamma - d_c)^2}, {Q_2}^*, \frac{\beta_2(N_T(\alpha\gamma - d_c) - hq\gamma(b_2 - d_{P_2 1}) - \frac{d_c q\gamma h^2 \lambda_{22}}{\alpha\gamma - d_c})}{\alpha\gamma - d_c(h\beta_2 - 1)}).$$

The following are the new coexistence equilibria in the two-producer-one-consumer model.

The coexistence equilibrium without consumer $(\text{P1P2})_H$:

Set $C = 0$ and assume all other variables are positive. The equilibrium solution is

$$(\frac{\lambda_{22}(b_1 - d_{P_1}) - \lambda_{12}(b_2 - d_{P_2})}{\lambda_{11}\lambda_{22} - \lambda_{12}\lambda_{21}}, \frac{\lambda_{11}(b_2 - d_{P_2}) - \lambda_{21}(b_1 - d_{P_1})}{\lambda_{11}\lambda_{22} - \lambda_{12}\lambda_{21}}, 0,$$

$$\frac{N_T\beta_1(\lambda_{11}\lambda_{22} - \lambda_{12}\lambda_{21})}{(b_1 - d_{P_1})(\beta_1\lambda_{22} - \beta_2\lambda_{21}) + (b_2 - d_{P_2})(\beta_2\lambda_{11} - \beta_1\lambda_{12}) + \lambda_{11}\lambda_{22} - \lambda_{12}\lambda_{21}},$$

$$\frac{N_T\beta_2(\lambda_{11}\lambda_{22} - \lambda_{12}\lambda_{21})}{(b_1 - d_{P_1})(\beta_1\lambda_{22} - \beta_2\lambda_{21}) + (b_2 - d_{P_2})(\beta_2\lambda_{11} - \beta_1\lambda_{12}) + \lambda_{11}\lambda_{22} - \lambda_{12}\lambda_{21}}).$$

In the absence of consumers, both producers co-exist under the competition of sharing resources. Note that the sum of the self-limitations $\lambda_{11} + \lambda_{22}$ is assumed to be larger than the sum of the interference-limitations $\lambda_{12} + \lambda_{21}$.

The coexistence equilibrium $(\text{P1P2C})_H$:

When the growth terms are positive, the equilibrium solution is

$$(\frac{(b_1 - d_{P_1} - b_2 + d_{P_2} - \frac{d_c h(\lambda_{22} - \lambda_{12})}{\alpha\gamma - d_c})}{\lambda_{11} + \lambda_{22} - \lambda_{12} - \lambda_{21}}, \frac{(b_2 - d_{P_2} - b_1 + d_{P_1} - \frac{d_c h(\lambda_{11} - \lambda_{21})}{\alpha\gamma - d_c})}{\lambda_{11} + \lambda_{22} - \lambda_{12} - \lambda_{21}},$$

$$\frac{\frac{\gamma h((b-1-d_{P_1})(\lambda_{22} - \lambda_{21}) - (b_2 - d_{P_2})(\lambda_{11} - \lambda_{12}))}{\alpha\gamma - d_c} + \frac{\gamma d_c h^2(\lambda_{11}\lambda_{22} - \lambda_{12}\lambda_{21})}{(\alpha\gamma - d - c)^2}}{\lambda_{11} + \lambda_{22} - \lambda_{12} - \lambda_{21}},$$

$$\frac{\beta_1(N_T - q\frac{\frac{\gamma h((b-1-d_{P_1})(\lambda_{22} - \lambda_{21}) - (b_2 - d_{P_2})(\lambda_{11} - \lambda_{12}))}{\alpha\gamma - d_c} + \frac{\gamma d_c h^2(\lambda_{11}\lambda_{22} - \lambda_{12}\lambda_{21})}{(\alpha\gamma - d - c)^2}}{\lambda_{11} + \lambda_{22} - \lambda_{12} - \lambda_{21}})}{1 + \beta_1\frac{(b_1 - d_{P_1} - b_2 + d_{P_2} - \frac{d_c h(\lambda_{22} - \lambda_{12})}{\alpha\gamma - d_c})}{\lambda_{11} + \lambda_{22} - \lambda_{12} - \lambda_{21}} + \beta_2\frac{(b_2 - d_{P_2} - b_1 + d_{P_1} - \frac{d_c h(\lambda_{11} - \lambda_{21})}{\alpha\gamma - d_c})}{\lambda_{11} + \lambda_{22} - \lambda_{12} - \lambda_{21}}},$$

$$\frac{\beta_2(N_T - q\frac{\frac{\gamma h((b-1-d_{P_1})(\lambda_{22} - \lambda_{21}) - (b_2 - d_{P_2})(\lambda_{11} - \lambda_{12}))}{\alpha\gamma - d_c} + \frac{\gamma d_c h^2(\lambda_{11}\lambda_{22} - \lambda_{12}\lambda_{21})}{(\alpha\gamma - d - c)^2}}{\lambda_{11} + \lambda_{22} - \lambda_{12} - \lambda_{21}})}{1 + \beta_1\frac{(b_1 - d_{P_1} - b_2 + d_{P_2} - \frac{d_c h(\lambda_{22} - \lambda_{12})}{\alpha\gamma - d_c})}{\lambda_{11} + \lambda_{22} - \lambda_{12} - \lambda_{21}} + \beta_2\frac{(b_2 - d_{P_2} - b_1 + d_{P_1} - \frac{d_c h(\lambda_{11} - \lambda_{21})}{\alpha\gamma - d_c})}{\lambda_{11} + \lambda_{22} - \lambda_{12} - \lambda_{21}}}).$$

Note that when either or both growth terms are zero, the equilibrium solution does not exist.

Since the equilibria $(\text{P1})_H$ and $(\text{P2})_H$, $(\text{P1C})_H$ and $(\text{P2C})_H$ are conjugates, we just study $(\text{P1})_H$ and $(\text{P1C})_H$. The eigenvalue plots of these equilibrium solutions in parametric space

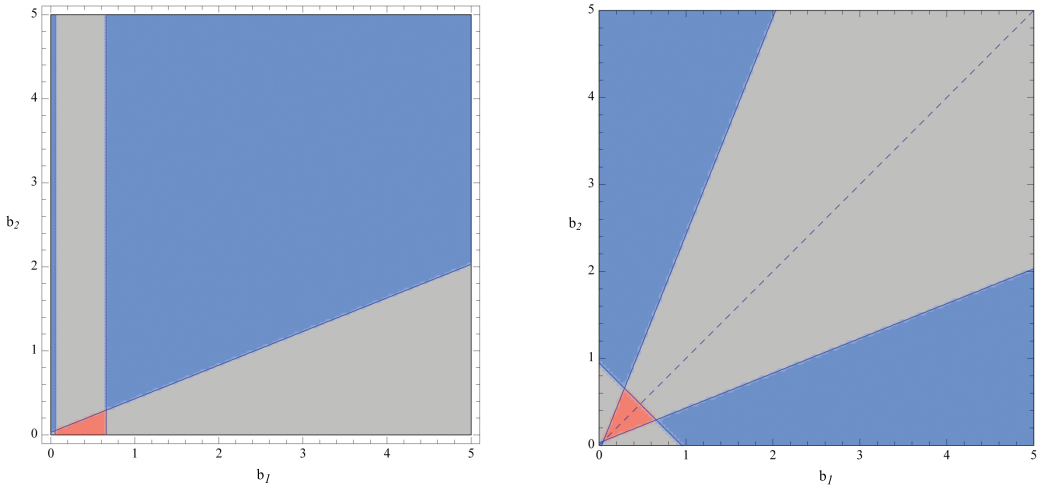

(a) (P1) (b) (P1P2)

Figure 5.2.2: **Eigenvalue Diagrams in case H**
Equilibrium (P1P2) is in the first quadrant when (b_1, b_2) is in the wedge shape gray area in figure (5.2.2(b)). The wedge shape is caused by the competition between the two producers. Equilibrium (P1P2) is outside the first quadrant when (b_1, b_2) is in the blue areas to the left and right of the gray wedge. That implies one of the producers is going to be extinct under the competition. (The color scheme is described in table(5.2.1))

$b_1 : [0, 5] \times b_2 : [0, 5]$ with a fixed N_T are shown individually in figures (5.2.2) and (5.2.3). They are computed numerically using Mathematica 6.0.

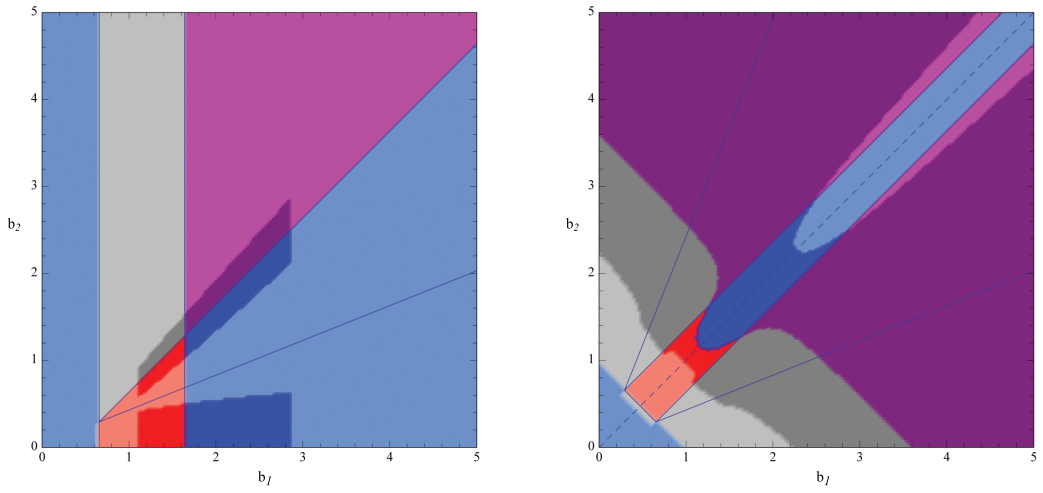

(a) (P1C)

(b) (P1P2C)

Figure 5.2.3: **Eigenvalue Diagrams in case H**
The diagonal dashed line in figure (3(b)) is when $b_1 = b_2$. The blue lines are the boundaries of equilibrium (P1P2) being in the positive quadrant. (The color scheme is in the table(5.2.1))

Color	Number of Eigenvalues with a Positive Real Part	Stability
	All Real Eigenvalues	
Pink / Salmon	0	Attracting
Silver	1	Saddle
Light Blue	2	Saddle
Magenta	3	Saddle
Light Orange	4	Saddle
Lime	5	Repelling
	Containing Complex Eigenvalues	
Red	0	Attracting
Gray	1	Saddle
Blue	2	Saddle
Purple	3	Saddle
Orange	4	Saddle
Green	5	Repelling

Table 5.2.1: Color Scheme For The Stability diagrams

A bifurcation diagram for case H is shown in figure (5.2.4). The difference between (P1) and (P1P2) is that (P1) lies on the side P_1C plane and (P1P2) lies on the plane $C = 0$. There are two layers in the bifurcation graph. When the consumer C is zero, the light color dashed lines are the transcritical bifurcations. Two-producer coexistence (P1P2) is attracting in the wedge, while monoculture (P1) and (P2) are attrating on the right and left of the wedge, respectively. (Refers to figure (5.2.2(b))) Equilibrium (O) is attracting in region $(0 \leq b_1 \leq d_{P_1}) \cup (0 \leq b_2 \leq d_{P_2})$. Since the death rates of both producers are relatively small, this (O) attracting region cannot be displayed at this scale. Region A is the case where two producers coexist but $C = 0$. From region A to B, there is a transcritical bifurcation. In region B, solutions of populations approach the equilibrium point $(\text{P1P2C})_H$. From region B to C, there is a Hopf bifurcation. In region C, solutions approach a limit cycle around $(\text{P1P2C})_H$ in the interior space of the first quadrant. In region Z and $\tilde{\text{Z}}$, solutions also approach a limit cycle in the interior but $(\text{P1P2C})_H$ is no longer in the first quadrant. From region F to Z, there is a transcritical bifurcation of periodic orbits. This is a new bifurcation that the single producer single consumer model does not have. Also, the geometry of limit cycle changes due to this new bifurcation. There is a discussion about the geometry of limit cycles in next section. Regions D, E, and F are the regions where solutions approach the side plane $P_2 = 0$ since $b_1 > b_2$. Therefore, D corresponds to the monoculture region in the one-producer-one-consumer model. E corresponds to the coexisting region, and F corresponds to the coexisting region with the population oscillating in the long run.

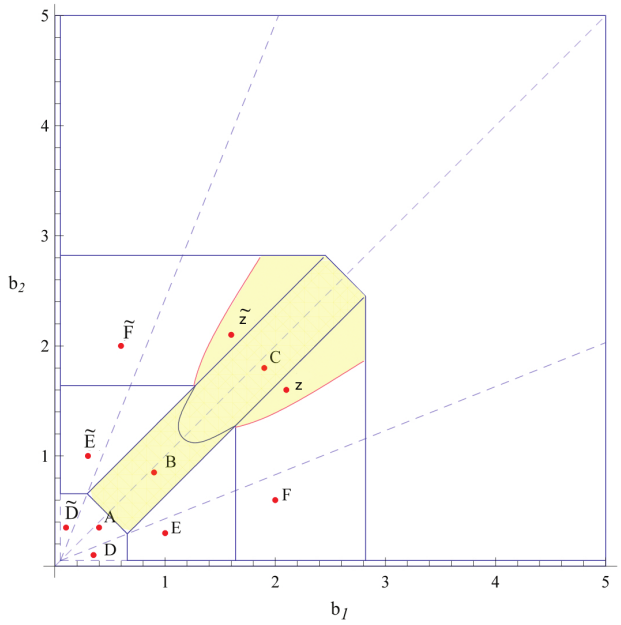

Figure 5.2.4: **A Bifurcation Diagram In Case H (5.2.2)**
The diagonal dashed line is $b_1 = b_2$ for reference. The other dashed lines indicate the bifurcations when $C = 0$, while the solid curves indicate the bifurcations in the space $C > 0$. The yellow colored regions are the regions where two-producer-one-consumer coexistence solutions can exist. In the unlabeled region, equilibrium solutions $(\text{P1C})_H$ and $(\text{P1P2C})_H$ do not satisfy $\frac{1}{q}\frac{Q_1P_1+Q_2P_2}{P_1+P_2} \geq \gamma$. From region Z to F, there is a transcritical bifurcation of periodic orbits. The parameter values of that bifurcation are numerically approximated by the pink curve.

Equilibria In Case L

In this case the biomass conversion efficiency becomes $\frac{1}{q}\frac{Q_1P_1+Q_2P_2}{P_1+P_2}$.

$$\begin{cases} \frac{dP_1}{dt} &= ((b_1-\lambda_{12}P_2-\lambda_{11}P_1)^+ - d_{P_1} - \frac{\alpha C}{h+P_1+P_2})P_1 \\ \frac{dP_2}{dt} &= ((b_2-\lambda_{21}P_1-\lambda_{22}P_2)^+ - d_{P_2} - \frac{\alpha C}{h+P_1+P_2})P_2 \\ \frac{dC}{dt} &= (\frac{Q_1P_1+Q_2P_2}{q(P_1+P_2)}\frac{\alpha(P_1+P_2)}{h+P_1+P_2} - d_c)C \\ \frac{dQ_1}{dt} &= ((N_T-qC-Q_1P_1-Q_2P_2)\beta_1 - Q_1)(b_1-\lambda_{12}P_2-\lambda_{11}P_1)^+ \\ \frac{dQ_2}{dt} &= ((N_T-qC-Q_1P_1-Q_2P_2)\beta_2 - Q_2)(b_2-\lambda_{21}P_1-\lambda_{22}P_2)^+ \end{cases} \tag{5.2.3}$$

Equilibrium solutions are the following (in (P_1, P_2, C, Q_1, Q_2) format):

The origin $(\mathrm{O})_L$ and all monoculture equilibrium $(\mathrm{P1})_L$, $(\mathrm{P2})_L$, and $(\mathrm{P1P2})_L$ are the same as the ones in case H.

The procedure of finding $(\mathrm{P1C})_L$ is described in the last section (one producer and one consumer model). The coexistence equilibrium $(\mathrm{P1P2C})_L$ are also the roots of a cubic equation $F(P_1)$ (See Appendix V).

$$\begin{aligned} F(P_1) &= (N_T - \tfrac{q}{\alpha}(\tfrac{1}{2}(b_1+b_2-d_{P_1}-d_{P_2}-\lambda_{12}\tfrac{b_1-b_2-d_{P_1}+d_{P_2}-P_1\lambda_{11}+P_1\lambda_{21}}{\lambda_{12}-\lambda_{22}} \\ &\quad -\lambda_{11}P_1-\lambda_{21}P_1-\lambda_{22}\tfrac{b_1-b_2-d_{P_1}+d_{P_2}-P_1\lambda_{11}+P_1\lambda_{21}}{\lambda_{12}-\lambda_{22}})) \\ &\quad (h+P_1+\tfrac{b_1-b_2-d_{P_1}+d_{P_2}-P_1\lambda_{11}+P_1\lambda_{21}}{\lambda_{12}-\lambda_{22}})) \\ &\quad (\beta_1P_1+\beta_2\tfrac{b_1-b_2-d_{P_1}+d_{P_2}-P_1\lambda_{11}+P_1\lambda_{21}}{\lambda_{12}-\lambda_{22}}) \\ &\quad -\tfrac{qd_c}{\alpha}(1+P_1\beta_1+\beta_2\tfrac{b_1-b_2-d_{P_1}+d_{P_2}-P_1\lambda_{11}+P_1\lambda_{21}}{\lambda_{12}-\lambda_{22}}) \\ &\quad (h+P_1+\tfrac{b_1-b_2-d_{P_1}+d_{P_2}-P_1\lambda_{11}+P_1\lambda_{21}}{\lambda_{12}-\lambda_{22}}) \end{aligned} \tag{5.2.4}$$

The explicit coefficients of F are too long to display. The coefficient of the ${P_1}^3$ term does not depend on the parameters b_1, b_2, and N_T. Numerically, it is apparently always positive with the parameter setting in this paper. However, the y-intercept is no longer independent of the parameters b_1, b_2, and N_T. Let P_+ and P_- be the locations of the extreme values of $F(P_1)$. As b_1 and b_2 change, P_+ and P_- also move. When $F(P_-) > 0$ and $F(P_+) < 0$, the cubic equation F has three real roots. When $F(P_+) > 0$ and $F(P_-) > 0$, the cubic F changes back having one real root. The changes in the number of roots is likely due to saddle-node bifurcations (see graphs (5.2.5)). Not all solutions of the cubic equation satisfy $\frac{1}{q}\frac{Q_1P_1+Q_2P_2}{P_1+P_2} < \gamma$. The details of selecting valid coexistence equilibria is shown in the next section figure (5.4.9).

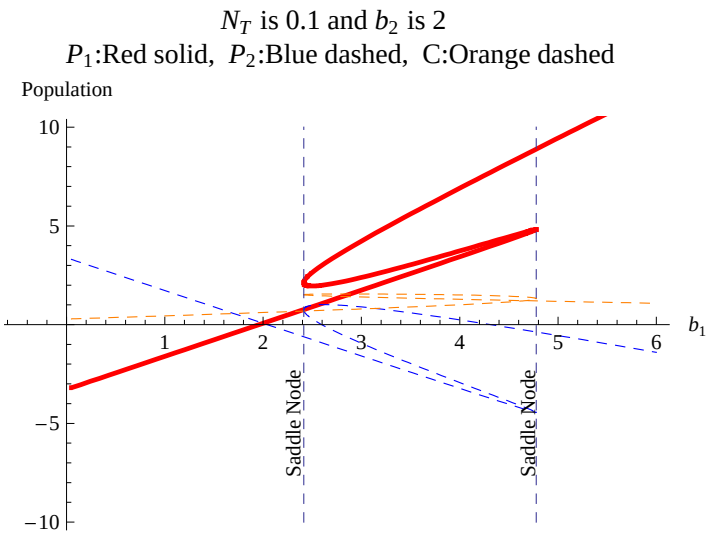

(a) Solutions for P_1, P_2, and C

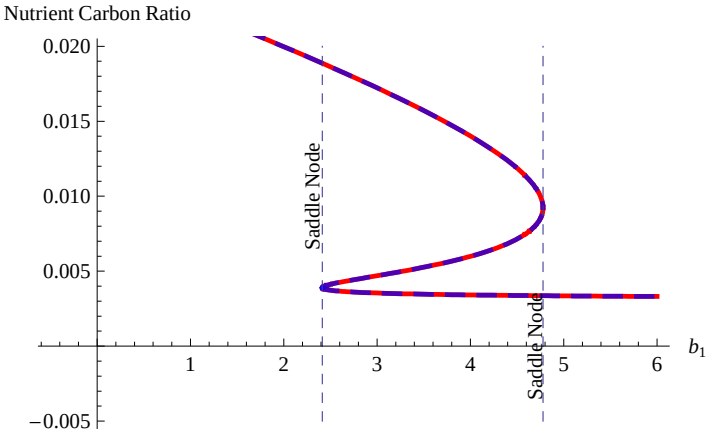

(b) Solutions for Q_1 and Q_2

Figure 5.2.5: Fixing N_T and b_2, as b_1 increases, a saddle-node bifurcation occurs and creates two additional solutions. As b_1 increase further, another saddle-node bifurcation occurs eliminating two solutions. Here Q_1 and Q_2 are the same because both transpiration rates are the same ($\beta_1 = \beta_2$).

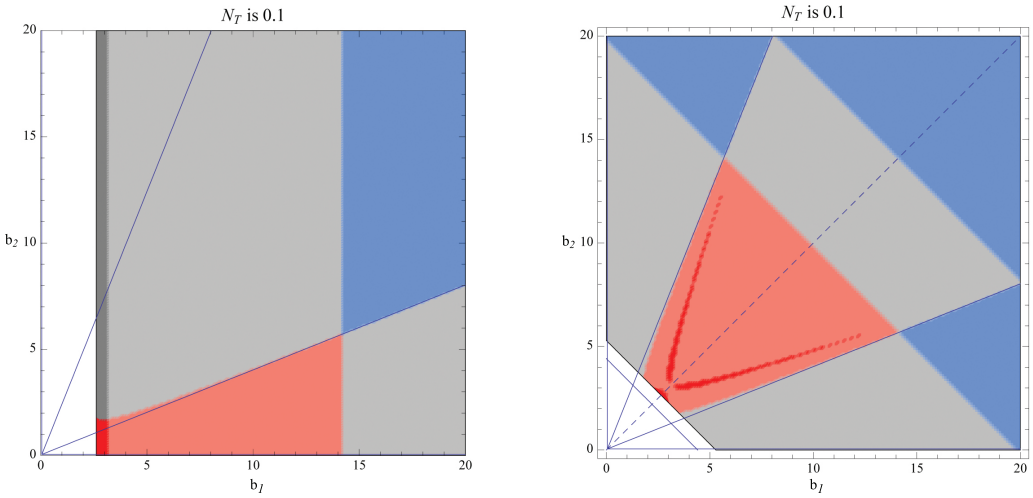

(a) $(\text{P1C})_L$ (b) $(\text{P1P2C})_L$

Figure 5.2.6: **Eigenvalue Diagrams in Case L**
The eligible equilibrium solutions are born via a saddle-node bifurcation. An equilibrium $(\text{P1P2C})_L$ is in the first quadrant when (b_1, b_2) is in the diagonal wedge region (pink and gray). At the end of the wedge (gray) and in other areas, equilibrium $(\text{P1P2C})_L$ is outside of the first quadrant.

The eigenvalue diagrams of the equilibrium solutions in parametric space $b_1 : [0, 5] \times b_2 : [0, 5]$ with a fixed N_T are shown individually in figure (5.2.6). The overall bifurcation diagram for case L is shown in figure (5.2.7). In region J there are two valid $(\text{P1P2C})_L$ equilibria and one valid $(\text{P1P2C})_H$ equilibrium. Thus, there are three (P1P2C) equilibrium solutions in the full model. A non-smooth saddle-node bifurcation occurs on the boundary of regions J and K. It makes the saddle $(\text{P1P2C})_L$ and $(\text{P1P2C})_H$ vanish. Thus, there is only one (P1P2C) equilibrium in region K (the node $(\text{P1P2C})_L$). A transcritical bifurcation occurs on the boundary of regions K and M. So the system changes back to two producer coexistence. Region N is the region after a saddle-node bifurcation on the side plane P_1C. Region N, O, and P represent corresponding results in the one-producer-one-consumer model. (The same holds for regions $\tilde{\text{N}}$, $\tilde{\text{O}}$, and $\tilde{\text{P}}$ since they are the conjugates of N, O, and P).

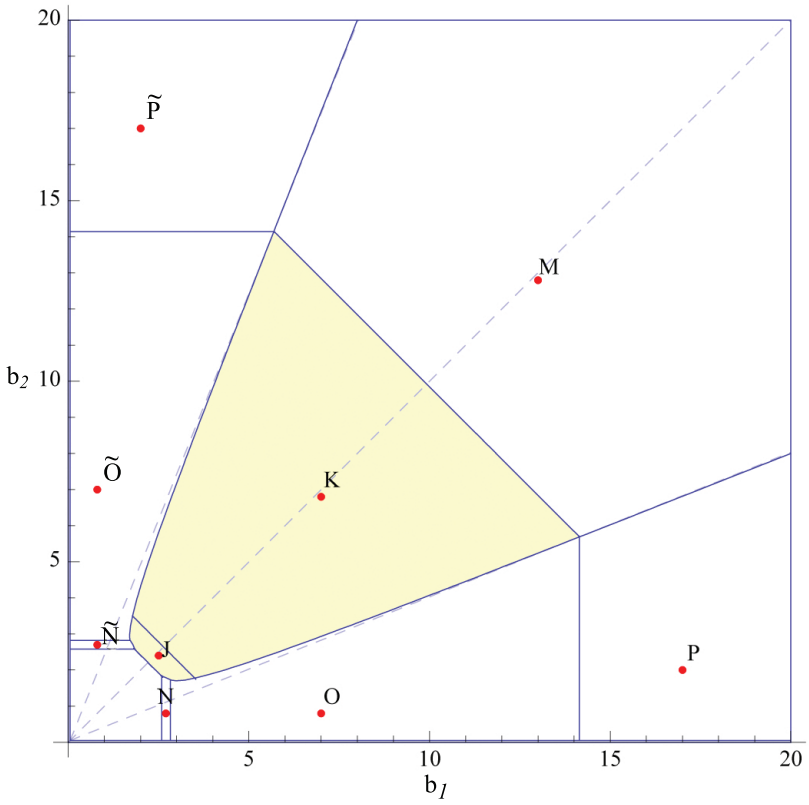

Figure 5.2.7: **A Bifurcation Diagram In Case L (5.2.3)**
There are two layers in this figure. The diagonal dashed line is $b_1 = b_2$ for reference. The other dashed curves indicate the bifurcations on the plane $C = 0$. (Refer to figure (5.2.2(b))) The solid curves indicate the bifurcations in the space $C > 0$. The yellow colored regions are the regions where solutions approach the two producer-consumer coexistence equilibrium or limit cycle.

5.3 The Geometry Of The Limit Cycles

The geometry of the limit cycles seems not to be caused by the stoichiometry since limit cycles come after the Hopf bifurcation and are destroyed by the saddle-node bifurcation in the case L (It happens in one-producer-one-consumer model). The geometry that we concerned in this paper is the order of population growth. It is defined in below.

Definition 1. *In every limit cycle, there is a point V_0 on the cycle that has the shortest distance from the origin. Starting from V_0 and moving along the limit cycle in a forward time, a population that grows at the fastest rate is said to be the "first". The population that grows at the second fastest rate is the "second", and so on. The order of the population growth starting at V_0 is called the sequence of a limit cycle.*

According to the bifurcation diagram (5.2.4), the regions that have limit cycles are C, F, Z, $\tilde{\text{F}}$, and $\tilde{\text{Z}}$. In region C, the whole limit cycle exists in the interior space of P_1P_2C space (See figure (5.3.8(a))). The sequence of a cycle usually is that the producer with the highest growth rate would be the first, the other producer is the second, and the consumer is the last. Depending on the difference between b_1 and b_2 (assuming $b_1 > b_2$), the producer P_1 will grow first, approaching its $C = 0$ carrying capacity, and then the producer P_2 will grow if the difference in b_1 and b_2 is significant. Otherwise, both producers growth simultaneously.

In regions F and $\tilde{\text{F}}$, the limit cycles are on the side plane $P_2 = 0$ and $P_1 = 0$, respectively. The sequence of a cycle is that the producer is first and then consumer is second (last) (See figure (5.3.8(b))).

In regions Z and $\tilde{\text{Z}}$, the limit cycle exists in the interior space without an equilibrium point in the interior. The sequence of a cycle is that the producer with the highest growth rate would be the first. The consumer then starts to grow and the second producer starts to grow at a high rate and then the consumer population continues to increase (See figure (5.3.8(c))).

5.4 A Full Model Of Two Producers And One Consumer

The biomass conversion efficiency is a min function. The system of equations is (5.0.1). A process of selecting valid coexistence equilibria is described in figure (5.4.9). An overall bifurcation diagram with a fixed $N_T = 0.1$ is shown in figure (5.4.10). The figures have two layouts. The light color dashed curves indicate the bifurcations on the plane $C = 0$. (Refers to figure (5.2.2(b))) The solid curves indicate the bifurcations in the space

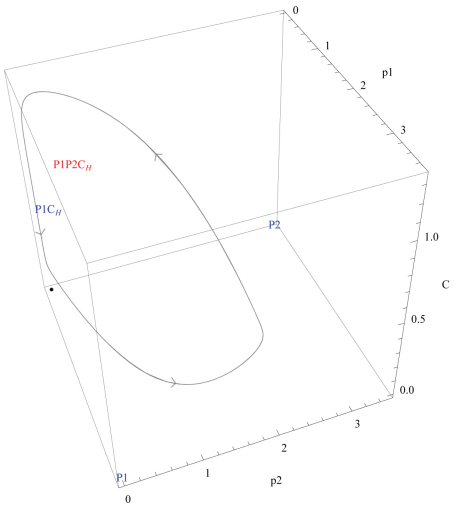

(a) A Limit Cycle In Region C

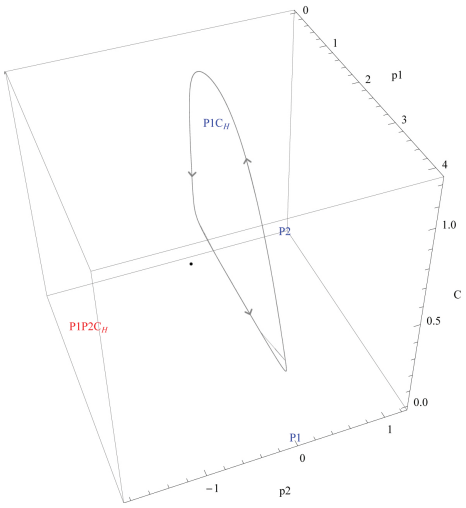

(b) A Limit Cycle In Region F

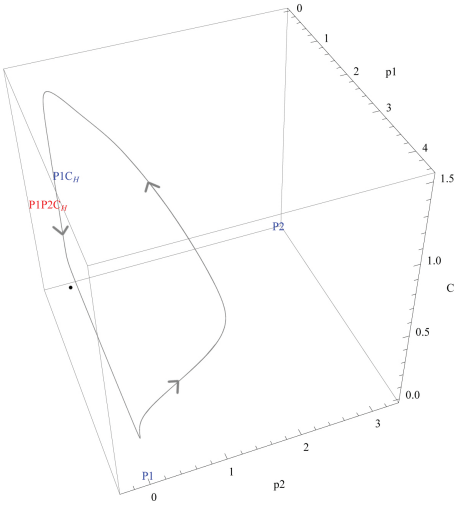

(c) A Limit Cycle In Region Z

Figure 5.3.8: **Limit Cycles**

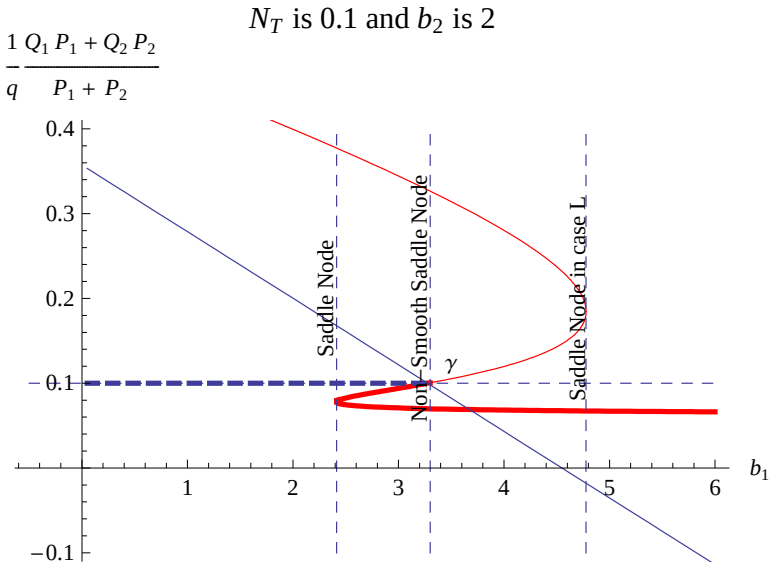

Figure 5.4.9: **A Plot of $\frac{1}{q}\frac{Q_1P_1+Q_2P_2}{P_1+P_2}$ At Coexistence Equilibrium Against b_1 with Fixed N_T and b_2**
The red curve is the efficiency $\frac{1}{q}\frac{Q_1P_1+Q_2P_2}{P_1+P_2}$ according to $(\text{P1P2C})_L$, and the blue line is the efficiency $\frac{1}{q}\frac{Q_1P_1+Q_2P_2}{P_1+P_2}$ according to $(\text{P1P2C})_H$. The horizontal dashed line is γ. The first and second vertical dashed lines indicate the first and non-smooth saddle-node bifurcations. The third dashed line is the saddle-node bifurcation in case L only and does not exist in the full model. Before the first saddle bifurcation, the efficiencies from both cases are always above γ. After the first saddle-node bifurcation, there are two additional efficiencies in case L, which are below γ. As b_1 increases, the efficiency in case H decreases and passes below γ. When the efficiency in case H is equal to γ, one of the case L efficiencies is also equal to γ. Thus, the non-smooth saddle-node bifurcation occurs where $\frac{Q_H}{q} = \gamma$ in the full model.

$C > 0$. The yellow colored regions are the regions where solutions approach the two-producers-one-consumer coexistence equilibrium or limit cycle. A bifurcation diagram of the two-producer-one-consumer model without stoichiometry is shown in figure (5.4.12).

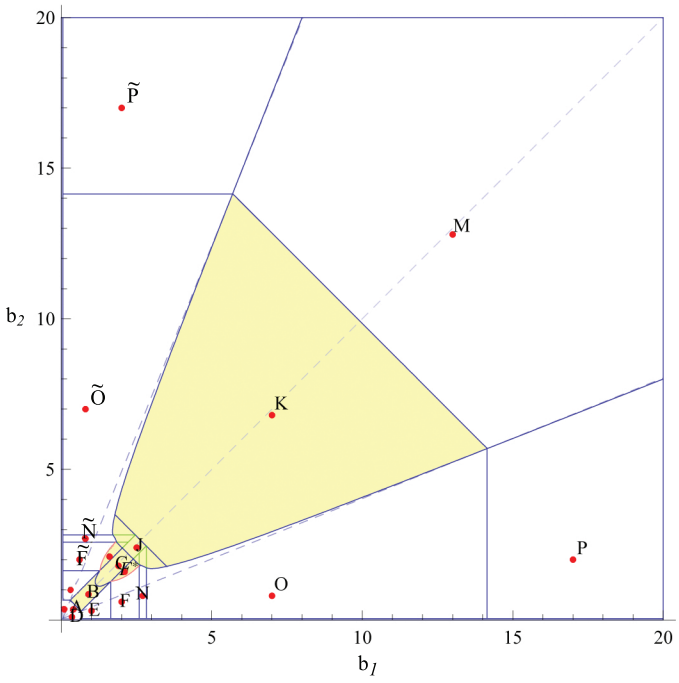

Figure 5.4.10: **A Bifurcation Diagram For The Full System (5.0.1) With Fixed Total Nutrient** $N_T = 0.1$
In the lower left corner, the system behaves more like the case H since the growth rates are relatively low and thus allow high nutrient level in the system. A zoom in on the lower left corner is the next graph (5.4.11).

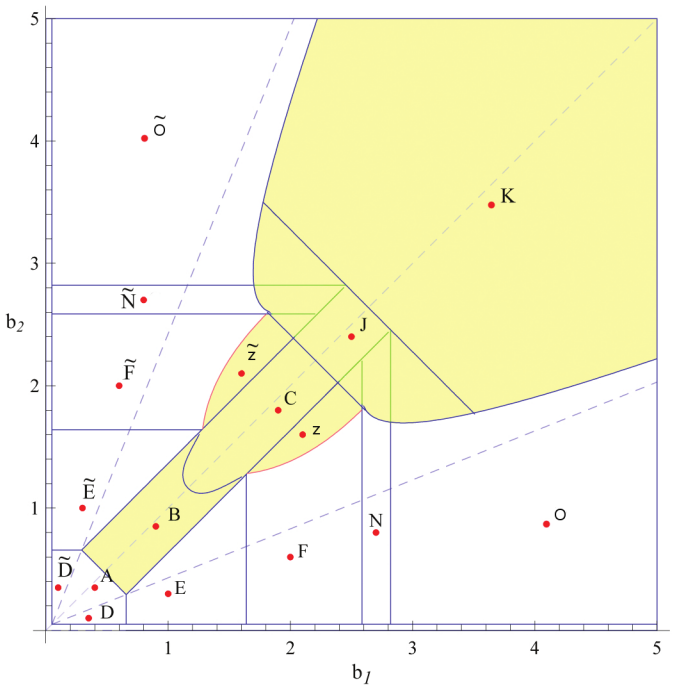

Figure 5.4.11: **A Bifurcation Diagram For The Full System (5.0.1) (Zoom In)** The diagonal dashed line is where $b_1 = b_2$. The other two diagonal dashed lines indicate the wedge-shaped region where (P1P2) is in the first quadrant. There are three coexistence (P1P2C) equilibria in regions N, J, and $\tilde{\text{N}}$. The green lines in region J denote the transcritical bifurcations of $(\text{P1P2C})_H$ and $(\text{P1C})_H$, but do not affect the attracting equilibrium. Crossing the solid border between regions J and N, one of the $(\text{P1P2C})_L$ and one of the $(\text{P1C})_L$ would have a transcritial bifurcation.

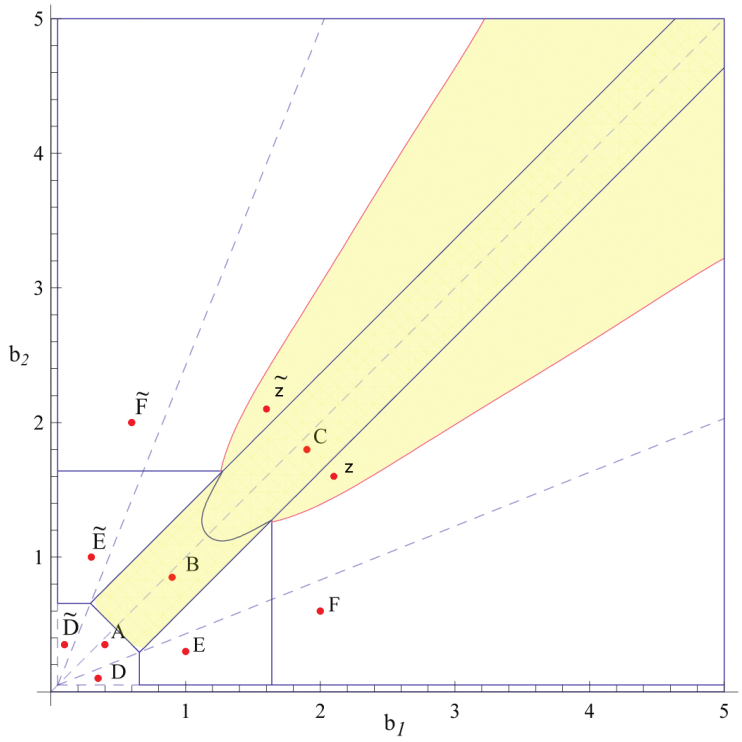

Figure 5.4.12: **A Bifurcation Diagram Of The Two Producer And One Consumer Model Without Stoichiometry**

Regions	Species		Regions	Species
A, M	P_1, P_2		B, J, K	P_1, P_2, C
D, P	P_1		E, N, O	P_1, C
$\tilde{\text{D}}$, $\tilde{\text{P}}$	P_2		$\tilde{\text{E}}$, $\tilde{\text{N}}$, $\tilde{\text{O}}$	P_2, C
C, Z, $\tilde{\text{Z}}$, F, $\tilde{\text{F}}$	P_1, P_2, C (cycle)			

Model (5.0.1) with the parameter settings chosen in this paper supports a typical sequence of bifurcations as the producer growth rates increase. First, one producer is able to survive. Second, the consumer is able to survive. Third, a Hopf bifurcation occurs causing oscillations in the populations of the producer and consumer. Fourth, the population oscillations are stopped by a saddle-node bifurcation. Fifth, consumer is unable to survive due to the poor food quality, and the system changes back to have producers only.

The phase portraits of the regions are shown in figures (5.4.13). Since regions $\tilde{\text{D}}$, $\tilde{\text{P}}$, $\tilde{\text{E}}$, $\tilde{\text{F}}$, $\tilde{\text{Z}}$, $\tilde{\text{N}}$, and $\tilde{\text{O}}$ are the conjugates of regions D, P , E, F, Z, N, and O, the phase portraits in these regions are not shown. In each phase portrait, solutions of P_1, P_2, C, Q_1 and Q_2 with initial values are plotted against the time. Solution orbits are also projected into the P_1P_2C space, and the center of the equilibrium labels are the locations of the equilibria.

The table below describes the bifurcations between any two regions.

Denoting W to this region $(0 \leq b_1 \leq d_{P_1}) \cup (0 \leq b_2 \leq d_{P_2})$.

Regions	Type of Bifurcation	Involved Attractors	Involved Non-Attractors
W → A	Transcritical	(O) → (P1P2)	
W → D	Transcritical	(O) → (P1)	
D → A	Transcritical	(P1) → (P1P2)	
A → B	Transcritical	(P1P2) → $(P1P2C)_H$	
D → E	Transcritical	(P1) → $(P1C)_H$	
E → B	Transcritical	$(P1C)_H$ → $(P1P2C)_H$	
B → C	Hopf	$(P1P2C)_H$ → Interior limit cycle	
E → F	Hopf	$(P1C)_H$ → P_1C plane limit cycle	
F → Z	Transcritical	Limit cycle in P_1C plane → the interior limit cycle	
Z → C	Transcritical	Interior limit cycle → Interior limit cycle	$(P1C)_H$ → $(P1P2C)_H$
C → J	Saddle-node	Interior limit cycle → Stable $(P1P2C)_L$	Two $(P1P2C)_L$ are born
Z → J	Saddle-node	Interior limit cycle → Stable $(P1P2C)_L$	Two $(P1P2C)_L$ are born
F → N	Saddle-node	P_1C plane limit cycle → Stable $(P1C)_L$	Two $(P1C)_L$ are born
N → J	Transcritical	$(P1C)_L$ → $(P1P2C)_L$	
J → K	Non-Smooth Saddle-node	Stable $(P1P2C)_L$ → Stable $(P1P2C)_L$	$(P1P2C)_H$ and $(P1P2C)_L$ (eliminated)
N → O	Non-Smooth Saddle-node	Stable $(P1C)_L$ → Stable $(P1C)_L$	$(P1C)_H$ and $(P1C)_L$ (eliminated)
O → J	Transcritical	$(P1C)_L$ → $(P1P2C)_L$	
O → K	Transcritical	$(P1C)_L$ → $(P1P2C)_L$	
K → M	Transcritical	$(P1P2C)_L$ → (P1P2)	
O → P	Transcritical	$(P1C)_L$ → (P1)	
P → M	Transcritical	(P1) → (P1P2)	

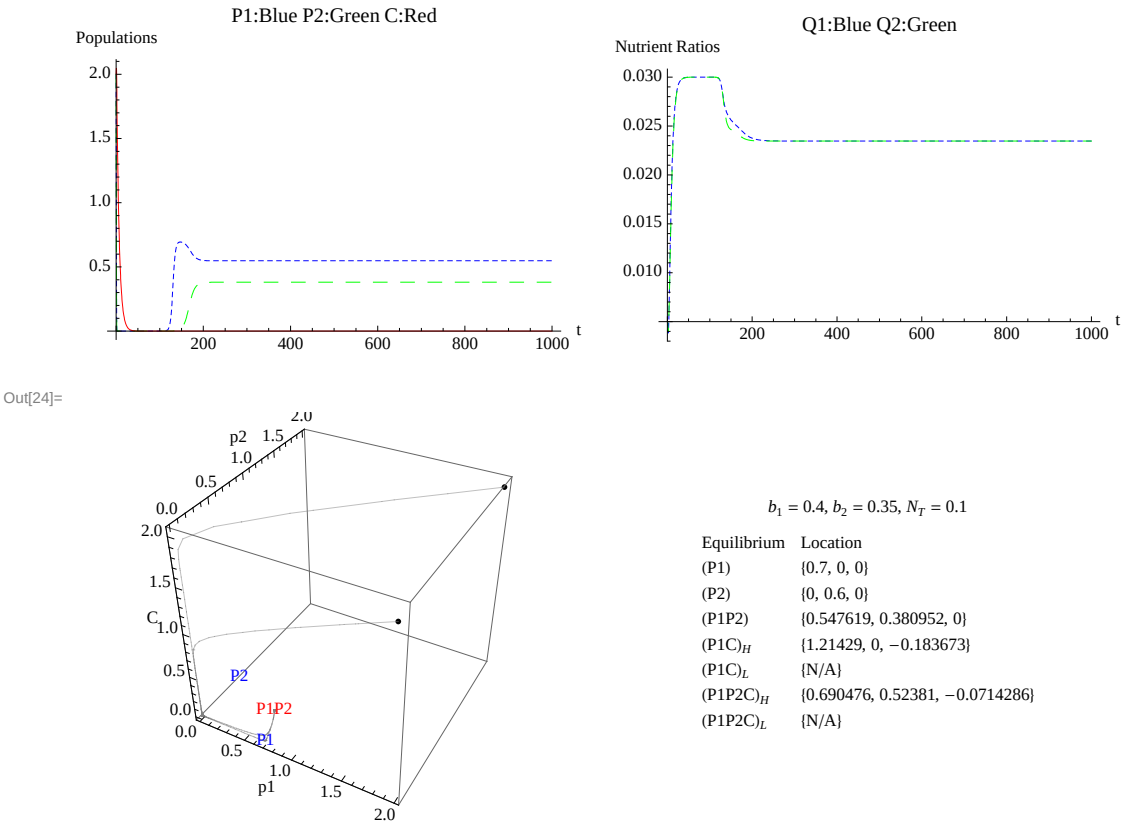

Equilibrium	Location
(P1)	{0.7, 0, 0}
(P2)	{0, 0.6, 0}
(P1P2)	{0.547619, 0.380952, 0}
$(P1C)_H$	{1.21429, 0, −0.183673}
$(P1C)_L$	{N/A}
$(P1P2C)_H$	{0.690476, 0.52381, −0.0714286}
$(P1P2C)_L$	{N/A}

Figure 5.4.13: **A Phase Portrait in Region A**
This is a multiculture system with both producers coexisting under the resource competitions. Two-producer-coexistence equilibrium (P1P2) is in the first quadrant and attracting.

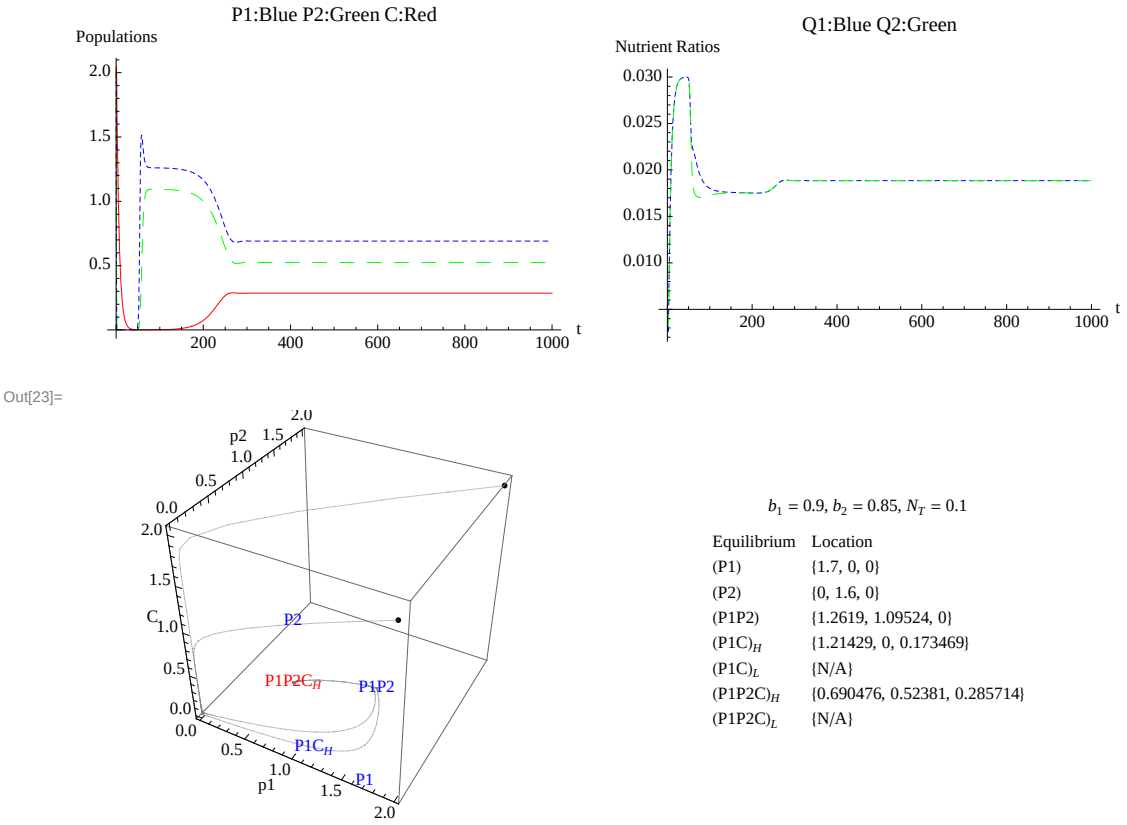

Equilibrium	Location
(P1)	{1.7, 0, 0}
(P2)	{0, 1.6, 0}
(P1P2)	{1.2619, 1.09524, 0}
$(P1C)_H$	{1.21429, 0, 0.173469}
$(P1C)_L$	{N/A}
$(P1P2C)_H$	{0.690476, 0.52381, 0.285714}
$(P1P2C)_L$	{N/A}

Figure 5.4.14: **A Phase Portrait in Region B**
Coexistence equilibrium $(P1P2C)_H$ moves into the first positive quadrant and becomes attracting. Consumers are able to enter the system.

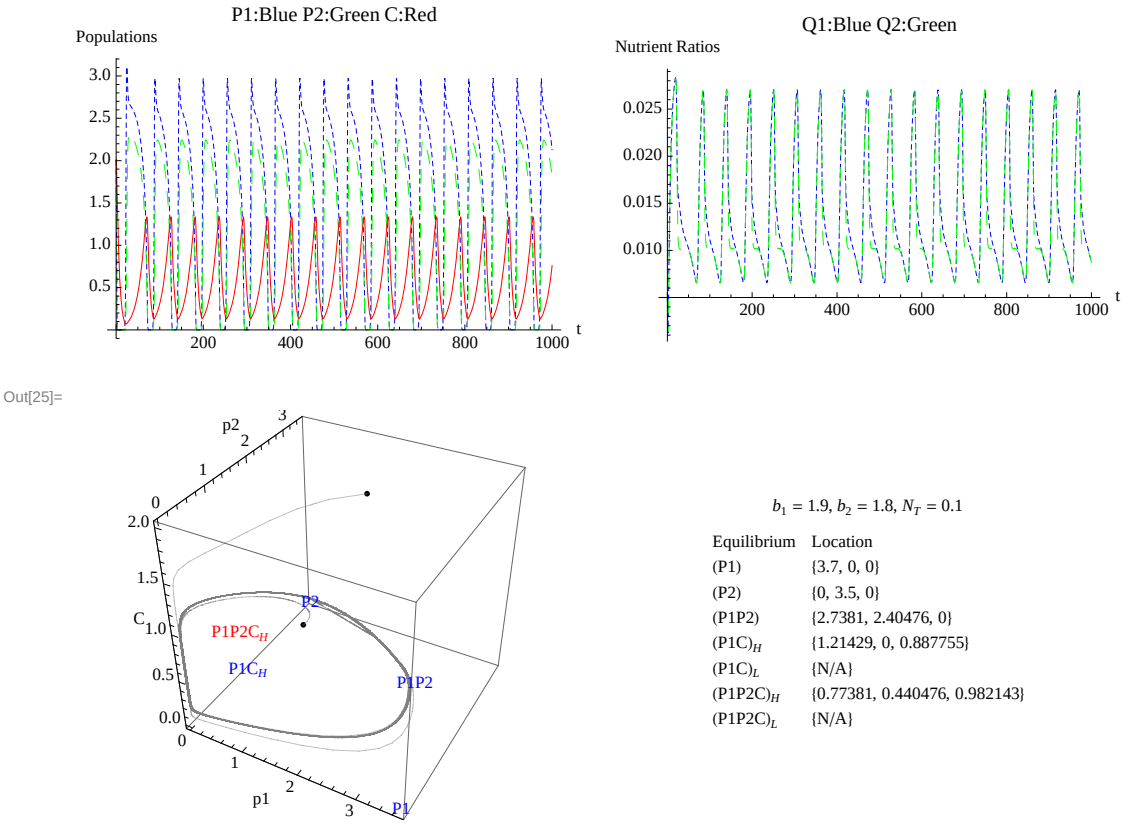

Figure 5.4.15: **A Phase Portrait in Region C**
Solutions of the model approach a limit cycle and equilibrium $(\text{P1P2C})_H$ is in the first positive quadrant.

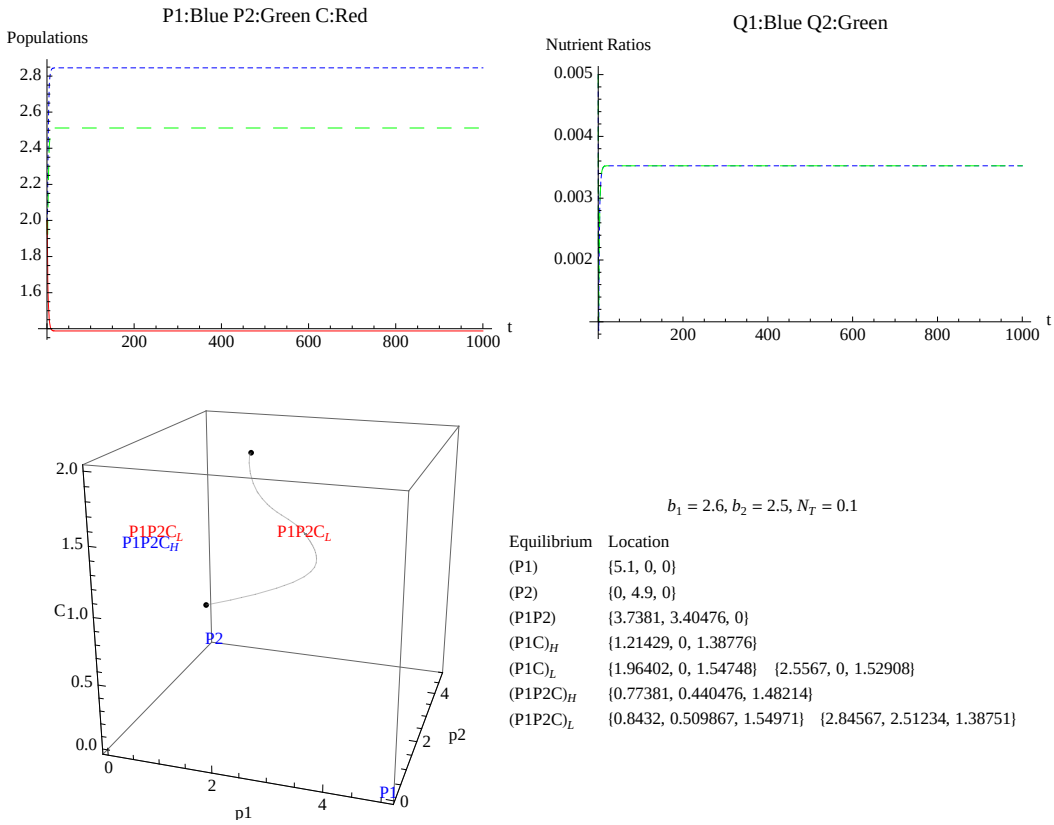

$b_1 = 2.6, b_2 = 2.5, N_T = 0.1$

Equilibrium	Location
(P1)	{5.1, 0, 0}
(P2)	{0, 4.9, 0}
(P1P2)	{3.7381, 3.40476, 0}
$(P1C)_H$	{1.21429, 0, 1.38776}
$(P1C)_L$	{1.96402, 0, 1.54748} {2.5567, 0, 1.52908}
$(P1P2C)_H$	{0.77381, 0.440476, 1.48214}
$(P1P2C)_L$	{0.8432, 0.509867, 1.54971} {2.84567, 2.51234, 1.38751}

Figure 5.4.16: **A Phase Portrait in Region J**
Solutions approach a stable equilibrium $(P1P2C)_L$. There are two additional two-producer-one-consumer coexistence equilibria.

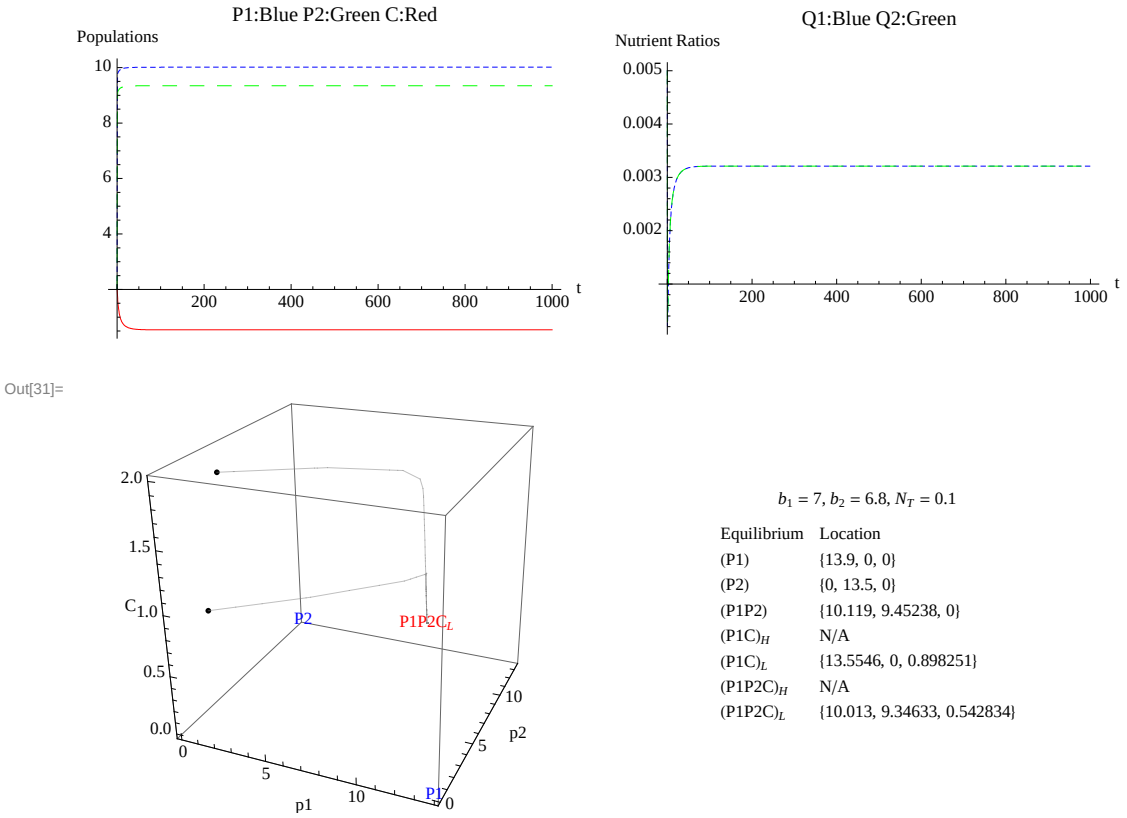

$b_1 = 7, b_2 = 6.8, N_T = 0.1$

Equilibrium	Location
(P1)	{13.9, 0, 0}
(P2)	{0, 13.5, 0}
(P1P2)	{10.119, 9.45238, 0}
$(P1C)_H$	N/A
$(P1C)_L$	{13.5546, 0, 0.898251}
$(P1P2C)_H$	N/A
$(P1P2C)_L$	{10.013, 9.34633, 0.542834}

Figure 5.4.17: **A Phase Portrait in Region K**
Solutions approach a stable equilibrium $(P1P2C)_L$, and there is one two-producer-one-consumer coexistence equilibrium.

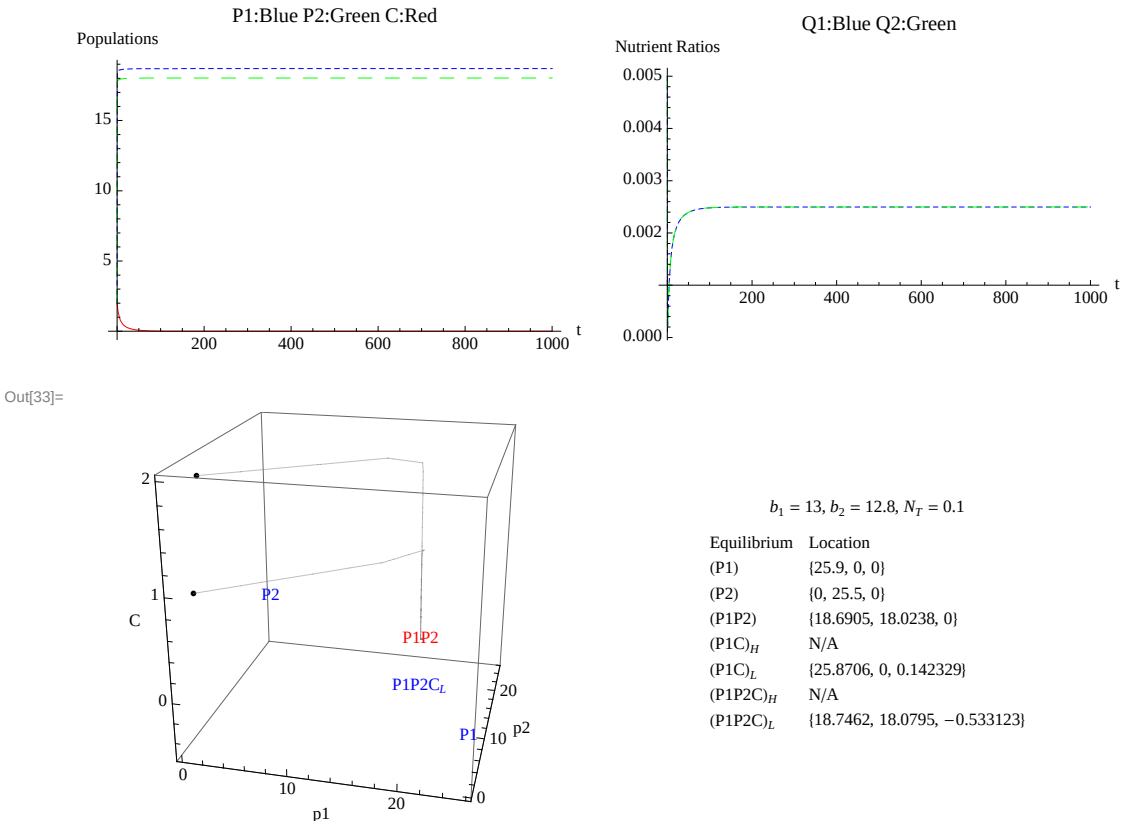

$b_1 = 13, b_2 = 12.8, N_T = 0.1$

Equilibrium	Location
(P1)	{25.9, 0, 0}
(P2)	{0, 25.5, 0}
(P1P2)	{18.6905, 18.0238, 0}
$(P1C)_H$	N/A
$(P1C)_L$	{25.8706, 0, 0.142329}
$(P1P2C)_H$	N/A
$(P1P2C)_L$	{18.7462, 18.0795, −0.533123}

Figure 5.4.18: **A Phase Portrait in Region M**Equilibrium (P1P2) is the attractor.

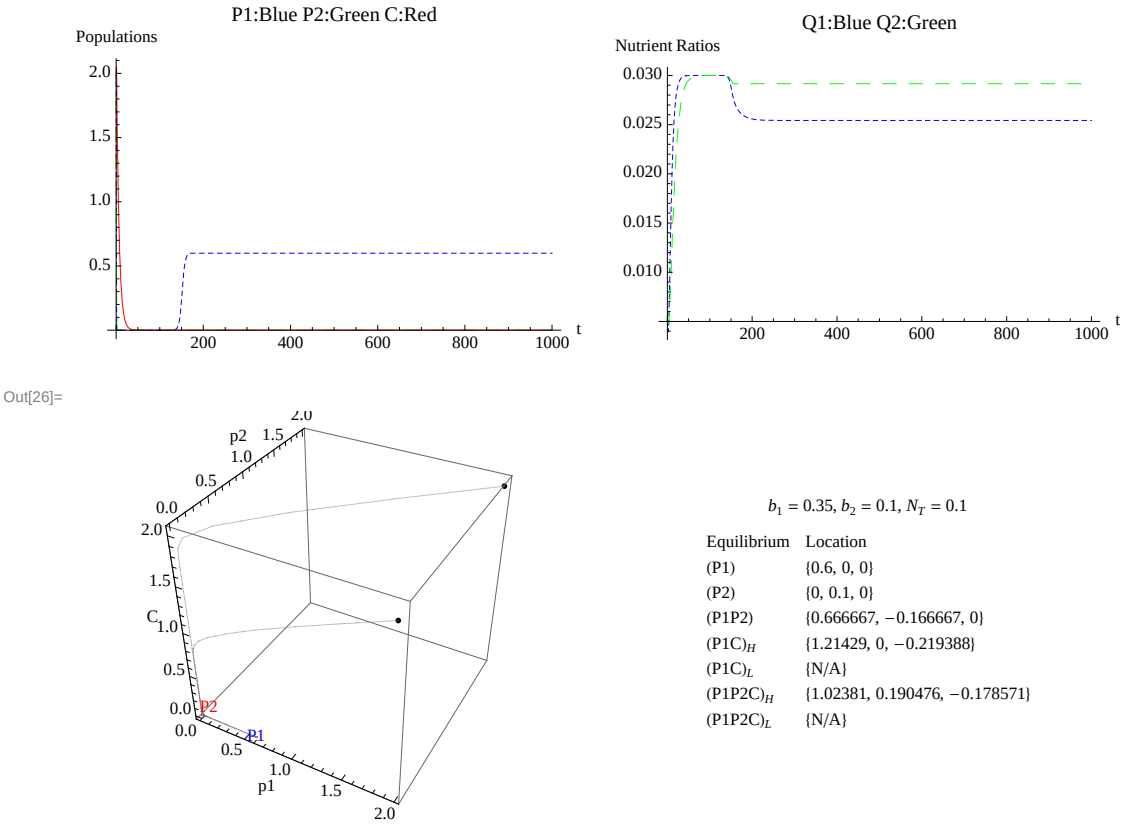

Equilibrium	Location
(P1)	{0.6, 0, 0}
(P2)	{0, 0.1, 0}
(P1P2)	{0.666667, −0.166667, 0}
$(P1C)_H$	{1.21429, 0, −0.219388}
$(P1C)_L$	{N/A}
$(P1P2C)_H$	{1.02381, 0.190476, −0.178571}
$(P1P2C)_L$	{N/A}

Figure 5.4.19: **A Phase Portrait in Region D**
This is a monoculture system with only one producer. Equilibrium (P1) is attracting.

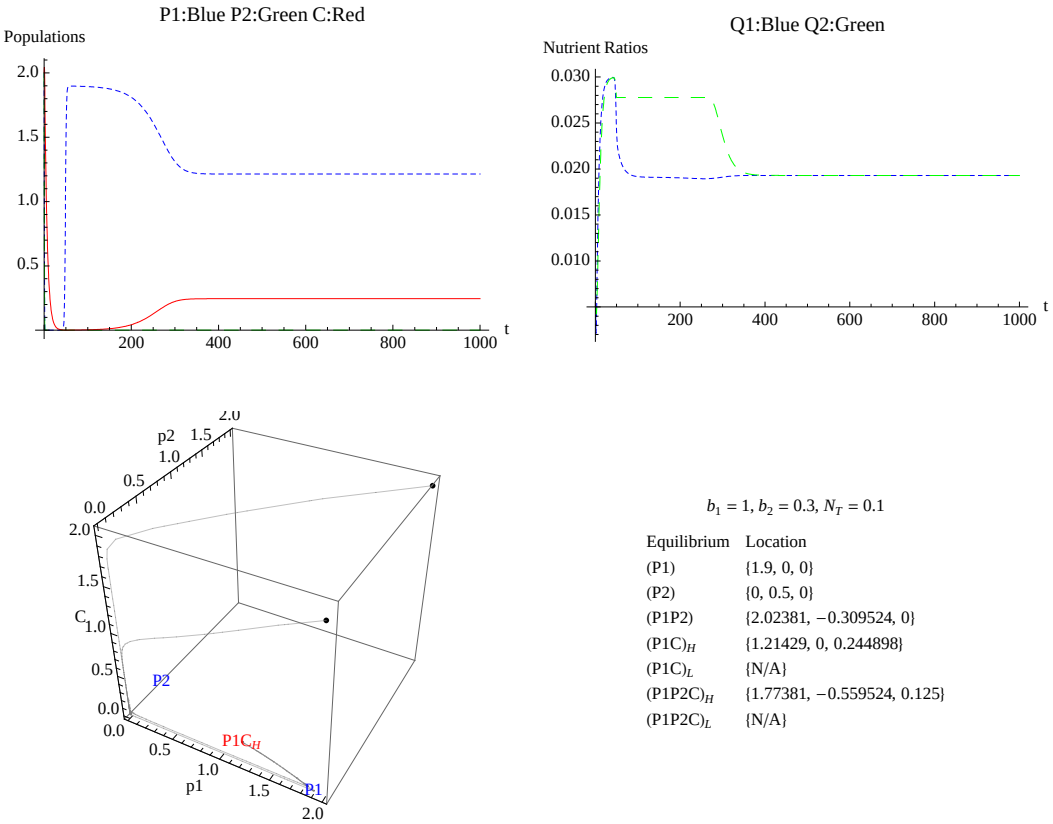

$b_1 = 1, b_2 = 0.3, N_T = 0.1$

Equilibrium	Location
(P1)	{1.9, 0, 0}
(P2)	{0, 0.5, 0}
(P1P2)	{2.02381, −0.309524, 0}
$(P1C)_H$	{1.21429, 0, 0.244898}
$(P1C)_L$	{N/A}
$(P1P2C)_H$	{1.77381, −0.559524, 0.125}
$(P1P2C)_L$	{N/A}

Figure 5.4.20: **A Phase Portrait in Region E**
Equilibrium $(P1C)_H$ is attracting in the P_1C plane.

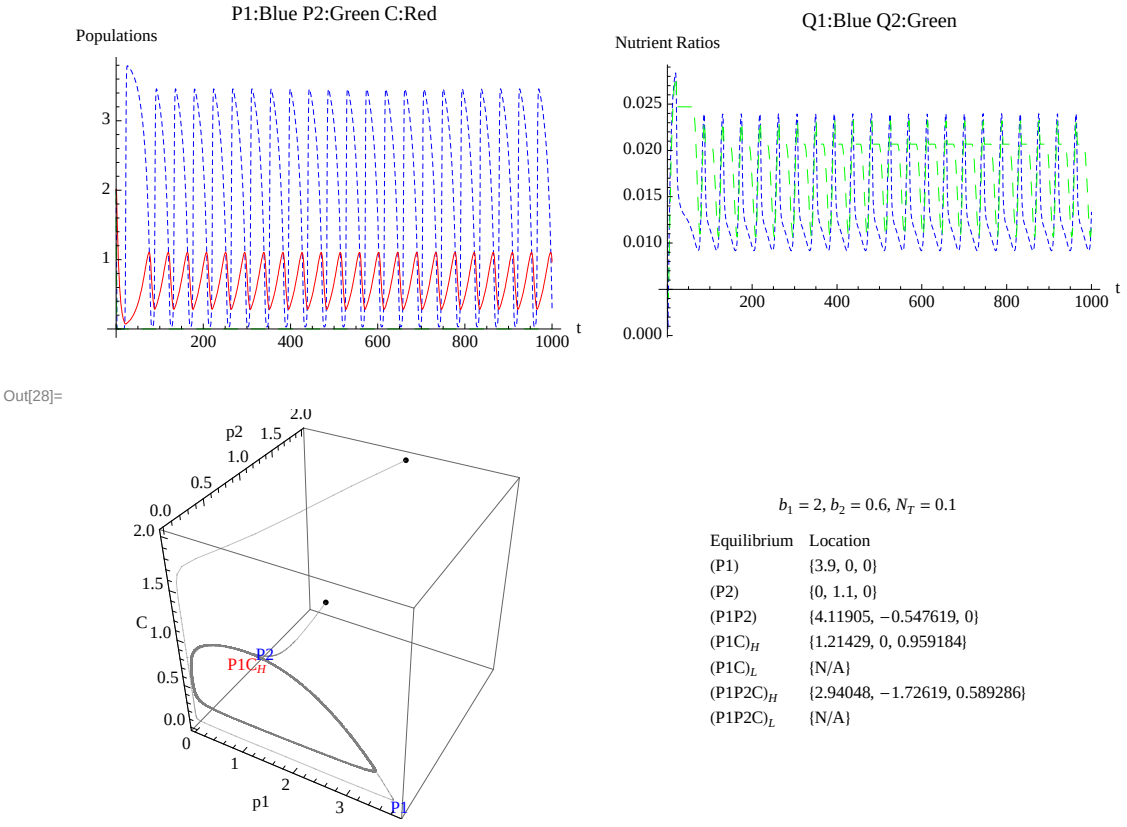

$b_1 = 2, b_2 = 0.6, N_T = 0.1$

Equilibrium	Location
(P1)	{3.9, 0, 0}
(P2)	{0, 1.1, 0}
(P1P2)	{4.11905, −0.547619, 0}
$(P1C)_H$	{1.21429, 0, 0.959184}
$(P1C)_L$	{N/A}
$(P1P2C)_H$	{2.94048, −1.72619, 0.589286}
$(P1P2C)_L$	{N/A}

Figure 5.4.21: **A Phase Portrait in Region F**
Solutions approaches a limit cycle on the P_1C plane.

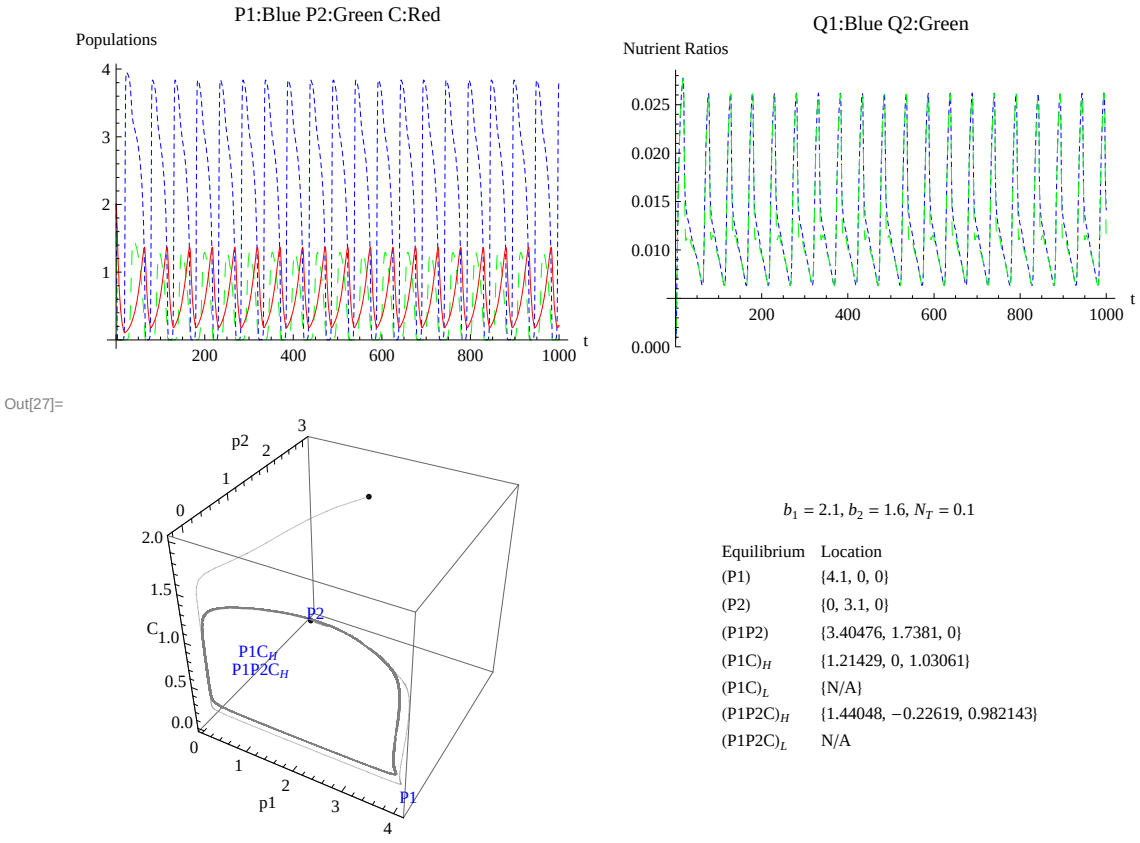

$b_1 = 2.1, b_2 = 1.6, N_T = 0.1$

Equilibrium	Location
(P1)	{4.1, 0, 0}
(P2)	{0, 3.1, 0}
(P1P2)	{3.40476, 1.7381, 0}
$(P1C)_H$	{1.21429, 0, 1.03061}
$(P1C)_L$	{N/A}
$(P1P2C)_H$	{1.44048, −0.22619, 0.982143}
$(P1P2C)_L$	N/A

Figure 5.4.22: **A Phase Portrait in Region Z**
The limit cycle on the P_1C plane is unstable, and solutions approach a limit cycle in the interior positive quadrant. However, there is no equilibrium in the positive quadrant.

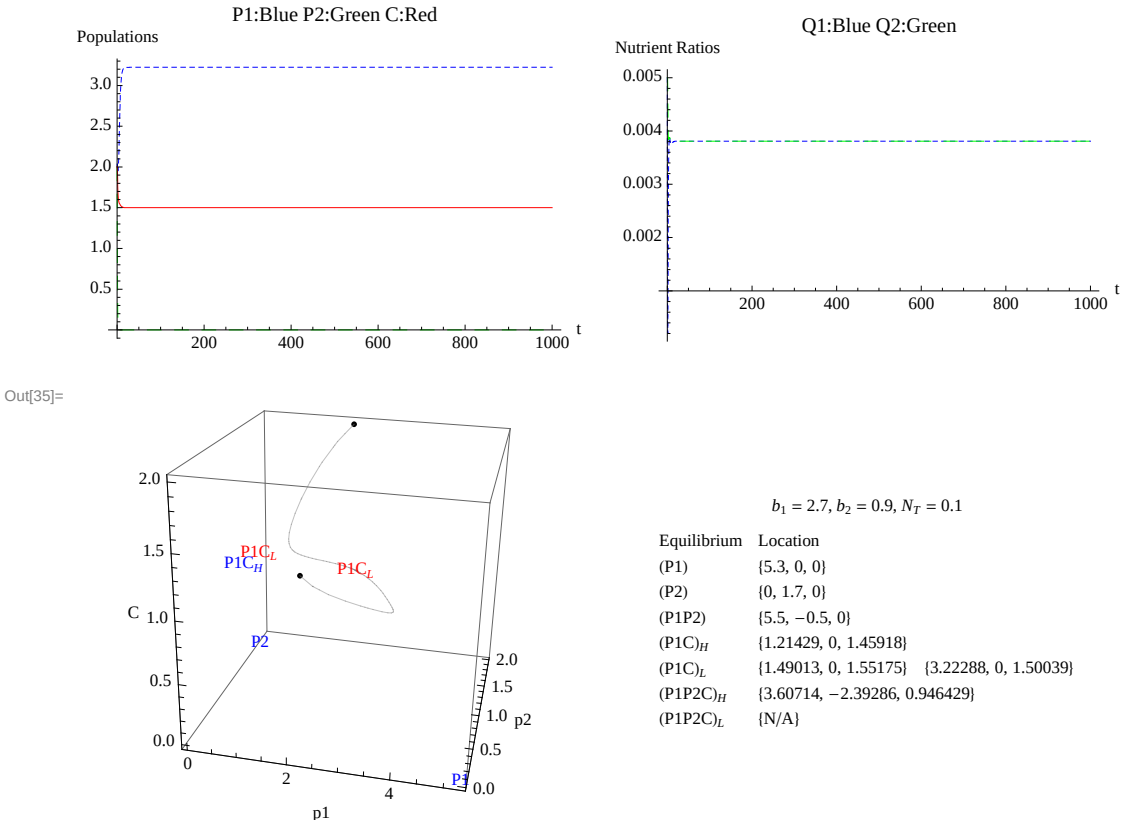

$b_1 = 2.7$, $b_2 = 0.9$, $N_T = 0.1$

Equilibrium	Location
(P1)	{5.3, 0, 0}
(P2)	{0, 1.7, 0}
(P1P2)	{5.5, −0.5, 0}
$(P1C)_H$	{1.21429, 0, 1.45918}
$(P1C)_L$	{1.49013, 0, 1.55175} {3.22288, 0, 1.50039}
$(P1P2C)_H$	{3.60714, −2.39286, 0.946429}
$(P1P2C)_L$	{N/A}

Figure 5.4.23: **A Phase Portrait in Region N**
Solutions approach an attracting coexistence equilibrium $(P1C)_L$ in the P_1C plane. There are two additional one-producer-one-consumer coexistence equilibria in the P_1C plane.

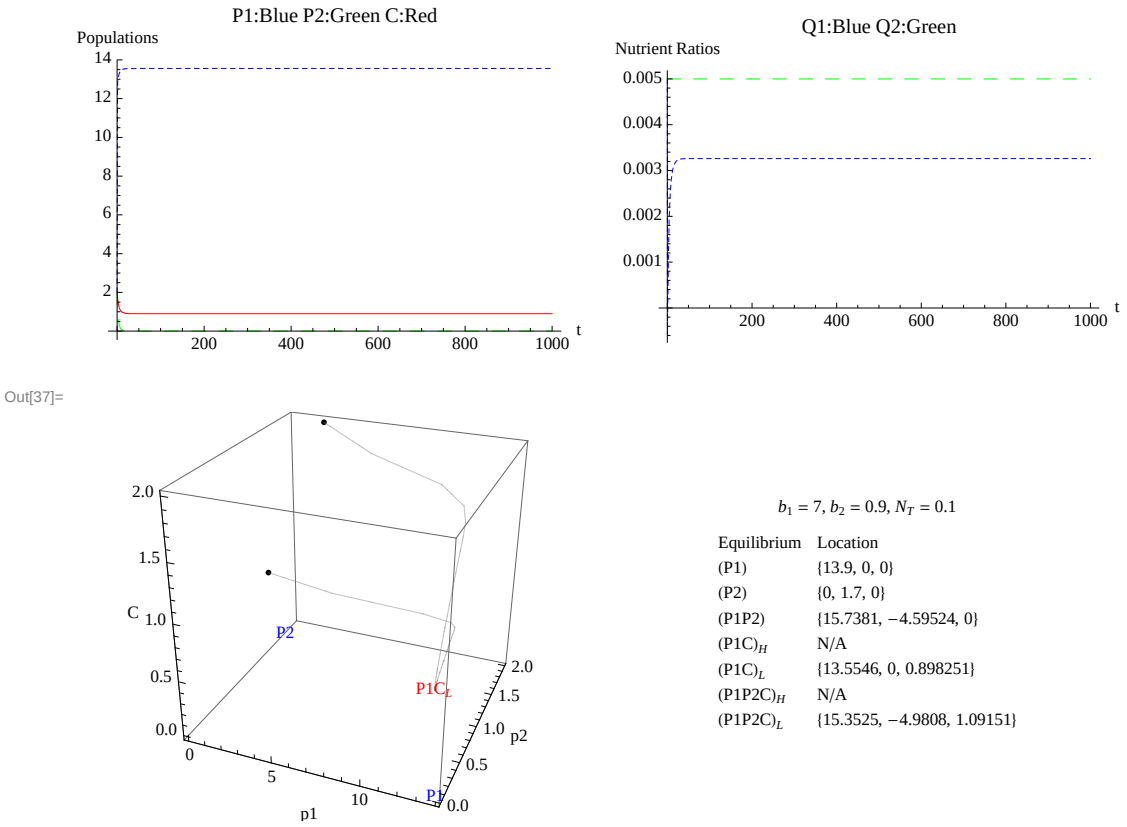

$b_1 = 7, b_2 = 0.9, N_T = 0.1$

Equilibrium	Location
(P1)	{13.9, 0, 0}
(P2)	{0, 1.7, 0}
(P1P2)	{15.7381, −4.59524, 0}
$(P1C)_H$	N/A
$(P1C)_L$	{13.5546, 0, 0.898251}
$(P1P2C)_H$	N/A
$(P1P2C)_L$	{15.3525, −4.9808, 1.09151}

Figure 5.4.24: **A Phase Portrait in Region O**
Solutions approach an attracting coexistence equilibrium $(P1C)_L$ in the P_1C plane; there is no other one-producer-one-consumer coexistence equilibrium (P1C) in the P_1C plane.

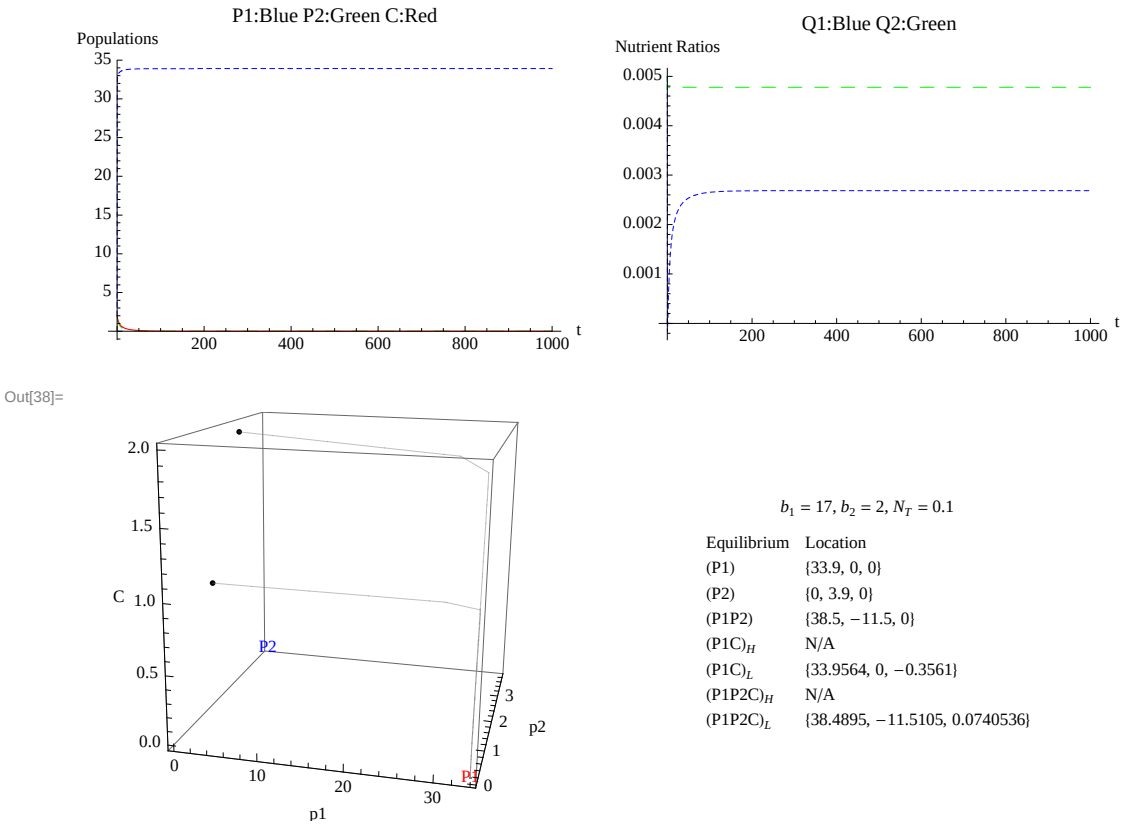

$b_1 = 17, b_2 = 2, N_T = 0.1$

Equilibrium	Location
(P1)	{33.9, 0, 0}
(P2)	{0, 3.9, 0}
(P1P2)	{38.5, −11.5, 0}
$(P1C)_H$	N/A
$(P1C)_L$	{33.9564, 0, −0.3561}
$(P1P2C)_H$	N/A
$(P1P2C)_L$	{38.4895, −11.5105, 0.0740536}

Figure 5.4.25: **A Phase Portrait in Region P**Equilibrium (P1) is attracting.

6 Conclusions

The model in this paper is a generalization of the Rosenzweig and MacArthur model (see equations (2.0.2)), which is a single-producer-single-consumer model. First, we introduce stoichiometry into Rosenzweig and MacArthur model. Second, we consider having two producers instead of one in Rosenzweig and MacArthur model. Finally we consider two producer one consumer model with stoichiometry.

Due to the stoichiometry, both models with one producer and two producers have more than the three bifurcations typically observed in the Rosenzweig and MacArthur model. As the producer's growth rates increase with a fixed amount of nutrient in the system, there is a typical sequence of bifurcations: a first transcritical for the producer entering the system, a second transcritical for the consumer entering and surviving, a Hopf creating coexistence limit cycles, a first saddle-node destroying the cycles, a second saddle-node taking the two "extra" saddle coexistence equilibria away, and a transcritical for the consumer leaving the system. The first saddle-node bifurcation occurs on the limit cycle, and destroys the periodic solution. Orbits which previously approached a limit cycle will now approach a coexistence equilibrium. That attracting equilibrium is the node born in the saddle-node bifurcation. Before the second saddle node bifurcation, there is a total of three coexistence equilibrium solutions, one from case H, and the other two from the first saddle node bifurcation in case L. When the second saddle node bifurcation occurs, the saddle coexistence equilibrium solution from case L and coexistence equilibrium solution from case H merge and vanished (see figure (4.3.6) and (5.4.9)).

By adding a second producer, some additional factors, such as the variation of producers (in terms of the growth rates) and the competition between the two producers, can be introduced into the model. When the producers' growth rates are low (allowing relatively high nutrient food to the consumer), the criteria for coexistence of both producers and the consumer is highly exclusive to the variations of producers' growth rates. If growth rates are not chosen from a narrow band along the $b_1 = b_2$ diagonal, the producer with a lower growth rate will go extinct, and the system changes to an one-producer-one-consumer model. When the producers' growth rates are high (providing relatively low nutrient to the consumer), the criteria for coexistence of both producers and the consumer is more tolerant to the variations of producers' growth rates, and approaches the criteria for coexistence of both producers in the absence of the consumer. (See the yellow coexistence regions in figures (5.4.10) and (5.4.11)). When the growth rates are sufficiently high, there is no more two-producer-one-consumer coexistence (region M).

Another impact of adding a second producer is to allow the limit cycles to have more interesting geometry. Limit cycles can exist in the case of two producers and one consumer for certain growth rates b_1 and b_2. All appear to have been born in Hopf bifurcations (see

figure (5.2.4)). Usually, the growth sequence starting from low population values is (1) the producer with a higher growth rate, (2) the producer with a lower growth rate, and then (3) the consumer. The time interval of traveling from step (1) to step (2) is short. If both producer growth rates are very close, then step (1) and step (2) happen simultaneously. Once the populations of producers approach their carrying capacities, consumers start to grow (See figure (5.3.8(a))). There are some exceptional cases in which the limit cycle starts with (1) the faster growing producer, (2) consumer, and (3) the slower growing producer (See figure (5.3.8(c))). This happens when the growth rates of both producers are significantly different.

In brief, the introduction of a stoichiometry to the model causes the loss of large amplitude limit cycles. Because the total nutrient N_T is fixed, a sufficiently high growth in producers results in the extinction of the consumer. Adding second primary parameter (the second growth rate) creates additional interesting bifurcations (see figures (5.4.10) and (5.4.11)) and provides the criteria of two-producer-one-consumer coexistence in the long run.

7 Appendix

I Biomass Conversion Rate With Two Food Sources

Assume there are two food sources for the consumers. f_1 and f_2 are the predation rates for producers P_1 and P_2. Let γ be the optimal biomass conversation efficiency, and Q be the stoichiometric ratio of the food (the producers) in the gut. Assume that $1-\gamma$ of ingested carbohydrates are excreted or respired. There is a relationship between γ and Q.

The nutrient concentration in the refined food in the gut is

$$Q_{gut} = \frac{1}{\gamma}[\frac{\text{rate of nutrient ingestion}}{\text{rate of carbohydrate ingestion}}]$$

The rate of consumer conversion of nutrients is

$$\begin{cases} q \times \text{rate of generating refined carbons} & , \quad \text{if Q} > \text{q}, \\ \frac{Q}{q} \times q \times \text{rate of generating refined carbons} & , \quad \text{if Q} \leq \text{q} \end{cases}$$

$$= \text{rate of generating refined carbons} \times \begin{cases} q & , \quad if\ Q > q, \\ Q & , \quad if\ Q \leq q \end{cases}$$

$$= \gamma \times \text{rate of carbohydrate ingestion} \times \min[\text{q}, \text{Q}]$$

$$= q \times \text{rate of carbohydrate ingestion} \times \min[\gamma, \tfrac{1}{\text{q}}[\tfrac{\text{rate of nutrient ingestion}}{\text{rate of carbohydrate ingestion}}]]$$

Note that the rate of generating refined carbons is assumed to be $\gamma\times$rate of carbohydrate ingestion.

From the above, $\{\text{rate of carbohydrate ingestion} \times \min[\gamma, \frac{1}{\text{q}}[\frac{\text{rate of nutrient ingestion}}{\text{rate of carbohydrate ingestion}}]]\}$ is the consumer biomass conversion rate. The ingestion rates of producers one and two are f_1C and f_2C. The ingestion rate of nutrient from producers one and two are Q_1f_1C and Q_2f_2C, respectively. Therefore, the biomass conversion rate is

$$\min[\gamma, \frac{1}{q}[\frac{Q_1f_1C + Q_2f_2C}{f_1C + f_2C}]](f_1C + f_2C)$$

$$= \min[\gamma, \frac{1}{q}[\frac{Q_1f_1 + Q_2f_2}{f_1 + f_2}]](f_1C + f_2C)].$$

In our model, $f_1 = af(P_1 + P_2) = \frac{P_1}{P_1+P_2} f(P_1 + P_2)$ and $f_2 = (1-a)f(P_1 + P_2) = \frac{P_2}{P_1+P_2} f(P_1 + P_2)$. Thus, the biomass conversion rate in our model is

$$\min[\gamma, \tfrac{1}{q}[\frac{Q_1 \frac{P_1}{P_1+P_2} f(P_1+P_2) + Q_2 \frac{P_2}{P_1+P_2} f(P_1+P_2)}{\frac{P_1}{P_1+P_2} f(P_1+P_2) + \frac{P_2}{P_1+P_2} f(P_1+P_2)}]](\frac{P_1}{P_1+P_2} f(P_1 + P_2)C + \frac{P_2}{P_1+P_2} f(P_1 + P_2)C)$$

$$= \min[\gamma, \tfrac{1}{q}[\frac{Q_1 P_1 + Q_2 P_2}{P_1+P_2}]] f(P_1 + P_2)C.$$

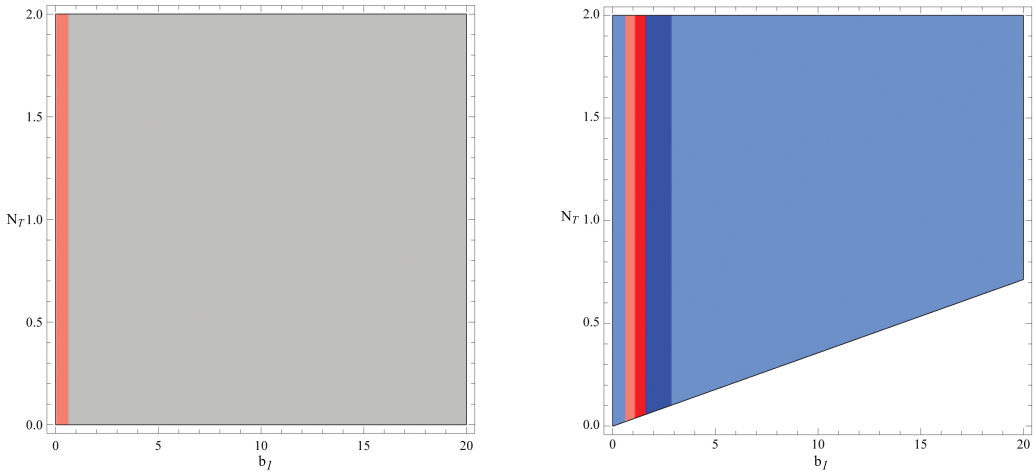

(a) $(P1)_H$ (b) $(P1C)_H$

Figure 7.2.1: Eigenvalue Plot (The color scheme is described in table (7.2.1))

II The Eigenvalue Plots For Equilibrium $(P1)_H$ And $(P1C)_H$

The Eigenvalue plots for equilibrium $(P1)_H$ and $(P1C)_H$ for model (4.2.2) in the parametric space $b_1 : [0, 20] \times N_T : [0, 2]$ are shown in figure (7.2.1). The colors indicate the eigenvalue states of the equilibrium solution in the sets of parameters b_1 and N_T. The lower right corners in graphs are not colored because the solutions $(P1)_H$ and $(P1C)_H$ are unable to provide enough nutrient Q_1 to satisfy $\frac{Q_1}{q} \geq \gamma$.

Color	Number of Eigenvalue with a Positive Real Part	Stability
	Real Eigenvalues	
Pink / Salmon	0	Attracting
Silver	1	Saddle
Light Blue	2	Saddle
Magenta	3	Repelling
	Complex Eigenvalues	
Red	0	Attracting
Gray	1	Saddle
Blue	2	Saddle
Purple	3	Repelling

Table 7.2.1: Color Scheme for figure (7.2.1)

$(\mathrm{P1})_H$ and $(\mathrm{P1C})_H$ are equilibrium solutions in case H when $\frac{N_T\lambda_{11}\beta}{\lambda_{11}+(b_1-d_{p_1})\beta} > q\gamma$ and $\frac{\beta(N_T(\alpha\gamma-d_c)-hq\gamma(b_1-d_{p_1}))}{\alpha\gamma-d_c(h\beta-1)} > q\gamma$ respectively. Between the region $b_1 = 0$ and $b_1 = d_{P_1} = 0.05$, the equilibrium $(\mathrm{O})_H$ is attracting. As b_1 increases, a transcritial bifurcation occurs at $b_1 = 0.05$. The stabilities of equilibrium $(\mathrm{O})_H$ and equilibrium $(\mathrm{P1})_H$ exchange. From $b_1 = 0.05$ to $b_1 = d_{P_1} + \frac{h\lambda_{11}d_c}{\alpha\gamma-d_c} = 0.6571$, equilibrium $(\mathrm{P1})_H$ is attracting. At $b = 0.6571$, another transcritial bifurcation occurs exchanging the stabilities of $(\mathrm{P1})_H$ and $(\mathrm{P1C})_H$. In other words, there is enough food supply for the consumer to entry the system. As b_1 increases further, a damped oscillation occurs in the solution curve of (P_1, C). At $b_1 = 1.6393$, a Hopf bifurcation occurs, which is indicated in the $(\mathrm{P1C})_H$ plot where the color is changed from RED to BLUE. The solution of (P_1, C) now forms a limit cycle. As b_1 further increases, the cycle enlarges in the geometric sense. The population curves of P_1 and C have a high amplitude oscillation. The phase portraits from different regions of parameter space $b_1 \times N_T$ are shown below.

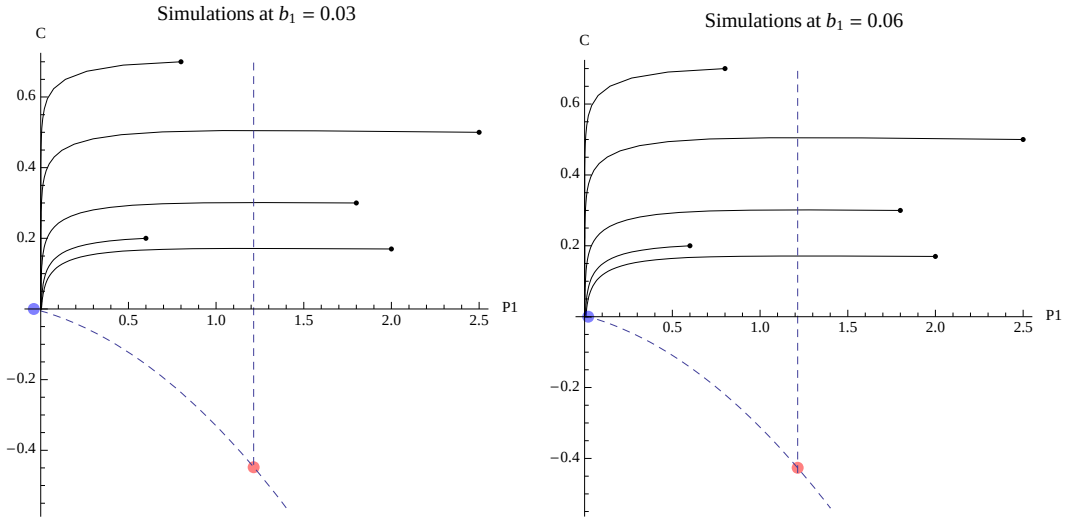

At $b_1 = 0.03$, both equilibrium solutions $(\text{P1})_H$ and $(\text{P1C})_H$ are outside the first octant. All five simulated solutions (with different initial values) are going to the origin, which is an attracting equilibrium point when $b_1 < d_{P_1} = 0.05$. When $b_1 = 0.06$, $(\text{P1})_H$ comes into the first octant and becomes attracting after a transcritical bifurcation with the origin at $b_1 = d_{P_1}$.

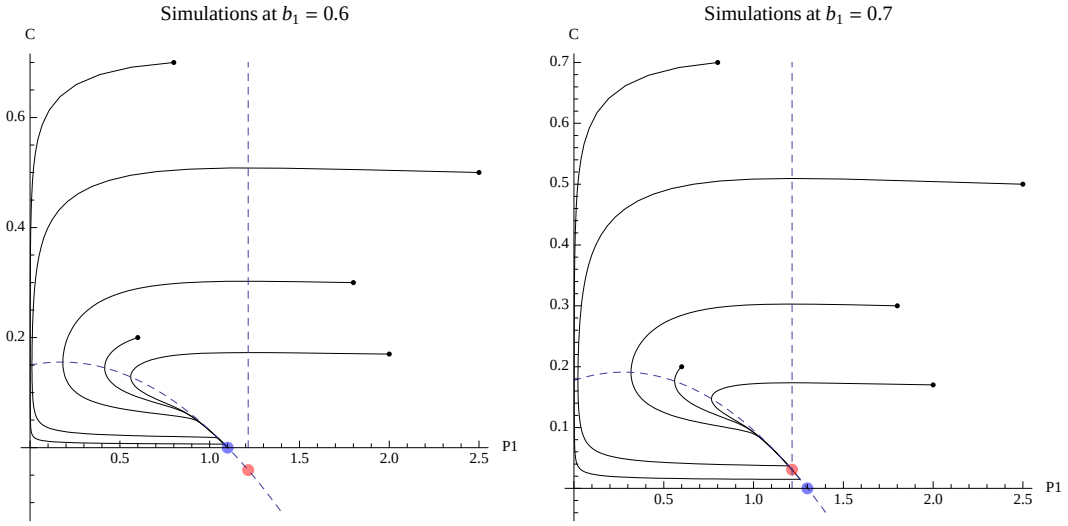

At $b_1 = 0.6$, the equilibrium $(\text{P1C})_H$ is outside the first octant. All simulated solutions approach $(\text{P1})_H$. At $b_1 = 0.7$, $(\text{P1C})_H$ comes into the first octant and becomes attracting after a transcritical bifurcation with $(\text{P1})_H$ at $b_1 = d_{P_1} + \frac{h\lambda_{11}d_c}{\alpha\gamma - d_c} = 0.6571$.

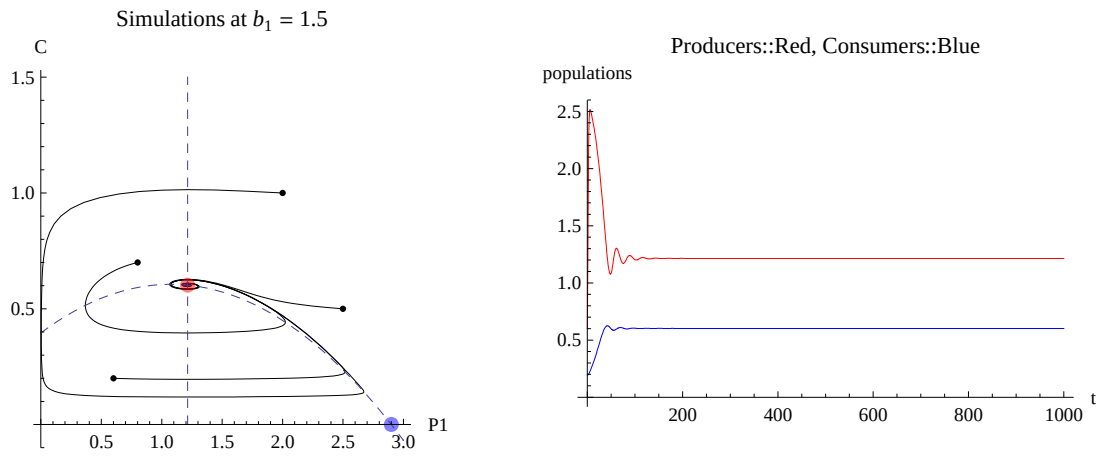

At $b_1 = 1.5$, $(\text{P1C})_H$ is still attracting, but populations have some damped oscillations at the beginning of time.

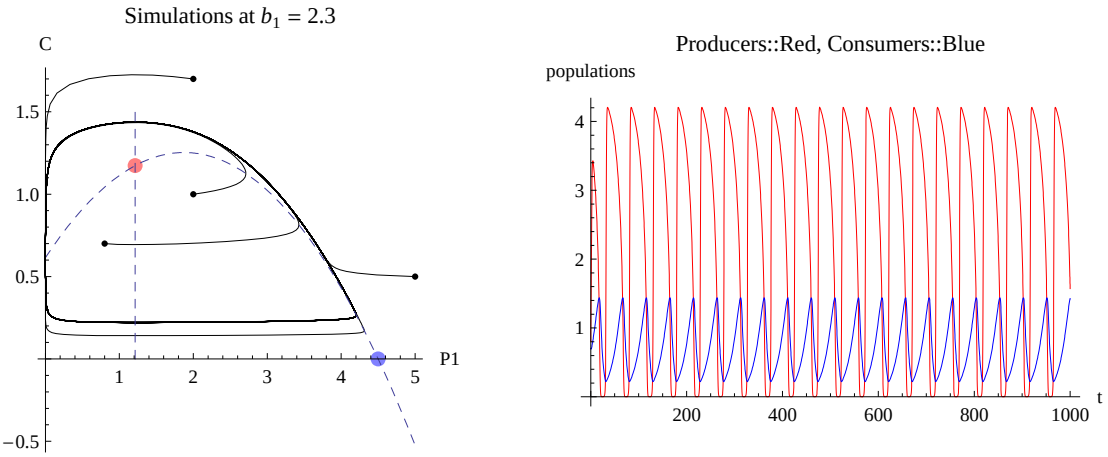

At $b_1 = 2.3$, $(\text{P1C})_H$ has gone through a Hopf bifurcation. The simulated solutions approach an attract limit cycle rather than the equilibrium point $(\text{P1C})_H$.

III Finding $(P1C)_L$ In The One-Producer-One-Consumer Model

Assuming the biomass conversion efficiency depends on the nutrient carbon ratio in producer.

$$\begin{cases} \frac{dC}{dt} &= (\frac{Q_1}{q}\frac{\alpha(P_1)}{h+(P_1)} - d_c)C \\ \frac{dP_1}{dt} &= (b_1 - \lambda_{11}P_1 - d_{p_1} - \frac{\alpha C}{h+(P_1)})P_1 \\ \frac{dQ_1}{dt} &= ((N_T - qC - Q_1P_1)\beta - Q_1)(b_1 - \lambda_{11}P_1) \end{cases} \tag{7.3.1}$$

Set $\frac{dC}{dt}$, $\frac{dP_1}{dt}$, and $\frac{dQ_1}{dt}$ to zero.

$$\begin{cases} \frac{Q_1}{h+(P_1)} &= \frac{qd_c}{\alpha}\frac{1}{P_1} \\ \frac{\alpha C}{h+(P_1)} &= b_1 - \lambda_{11}P_1 - d_{p_1} \\ \frac{N_T}{h+P_1} &= \frac{Q_1}{h+P_1}(\frac{1}{\beta} + P_1) + \frac{q}{\alpha}\frac{\alpha C}{h+P_1} \end{cases}$$

$$\frac{N_T}{h+P_1} = \frac{qd_c}{\alpha}\frac{1}{P_1}(\frac{1}{\beta} + P_1) + \frac{q}{\alpha}(b_1 - \lambda_{11}P_1 - d_{p_1})$$

$$N_TP_1 = \frac{qd_c}{\alpha}(\frac{1}{\beta} + P_1)(h+P_1) + \frac{qP_1}{\alpha}(b_1 - \lambda_{11}P_1 - d_{p_1})(h+P_1)$$

$$\frac{qd_c}{\alpha}(\frac{1}{\beta} + P_1)(h+P_1) + \frac{qP_1}{\alpha}(b_1 - \lambda_{11}P_1 - d_{p_1})(h+P_1) - N_TP_1 = 0$$

Expanding the products and regrouping the power terms of P_1, equation (10) is formed.

$$f(P_1) = (P_1)^3c3 + (P_1)^2c2 + (P_1)c1 + c0 = 0,$$

where

$c3 = -\lambda_{11}$

$c2 = b_1 - d_{p_1} + d_c - h\lambda_{11}$

$c1 = (b_1 - d_{p_1} + d_c)h - \frac{N_T \alpha}{q} + \frac{d_c}{\beta}$

$c0 = \frac{h d_c}{\beta}$

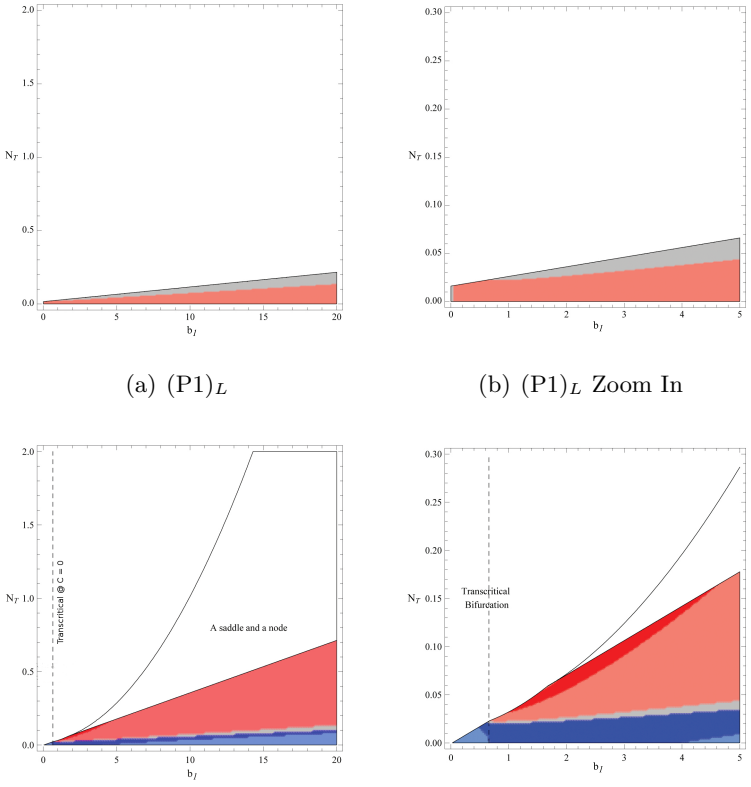

(a) $(P1)_L$

(b) $(P1)_L$ Zoom In

(c) $(P1C)_L$

(d) $(P1C)_L$ Zoom In

Figure 7.4.2: Eigenvalue Plots (The color scheme is described in table (7.4.2))

IV The Eigenvalue Plots For Equilibrium $(P1)_L$ And $(P1C)_L$

Color	Number of Eigenvalue with a Positive Real Part	Stability
	Real Eigenvalues	
Pink / Salmon	0	Attracting
Silver	1	Saddle
Light Blue	2	Saddle
Magenta	3	Repelling
	Complex Eigenvalues	
Red	0	Attracting
Gray	1	Saddle
Blue	2	Saddle
Purple	3	Repelling

Table 7.4.2: Color Scheme for figure (7.4.2)

The eigenvalue plots for equilibrium $(P1)_L$ and $(P1C)_L$ in the parametric space $b_1 : [0, 20] \times N_T : [0, 2]$ are shown in figures (7.4.2) and (7.4.3). The color scheme is described in the table below. The upper regions are not colored because for parameters in this region solutions $(P1)_L$ and $(P1C)_L$ do not satisfy the requirement $\frac{Q_1}{q} < \gamma$.

There are two $(P1C)_L$ solutions in the Saddle and Node region. One is a node and other one is a saddle. (They are shown in fig(7.4.3).) The vertical dashed line at $b_1 = \frac{d_c h \lambda_{11})}{\alpha\gamma - d_c} - d_p = 0.657143$ is the transcritical bifurcation between $(P1)_H$ and $(P1C)_H$ in case H. In graph (7.4.2), $b_1 = 0.657143$ is also the minimum producer's growth rate to permit a transcritical bifurcation allowing consumer's entry to the system in case L (same as in case H). Furthermore, the occurrence of transcritical bifurcation between $(P1)_L$ and $(P1C)_L$ now depends on both b_1 and N_T.

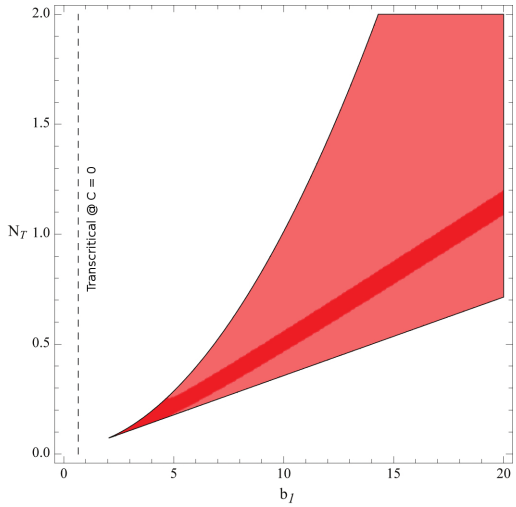

(a) $(P1)_L$ (A Node)

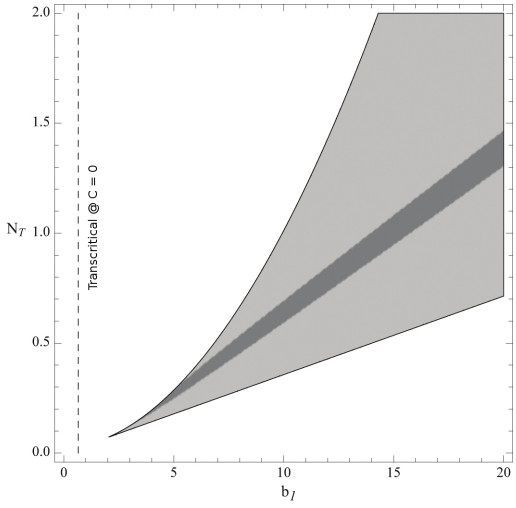

(b) $(P1)_L$ (A Saddle)

Figure 7.4.3: Eigenvalue Plots (The color scheme is described in table (7.4.2))

V Finding $(\text{P1P2C})_L$ In The Two-Producer-One-Consumer Model

Assuming the biomass conversion efficiency is $\frac{1}{q}\frac{Q_1P_1+Q_2P_2}{P_1+P_2}$

$$\begin{cases} \frac{dP_1}{dt} &= ((b_1-\lambda_{12}P_2-\lambda_{11}P_1)^+ - d_{P_1} - \frac{\alpha C}{h+P_1+P_2})P_1 \\ \frac{dP_2}{dt} &= ((b_2-\lambda_{21}P_1\lambda_{22}P_2)^+ - d_{P_2} - \frac{\alpha C}{h+P_1+P_2})P_2 \\ \frac{dC}{dt} &= (\frac{Q_1P_1+Q_2P_2}{q(P_1+P_2)}\frac{\alpha(P_1+P_2)}{h+P_1+P_2} - d_c)C \\ \frac{dQ_1}{dt} &= ((N_T-qC-Q_1P_1-Q_2P_2)\beta_1 - Q_1)(b_1-\lambda_{12}P_2-\lambda_{11}P_1)^+ \\ \frac{dQ_2}{dt} &= ((N_T-qC-Q_1P_1-Q_2P_2)\beta_2 - Q_2)(b_2-\lambda_{21}P_1-\lambda_{22}P_2)^+ \end{cases}$$

Set $\frac{dC}{dt}$, $\frac{dP_1}{dt}$, $\frac{dP_2}{dt}$, $\frac{dQ_1}{dt}$, and $\frac{dQ_2}{dt}$ to zero, and assume $(b_1-\lambda_{12}P_2-\lambda_{11}P_1)^+ > 0$ and $(b_1-\lambda_{21}P_1\lambda_{22}P_2)^+ > 0$.

$$\begin{cases} b_1-\lambda_{12}P_2-\lambda_{11}P_1-d_{P_1} &= \frac{\alpha C}{h+P_1+P_2} \\ b_1-\lambda_{21}P_1-\lambda_{22}P_2-d_{P_2} &= \frac{\alpha C}{h+P_1+P_2} \\ \frac{Q_1P_1+Q_2P_2}{q}\frac{\alpha}{h+P_1+P_2}-d_c &= 0 \\ (N_T-qC-Q_1P_1-Q_2P_2)\beta_1 &= Q_1 \\ (N_T-qC-Q_1P_1-Q_2P_2)\beta_2 &= Q_2 \end{cases}$$

By the last two equations,

$$Q_1 = \frac{(N_T-qC)\beta_1}{1+P_1\beta_1+P_2\beta_2}$$
$$Q_2 = \frac{(N_T-qC)\beta_2}{1+P_1\beta_1+P_2\beta_2}$$

Substitute Q_1 and Q_2 into the third equation,

$$(Q_1P_1 + Q_2P_2) = \frac{qd_c}{\alpha}(h + P_1 + P_2)$$

to obtain

$$(\frac{N_T}{h + P_1 + P_2} - \frac{q}{\alpha}\frac{\alpha C}{h + P_1 + P_2})(\beta_1P_1 + \beta_2P_2) = \frac{qd_c}{\alpha}(1 + P_1\beta_1 + P_2\beta_2)$$

By the first two equations,

$$P_2 = \frac{b_1 - b_2 - d_{P_1} + d_{P_2} - P_1\lambda_{11} + P_1\lambda_{21}}{\lambda_{12} - \lambda_{22}}$$

$$C = \frac{h + P_1 + P_2}{2\alpha}(b_1 + b_2 - d_{P_1} - d_{P_2} - \lambda_{11}P_1 - \lambda_{12}P_2 - \lambda_{21}P_1 - \lambda 22P_2)$$

Substitute P_2 and C into the third equation, equation (5.2.4) is formed.

$$\begin{aligned} F(P_1) \quad = \quad & (N_T - \tfrac{q}{\alpha}(\tfrac{1}{2}(b_1 + b_2 - d_{P_1} - d_{P_2} - \lambda_{12}\tfrac{b_1 - b_2 - d_{P_1} + d_{P_2} - P_1\lambda_{11} + P_1\lambda_{21}}{\lambda_{12} - \lambda_{22}} \\ & -\lambda_{11}P_1 - \lambda_{21}P_1 - \lambda_{22}\tfrac{b_1 - b_2 - d_{P_1} + d_{P_2} - P_1\lambda_{11} + P_1\lambda_{21}}{\lambda_{12} - \lambda_{22}})) \\ & (h + P_1 + \tfrac{b_1 - b_2 - d_{P_1} + d_{P_2} - P_1\lambda_{11} + P_1\lambda_{21}}{\lambda_{12} - \lambda_{22}})) \\ & (\beta_1P_1 + \beta_2\tfrac{b_1 - b_2 - d_{P_1} + d_{P_2} - P_1\lambda_{11} + P_1\lambda_{21}}{\lambda_{12} - \lambda_{22}} \\ & -\tfrac{qd_c}{\alpha}(1 + P_1\beta_1 + \beta_2\tfrac{b_1 - b_2 - d_{P_1} + d_{P_2} - P_1\lambda_{11} + P_1\lambda_{21}}{\lambda_{12} - \lambda_{22}}) \\ & (h + P_1 + \tfrac{b_1 - b_2 - d_{P_1} + d_{P_2} - P_1\lambda_{11} + P_1\lambda_{21}}{\lambda_{12} - \lambda_{22}})) \end{aligned}$$

Bibliography

[1] A. Sharov, *Quantitative Population Ecology*. Virginia Tech, Blacksburg, VA, 1996. URL: `http://www.ento.vt.edu/~sharov/PopEcol/lec10/lotka.html`.

[2] M. L. Rosenzweig and R. H. MacArthur, "Graphical representation and stability conditions for predator-prey interactions," *American Naturalist*, vol. 97, no. 895, pp. 209–223, 1963.

[3] S. Diehl, "Paradoxes of enrichment: Effects of increased light versus nutrient supply on pelagic producer-grazer systems," *The American Naturalist*, vol. 169, June 2007.

[4] I. Loladze, Y. Kuang, and J. Elser, "Stoichiometry in producer-grazer systems: Linking energy flow with element cycling," *Bulletin of Mathematical Biology*, vol. 62, pp. 1137–1162, 2000.

[5] J. Pastor and Y. Cohen, "Herbivores, the functional diversity of plants, and cycling of nutrients in ecosystems," *Theoretical Population Biology*, vol. 51, pp. 165–179, 1997.

[6] T. Anderson, J. Elser, and D. O. Hessen, "Stoichiometry and population dynamics," *Bulletin of Mathematical Biology*, vol. 7, pp. 884–900, 2004.

[7] L. Zimmermann, "A producer-consumer model with stoichiometry," Master's thesis, University of Minnesota Duluth, 2006.

[8] P. Yaodzis, *Introduction to Theoretical Ecology*. Harper and Row, 1989.

[9] A. King, *Population Fluctuations in Mammals*. University of Michigan, Ecology and Evolutionary Biology and Mathematics Departments, 1999. URL: `http://tsuga.biology.lsa.umich.edu/king/mam99/index.html`.